

**SUBSECTION 2.5.4:
STABILITY OF SUBSURFACE MATERIALS AND FOUNDATIONS
TABLE OF CONTENTS**

2.5.4	STABILITY OF SUBSURFACE MATERIALS AND FOUNDATIONS	...2.5.4-1
2.5.4.1	Geologic Features2.5.4-1
2.5.4.2	Properties of Subsurface Materials2.5.4-5
2.5.4.3	Foundation Interfaces2.5.4-34
2.5.4.4	Geophysical Surveys2.5.4-35
2.5.4.5	Excavations and Backfill2.5.4-48
2.5.4.6	Groundwater Conditions2.5.4-54
2.5.4.7	Response of Soil and Rock to Dynamic Loading2.5.4-56
2.5.4.8	Liquefaction Potential2.5.4-61
2.5.4.9	Earthquake Site Characteristics2.5.4-65
2.5.4.10	Static Stability2.5.4-65
2.5.4.11	Design Criteria and References2.5.4-76
2.5.4.12	Techniques to Improve Subsurface Conditions2.5.4-77
2.5.4.13	References2.5.4-78

SUBSECTION 2.5.4 LIST OF TABLES

<u>Number</u>	<u>Title</u>
2.5.4-201	Summary of Layer Thicknesses
2.5.4-202	Summary of Uncorrected N-Values
2.5.4-203	SPT Hammer Efficiency Corrections
2.5.4-204	Summary of Corrected N-Values (N_{60})
2.5.4-205	Summary of General Physical and Chemical Properties Test Results
2.5.4-206	Summary of Recovery and RQD Values for Rock Strata
2.5.4-207	Summary of Unconfined Strength Testing of Rock
2.5.4-208	Summary of Triaxial Testing Results
2.5.4-209	Summary of Recommended Geotechnical Engineering Parameters
2.5.4-210	Summary of Calcite Content Testing Results
2.5.4-211	Guidelines for the Evaluation of Soil Chemistry
2.5.4-212	As-built Boring and CPT Probe Information
2.5.4-213	Summary of Test Pit Location
2.5.4-214	Summary of Laboratory Compaction, and CBR Results
2.5.4-215	Summary of Measured Shear Wave Velocities and Compressive Wave Velocities
2.5.4-216	Summary of Recommended Shear Modulus Degradation and Damping Curves
2.5.4-217	Summary of Bearing Capacity
2.5.4-218	Summary of Liquefaction Resistance Calculation Results
2.5.4-219	Estimated Foundation Settlements

SUBSECTION 2.5.4 LIST OF FIGURES

<u>Number</u>	<u>Title</u>
2.5.4-201	Site Plan Showing Structures and Finish Grade
2.5.4-202	Site Plan Showing Boring Locations
2.5.4-203	Geotechnical Cross Section D-D' Through Unit 6 Power Block
2.5.4-204	Geotechnical Cross Section E-E' Through Unit 6 Power Block
2.5.4-205	Geotechnical Cross Section F-F' Through Unit 6 Power Block
2.5.4-206	Geotechnical Cross Section A-A' Through Unit 7 Power Block
2.5.4-207	Geotechnical Cross Section B-B' Through Unit 7 Power Block
2.5.4-208	Geotechnical Cross Section C-C' Through Unit 7 Power Block
2.5.4-209	Plan Showing Geotechnical Cross Section Locations
2.5.4-210	Sonic Log Locations
2.5.4-211	Shear Wave Velocity at Greater Depth
2.5.4-212	Plot of Uncorrected SPT N-Values with Depth
2.5.4-213	Plot of Corrected SPT N_{60} -Values with Depth
2.5.4-214	Plot of CPT Data with Depth
2.5.4-215	Plot of Rock RQD Data with Depth (Sheet 1 of 2)
2.5.4-215	Plot of Rock RQD Data with Depth (Sheet 2 of 2)
2.5.4-216	Plot of Fines Content with Depth
2.5.4-217	Plot of Rock Unconfined Compressive Strength with Depth
2.5.4-218	Plot of Shear Wave Velocity Measurements with Depth
2.5.4-219	Plot of Compression Wave Velocity with Depth
2.5.4-220	Plot of Recommended Shear Wave Velocity with Depth
2.5.4-221	Profile of Site Grading
2.5.4-222	Excavation at Power Block
2.5.4-223	Geophysical Survey Lines
2.5.4-224	Microgravity Models for Water-Filled Spherical Cavities in Limestone (Sheet 1 of 2)
2.5.4-224	Microgravity Models for Water-Filled Spherical Cavities in Limestone (Sheet 2 of 2)

SUBSECTION 2.5.4 LIST OF FIGURES (CONT.)

<u>Number</u>	<u>Title</u>
2.5.4-225	Microgravity Models for Water-Filled Horizontal Conduits in Limestone
2.5.4-226	Line 5 Geophysical Data
2.5.4-227	Line 9 Geophysical Data
2.5.4-228	Microgravity Contour Map
2.5.4-229	Line 9 Microgravity Model
2.5.4-230	Line 5 Microgravity Model
2.5.4-231	Microgravity Contour Map with Muck Effects Removed
2.5.4-232	Shear Modulus Degradation Based on RCTS Testing
2.5.4-233	Recommended Shear Modulus Degradation Curves
2.5.4-234	Damping Curve Measurements Based on RCTS Testing
2.5.4-235	Recommended Damping Curves
2.5.4-236	Recommended Shear Wave Velocity and Shear Modulus for Fill
2.5.4-237	Comparison of Normalized SPT N-Value (N1) Measured by SPT and Correlated from CPT
2.5.4-238	Factor of Safety Against Liquefaction Based on CPT Values
2.5.4-239	Lateral Earth Pressure Diagram: Active Case
2.5.4-240	Lateral Earth Pressure Diagram: At-Rest Case
2.5.4-241	Line 10 Geophysical Data
2.5.4-242	EW-1 Location at the Turkey Point Site
2.5.4-243	EW-1 Profiles of Vs, Average Vs, Standard Deviation, +/- Standard Deviation and 2008 Average Vs versus Depth Beneath Finished Site Grade

2.5.4 STABILITY OF SUBSURFACE MATERIALS AND FOUNDATIONS

PTN COL 2.5-1
PTN COL 2.5-5

This subsection presents information on the properties and stability of soils and rocks that may affect the safety of the Seismic Category I facilities (nuclear islands), under both static and dynamic conditions including the vibratory ground motions associated with the ground motion response spectrum (GMRS). An evaluation of the site conditions and geologic features that may affect the nuclear islands or their foundations is also provided.

This subsection is organized into the following subsections:

- Geologic Features ([Subsection 2.5.4.1](#))
- Properties of Subsurface Materials ([Subsection 2.5.4.2](#))
- Foundation Interfaces ([Subsection 2.5.4.3](#))
- Geophysical Surveys ([Subsection 2.5.4.4](#))
- Excavations and Backfill ([Subsection 2.5.4.5](#))
- Groundwater Conditions ([Subsection 2.5.4.6](#))
- Response of Soil and Rock to Dynamic Loading ([Subsection 2.5.4.7](#))
- Liquefaction Potential ([Subsection 2.5.4.8](#))
- Earthquake Site Characteristics ([Subsection 2.5.4.9](#))
- Static Stability ([Subsection 2.5.4.10](#))
- Design Criteria ([Subsection 2.5.4.11](#))
- Techniques to Improve Subsurface Conditions ([Subsection 2.5.4.12](#))

Subsection headings and heading numbers follow RG 1.206 for [Subsection 2.5.4](#).

2.5.4.1 Geologic Features

This subsection presents a summary of the non-tectonic processes and geologic features that could relate, if present, to permanent ground deformations or foundation instability at the Units 6 & 7 safety-related facilities. A summary of the

subsurface conditions based on the Units 6 & 7 subsurface investigation results is presented first, followed by descriptions of the foundation soil and rock properties and the stability of these materials. Processes and features evaluated include: areas of actual or potential subsurface subsidence, solution activity, uplift, or collapse; zones of alteration, irregular weathering, or structural weakness; unrelieved stresses in bedrock; rocks or soils that may become unstable; and a history of deposition and erosion.

The following description is based on the site geology presented in [Subsection 2.5.1](#), surface faulting described in [Subsection 2.5.3](#), and results of the site-specific subsurface investigation activities presented in [Subsection 2.5.4.2](#).

2.5.4.1.1 Summary of Subsurface Conditions

The Units 6 & 7 nuclear island locations are shown on [Figure 2.5.4-201](#). To evaluate the subsurface conditions at these locations, a subsurface investigation program is executed. A total of 88 geotechnical borings and 2 additional geophysical borings are drilled and sampled at the locations shown on [Figure 2.5.4-202](#). Soil boring and rock coring logs are presented in [Reference 257](#). [Figures 2.5.4-203](#) through [2.5.4-205](#) present geologic cross sections through Unit 6 based on these boreholes, and [Figures 2.5.4-206](#) through [2.5.4-208](#) present geologic cross sections through Unit 7. The cross section locations are shown on [Figure 2.5.4-209](#).

The depth of sediments and the estimated top of rock are indicated on the cross sections ([Figures 2.5.4-203](#) through [2.5.4-208](#)). [Table 2.5.4-201](#) summarizes the thickness of each stratum encountered and its respective base elevation. Geophysical methods used to identify top of rock are presented in [Subsection 2.5.4.4](#).

2.5.4.1.1.1 Description of Surficial Soil and Rock

The original site was covered by organic muck and the Miami Limestone ([Figure 2.5.1-332](#)). The organic muck was the dominant surface cover, whereas the Miami Limestone was at the ground surface in the northwestern portion of the site. The Miami Limestone is a marine carbonate rock, as presented in [Subsection 2.5.4.2](#).

The original site was at or near sea level with a natural relief of approximately 3 feet from its northern-to-southern boundary and approximately 0.5 feet of relief from its western-to-eastern boundary, except where the ground surface was

raised to create berms adjacent to the canals. Other than the berms, the site is flat and uniform throughout with the exception of the vegetative depressions as seen in [Figure 2.5.1-333](#). The vegetative depressions are reported to be dissolution features within the Miami Limestone.

2.5.4.1.1.1.1 Correlation with Site Geologic Setting

As presented in [Subsection 2.5.1.1.1.1.1](#), the site is within the Southern Slope subprovince of the Atlantic Coastal Plain. The geologic setting is characterized by broad bands of swamps and marshes that are flooded by tides or by freshwater runoff ([Figure 2.5.1-217](#)).

The boring logs presented in [Reference 257](#) indicate that the site subsurface is consistent with the Southern Slope subprovince. The results of petrographic examinations of rock core samples, as described in [Subsection 2.5.4.2.1](#), are also consistent with rock of this geomorphic province.

2.5.4.1.2 Subsidence, Dissolution Activity, Uplift, or Collapse

As described in [Subsections 2.5.1.2.4](#) and [2.5.1.2.5.2](#), no geologic hazards have been identified within the site or site area (5-mile radius). No unusual zones of alteration, weathering profiles, or structural weakness are encountered at the location of the site investigation. As described in [Subsection 2.5.1.2.5.3](#), no geomorphic disturbances or fault-related features are observed by the field reconnaissance. As a result of the reconnaissance investigation, no geomorphic, stratigraphic, or other evidence suggesting the presence of active or recent tectonic deformation within the site vicinity (25-mile radius) is observed.

As described in [Subsection 2.5.1.2.5.4](#), anthropogenic effects in southeastern Florida of urban development, water mining, limestone mining, agriculture, and construction of drainage canals impact the regional groundwater table and associated saltwater intrusion. [Subsection 2.4.12](#) contains a more detailed description of the Units 6 & 7 groundwater conditions.

The potential for subsidence or collapse pertaining to future subsurface solution activity below Units 6 & 7 is described in [Subsection 2.5.4.1.2.1](#). The potential for uplift is described in [Subsection 2.5.4.1.2.2](#).

2.5.4.1.2.1 Dissolution Activity

The majority of the near-surface geologic units are composed of limestone rock. Based on Florida Geological Survey records, sinkholes in the limestone of

southeastern Florida are few in number, shallow, broad, and develop gradually. The Florida Geological Survey has stated that “there is not a great degree of dissolution activity; what does occur is numerous small cavities in rock cores and is considered micro-karst. The Florida Geological Survey does not expect any large cavities or collapse in the site area.”

Florida Geological Survey publications have no documentation of significant karst development in this region of Florida (References 202 and 203). However, according to Renken et al. (Reference 204), there is evidence of karst development in Miami-Dade County along the Atlantic Coastal ridge extending southward from South Miami to the Everglades National Park. Vanlier et al. (Reference 205) state that most of Miami-Dade County is underlain by limestone having solution cavities. Vanlier et al. further indicate that a few localities in the Homestead and Turkey Point area are underlain by exceptionally large cavities between depths of approximately 18 to 31 feet. Parker (Reference 206) states that the Miami Limestone and Fort Thompson Formation have significant permeability and solution features that have created turbulent flow conditions in some wells. According to Cunningham et al. (Reference 207), paleokarst is well-documented in the Lake Belt area of north central Miami-Dade County.

Small dissolution features are present in limestone drill core samples collected during the subsurface investigation at the site and described in Reference 257. They occur in the form of vugs and moldic secondary porosity, particularly in the Miami and Key Largo limestones. During the site subsurface investigation, six rod drops, indicating the potential presence of voids, were noted during approximately 9000 feet of rock coring (Table 2.5.1-210 and Figure 2.5.1-378). Two of the rod drops (B-637 and B-805) occurred within the Miami Limestone, which will be removed from beneath the nuclear island during construction. These two rod drops had magnitudes of 2 and 3 feet. One rod drop (B-714) occurred at the base of the Fort Thompson Formation immediately before penetrating the sands of the Tamiami Formation and had a magnitude of 1 foot. The remaining three rod drops (B-738, B-811, and B-814) occurred within sandy zones of the Fort Thompson Formation in the elevation range of –62.7 to –79.1. These three rod drops, which are all located outside the nuclear island footprint, had magnitudes ranging from 0.5 to 4 feet. While caliper and acoustic logs from the 10 boreholes where downhole geophysical data were obtained do not indicate the presence of large voids, they do support the interpretation of two preferential secondary porosity flow zones. A more detailed discussion of the site geologic hazards is presented in Subsection 2.5.1.2.4. A description of the results of a geophysical survey using microgravity, seismic refraction, and multichannel analysis of surface waves

methods to investigate the potential for solution features beneath the site is provided in [Subsection 2.5.4.4.5](#).

2.5.4.1.2.2 Uplift or Collapse

Units 6 & 7 are located on the east coast of the Florida platform. As described in [Subsection 2.5.1.1.1.3.2.1](#), the Florida platform represents a flat, slowly subsiding region dominated by carbonate deposition from northern Cuba to Georgia and between the Florida escarpment in the eastern Gulf of Mexico and the Bahama platform in the east. As presented in [Subsection 2.5.3.2](#), no evidence of tectonic surface deformation is observed within the site vicinity. The absence of karst-related collapse is also described in [Subsection 2.5.3.2](#). Therefore, no uplift due to natural forces or human development is anticipated.

2.5.4.1.2.3 History of Deposition and Erosion

As described in [Subsection 2.5.1.2](#), the site area is characterized by flat, planar bedding in late Pleistocene and older units. The site vicinity geology ([Figure 2.5.1-331](#)) was influenced by sea level fluctuations, processes of carbonate and clastic deposition, and erosion. The Paleogene (early Cenozoic) is dominated by the deposition of carbonate rocks, while the Neogene (late Cenozoic) is influenced more by the deposition of quartzitic sands, silts, and clays ([Reference 208](#)). Within the site area, the dominant subsurface material types are limestones of the Miami Limestone, Key Largo Limestone, Fort Thompson Formation, and Arcadia Formation and sands and silts of the Tamiami and Peace River Formations ([Figure 2.5.1-332](#)). Minor units of alluvial soils, organic muck, and silt cover the site surface. During the Pleistocene, worldwide glaciation and fluctuating sea levels influenced the geology in the site vicinity. Drops in sea level caused by growth of glaciers increased Florida's land area significantly, which led to increased erosion and clastic deposition. Warm interglacial periods resulted in a rise in sea level and an increase in nutrient-rich waters leading to an increase in carbonate buildup ([Reference 208](#)).

2.5.4.2 Properties of Subsurface Materials

PTN COL 2.5-6

This subsection addresses the properties of subsurface materials and the methods of determining these properties. [Subsection 2.5.4.2.1](#) addresses the properties of subsurface materials encountered at the site, while [Subsections 2.5.4.2.2](#) and [2.5.4.2.3](#) describe the subsurface investigation and laboratory testing program conducted to obtain these properties.

2.5.4.2.1 Description of Subsurface Materials

This subsection addresses the properties of subsurface materials, as follows:

- [Subsection 2.5.4.2.1.1](#) provides an introduction to the soil and rock strata encountered at the site.
- [Subsection 2.5.4.2.1.2](#) describes each soil and rock stratum encountered.
- [Subsection 2.5.4.2.1.2.10](#) describes the subsurface materials below a depth of 600 feet bgs (i.e., below the maximum depth of this subsurface investigation).
- [Subsection 2.5.4.2.1.3](#) describes the evaluation of in situ properties of soil strata investigated (i.e., soils extending to a depth of approximately 600 feet bgs) and presents tables and figures of these properties.
- [Subsection 2.5.4.2.1.4](#) describes the chemical properties of the soil and rock.
- [Subsection 2.5.4.2.1.5](#) describes the field testing program.
- [Subsection 2.5.4.2.1.6](#) describes the laboratory testing program.

2.5.4.2.1.1 Summary of Soil and Rock Strata

Subsurface materials at the site consist of coastal marine sediments underlain by Paleozoic- and Mesozoic-age igneous and metamorphic bedrock (basement rock), which is estimated to be at a depth of at least 15,000 feet bgs ([Reference 209](#)). The uppermost 600 feet of site soils, consisting of limestones attributed to the Miami Limestone, Key Largo Limestone, and Fort Thompson Formation, and soils and soil-rock mixtures attributed to the Tamiami Formation and the Hawthorn Group, are the subject of this subsurface investigation. These subsurface materials are divided into eight individual strata, consisting of four predominantly rock strata (Strata 2, 3, 4, and 8), three predominantly soil strata (Strata 5, 6, and 7), and surficial muck (Stratum 1). The final site design includes an additional stratum of compacted limerock fill. The soil and rock strata are described in [Subsection 2.5.4.2.1.2](#).

Subsurface conditions deeper than 600 feet are characterized using information from the geologic literature, most notably [References 210](#) and [211](#), and from deeper borings drilled in the area for oil and gas exploration ([Reference 212](#)). While the depth to competent bedrock (“basement rock”) is significant at the site,

layers and lenses of limestone, dolostone, sand, and silt are present intermittently to this depth.

Identification and characterization of the investigated soil and rock strata are based on physical and engineering characteristics. Methods used in identification and characterization are described in detail in [Subsections 2.5.4.2.2](#) and [2.5.4.4](#) and include:

- Standard penetration testing (SPT) and rock coring in borings
- Cone penetration testing (CPT)
- Test pit (TP) excavations
- Geophysical downhole and P-S suspension logging to measure compression (P , V_p) and shear (S , V_s) wave velocities and other geophysical indices
- Groundwater observation well (OW) installations and related field testing
- Extensive laboratory testing of disturbed and intact soil samples and rock cores collected

The natural ground surface at and around the power block at the time of this subsurface investigation was generally level, ranging from approximately El. –2 feet to +1 foot, with an average of El. –1 foot. Note that all references to elevations given in this subsection are to the North American Vertical Datum of 1988 (NAVD 88). The power block finish grade elevation is +25.5 feet.

The natural ground surface at the makeup water reservoir at the time of this subsurface investigation was generally level at approximately El. –0.5 feet. A concrete retaining wall extends to El. +24 feet.

2.5.4.2.1.2 Description of Soil and Rock Strata

The following is a description of each soil stratum encountered in the subsurface investigation to the maximum investigated depth of 616 feet bgs in the power block and 150 feet bgs in the makeup water reservoir and perimeter areas. The stratum thickness indicated in each description for the power block is the calculated average within the two power block units (Unit 6 and Unit 7) because the subsurface conditions encountered in the subsurface boring program are relatively uniform. Note that the stratum thickness at a particular boring or CPT is only included in the average calculation when the stratum is encountered and fully

penetrated by the boring or CPT probe. The Unified Soil Classification System (USCS) ([References 213 and 214](#)) classifications included in each of the descriptions are based mainly on the results of grain size analyses and Atterberg limit tests. Most of the strata are present in each boring and CPT within the depth investigated, except as noted.

2.5.4.2.1.2.1 Stratum 1 (Muck)

Stratum 1 is removed from the plant area at the initiation of construction. Therefore, this stratum is not characterized to the same extent as the underlying strata. The following is a summary of the characterization of this stratum from the site investigation and previous data.

Stratum 1 (muck) is encountered at the ground surface in all borings in the Units 6 & 7 power block and within the entire site, except for boring B-814, which has fill covering Stratum 1. Stratum 1 consists primarily of light gray to black silty clay with varying amounts of sand and peat. Boreholes fully penetrated this stratum within the Units 6 & 7 power block and the entire site. Typically, the Stratum 1 soils contain trace organics near the surface. This stratum has a very soft to medium stiff consistency. The thickness of Stratum 1 ranges from 2 to 7 feet, with an average of 3.4 feet. The top of this layer is typically at El. -1.2 feet. The average base elevation of this stratum is -4.6 feet.

2.5.4.2.1.2.2 Stratum 2 (Miami Limestone)

The Miami Limestone (or the Miami Oolite, as it is referred to in some publications) is a soft rock unit that is generally sampled in South Florida using SPT equipment rather than rock coring. The top of this unit is encountered at elevations ranging from -3.3 to -8.3 feet. The range of thickness for the Miami Limestone varies from 17.2 to 30.3 feet with an average of 22.6 feet.

Boreholes fully penetrated this stratum at all of the boring locations. Two exploratory test pits partially penetrated this stratum at two locations, TP-601 and TP-701. This stratum consists of pale yellow, light brownish gray, and white limestone. Based on the logs included in Appendix B of [Reference 257](#), it has a porous, sometimes fossiliferous texture, comprising oolite grains with varying carbonate cementation. Observed fossils include mollusks, bryozoans, and corals. Stratum 2 is characterized as a boundstone using the Dunham carbonate classification scheme ([Reference 215](#)) included in Appendix B of [Reference 257](#). This stratum has a soft to very hard consistency depending on the degree of cementation. Because this stratum is primarily sampled with SPT rather than rock

core equipment, this hardness description is the one used in the “Geotechnical Exploration and Testing Report” found in Appendix B of [Reference 257](#) for rocks, which differs from both the standard hardness description for rocks ([Reference 216](#)) and the consistency descriptions for fine-grained soils.

2.5.4.2.1.2.3 Stratum 3 (Key Largo Limestone)

The top of Key Largo Limestone is encountered between El. –24.1 and El. –35.3 feet, at an average of El. –27.2 feet. The thickness varies between 13.5 and 28.0 feet in the borings, with an average thickness of 22.3 feet.

The Key Largo Limestone, or upper Fort Thompson Formation as it is referred to in [Reference 257](#), is a coralline, porous formation with recrystallized calcite infill visible in core samples. The color varies between white, pale yellow, light brownish gray, and gray. The properties of this stratum indicate a rock of medium hardness and strength based on [Reference 216](#).

2.5.4.2.1.2.4 Stratum 4 (Fort Thompson Formation)

The Fort Thompson Formation underlies the Key Largo Limestone across the entire site, except in boring B-802 where the Miami Limestone is directly above the Fort Thompson Formation. The Fort Thompson Formation is fully penetrated in the majority of boring locations. Borings B-622, B-623, B-624, B-626, B-627, B-629, B-631, B-632, B-633, B-639, B-722, B-723, B-724, B-727, B-729, B-730, B-731, B-732, B-733, B-738, and B-739 are terminated in the Fort Thompson Formation.

The top of this unit is encountered at elevations ranging from –44.1 to –53.4 feet. The range of thickness varies from 60.0 to 68.4 feet, with an average of 65.6 feet.

The Fort Thompson Formation consists of white limestone with varying amounts of vugs, shells, and some sand. It is medium hard to hard above approximately El. –60 feet and is medium hard to soft (based on [Reference 216](#)) below approximately El. –60 feet.

2.5.4.2.1.2.5 Stratum 5 (Upper Tamiami Formation)

The upper Tamiami Formation underlies the Fort Thompson Formation across the entire site. This stratum is fully penetrated in borings B-601(DH), B-602, B-604(DH), B-605, B-608(DH), B-630, B-701(DH), B-702, B-704(DH), and B-705 and at each of the four CPT locations. The top of the upper Tamiami Formation is

Turkey Point Units 6 & 7
COL Application
Part 2 — FSAR

encountered between El. –108.3 and –117.7 feet with an average top elevation of El. –115.1 feet. The base of this unit grades into the lower Tamiami Formation.

The bottom of the unit is estimated at El. –159 feet. The upper Tamiami Formation consists of light gray to greenish gray silty sands, with varying amounts of gravel. This stratum is generally dense to very dense.

2.5.4.2.1.2.6 Stratum 6 (Lower Tamiami Formation)

The lower Tamiami Formation is encountered below the upper Tamiami Formation in the Units 6 & 7 power block and is present in 11 of the 13 boring logs (included in [Reference 257](#)) that extend below El. –160 feet. This stratum is fully penetrated in boring locations B-601(DH), B-608(DH), B-610, B-630, B-701(DH), and B-710(DH), and CPT locations C-601, C-701, and C-702. The lower Tamiami Formation starts at approximately El. –159 feet.

The lower Tamiami Formation consists of light gray to greenish gray sandy silt with minor amounts of silty clay. It generally has a very stiff to hard consistency.

2.5.4.2.1.2.7 Stratum 7 (Peace River Formation)

The Peace River Formation of the Hawthorn Group is encountered in borings that extend to depths of approximately 220 feet or greater. The top of this stratum is encountered at elevations between El. –213.1 feet and –217.5 feet, at an average elevation of –215.5 feet. This unit is fully penetrated in one boring, B-701 (DH). The stratum thickness in B-701 (DH) is 239 feet.

The Peace River Formation is a very dense light gray to olive gray silty sand.

2.5.4.2.1.2.8 Stratum 8 (Arcadia Formation)

The Arcadia Formation of the Hawthorn Group is encountered in boring location B-701 DH. The top of the Arcadia Formation is encountered at approximately El. –452 feet. This stratum is not fully penetrated in B-701 (DH), with the bottom of boring at El. –617 feet.

The Arcadia Formation consists of several different types of limestone (wackestone, packstone, and mudstone), with occasional dolostone and thin silty sand layers near the top of the unit. The color ranges between pale yellow, white, and light greenish gray. This stratum ranges in hardness from soft to hard using [Reference 216](#) criteria. The induration ranges from friable to indurated. Shell molds are observed in some parts of this stratum.

2.5.4.2.1.2.9 Compacted Limerock Fill

Soil laboratory testing conducted on two bulk samples from test pits excavated into Miami Limestone during the subsurface investigation is performed to evaluate this material as a fill source. This excavated and re-compacted limestone is referred to as compacted limerock fill.

The muck layer underneath the power block area is removed and replaced with compacted limerock fill from onsite excavated Miami Limestone and offsite sources, with fill placement starting from approximately El. –5 feet and building up to El. +25.5 feet. Excavations and fill on other areas of the site as described in [Subsections 2.5.4.3](#) and [2.5.4.5](#) are completed. All other non-Category I structures are supported on compacted limerock fill.

2.5.4.2.1.2.10 Properties of Subsurface Materials Below 600 Feet

Evaluation of properties of materials deeper than 600 feet is performed through use of published data from the Florida Geological Survey (FGS) Oil and Gas Division and the U.S. Geological Survey (USGS) ([References 211](#) and [212](#)). Both sources contain logs of borings within approximately 115 miles of the site (see [Figure 2.5.4-210](#)). The FGS logs contain sonic data from which compression wave velocity can be calculated extending from as shallow as approximately El. –3550 feet to as deep as approximately El. –11,900 feet. The USGS logs, which include both lithology and sonic data, start out shallower than 600 feet and extend to as deep as approximately El. –2350 feet.

Two gaps in the data where compression wave velocity data are unavailable are identified. The shallower gap is between approximately El. –1800 and El. –2200 feet, and the deeper gap is between approximately El. –2350 and El. –3550 feet depth. Compression wave velocity values to fill the upper approximately 362-foot gap are assumed by estimating compression wave velocities from neutron porosity and porosity density logs obtained from the USGS publication ([Reference 211](#)) and by comparing the lithology and stratigraphy in the logged sections with the lithology of these upper data. Compression wave velocity values to fill the lower approximately 1200-foot gap are estimated by comparing the lithology in these lower data to the compression wave velocity values in logged sections with similar lithology.

Turkey Point Units 6 & 7
COL Application
Part 2 — FSAR

Compression wave velocities (V_p) from the sonic logs are converted to shear wave velocities (V_s) using the following equation (Reference 218):

$$V_s = V_p / [2(1 - \mu)/(1 + 2\mu)]^{1/2} \quad \text{Equation 2.5.4-1}$$

Poisson's ratio (μ) computed from P-S suspension shear and compression wave velocities measured in the semi-consolidated calcareous materials in the upper 600 feet was approximately 0.36. Typical values in South Florida reported in the literature below approximately El. -1100 feet are closer to 0.3. Thus, Poisson's ratio was assumed to reduce from 0.35 just below El. -600 feet. Published values for Poisson's ratio in southern Florida are typified by a value of 0.3 at El. -1100 feet (Reference 218). Thus, a Poisson's ratio of 0.3 is assumed for the calculation of shear wave velocity at and below El. -1100 feet.

As shown in Figure 2.5.4-211, the average V_s from the sonic logs initially increases fairly steadily starting at approximately 4000 feet/second at a depth of 600 feet beneath finished site grade until approximately 4500 feet beneath finished site grade, where an average V_s of approximately 10,000 feet/second is attained, which may coincide with the base of the thick anhydrite unit of the middle Cedar Keys formation. V_s then begins a trend of gradual decrease, which continues until a depth of approximately 6750 feet beneath finished site grade and velocities of around 7000 feet/second are attained, which may coincide with the base of the chalky limestones and dolomites of the Pine Key Formation. At this point, the average V_s from the logs begins a gradual increase to approximately 10,000 feet/second, which is estimated to occur at a depth of around 10,000 feet below finished site grade. Thereafter, the average V_s continues to fluctuate, generally in the range of 8500 feet/second to 10,000 feet/second.

The lithology and sonic data for the Class V exploratory well EW-1 at the Turkey Point Units 6 & 7 site (Figure 2.5.4-242) are provided in Reference 287. The sonic data, from which shear wave velocity is calculated, extends from approximately Elevation -1078 feet to Elevation -3226 feet (NAVD 88).

Compression wave velocities (V_p) from the EW-1 log are converted to shear wave velocities (V_s) using Equation 2.5.4-1. A Poisson's ratio value of 0.31 is assumed for the calculation of V_s down to Elevation -1100 feet and a value of 0.3 is assumed at and below Elevation -1100 feet (Reference 218). As shown in Figure 2.5.4-243, the average V_s from EW-1 is between 5000 and 6000 fps until a depth of approximately 1500 feet beneath finished site grade. Below this depth, the average V_s increases to between 6000 and 8000 to over 8000 fps at a depth of

approximately 2000 feet. V_s then remains between 6000 and 8000 fps until a depth of approximately 2800 feet where, again, an average V_s of over 8000 fps is attained. At this point, the average V_s begins to decrease and below a depth of approximately 3100 feet, the average V_s falls to between 4000 and 6000 fps.

The converted sonic data exhibit some V_s values greater than 9000 fps. Such high values generally indicate the presence of hard rock, such as the granitic rock at the V.C. Summer Units 2 & 3 site (Reference 288) and well-indurated Cambro-Ordovician marine carbonates such as those at the proposed Bellefonte Units 3 & 4 site (Reference 289). The detailed lithologic logs in Reference 287 document the absence of such lithologies at the Turkey Point site. Therefore, the V_s values greater than 9000 fps are not included in the average V_s shown in Figure 2.5.4-243. The V_s values that were less than 9000 fps were retained since, in general, they reflect the lithologies noted on the detailed boring log and average values appear to be similar to, although higher than, the previously obtained data.

2.5.4.2.1.3 Evaluation of Properties of In Situ Materials

Properties of in situ materials are evaluated using the results of field and laboratory testing for Units 6 & 7 and outside the power blocks. These results, in the form of boring logs, CPT records, test pit logs, laboratory test results, etc., are contained in Appendix B of Reference 257 and are summarized in tables and figures presented in the following subsections. Generally, the results from within Units 6 & 7 and outside the power blocks are similar. The majority of the average property values for each stratum presented in the following subsections are given in Table 2.5.4-209.

2.5.4.2.1.3.1 Stratum Thickness

The thickness of each stratum is estimated from borings that penetrate the particular stratum. Shear wave velocities and CPTs also provide an estimate of thickness for the shallower strata. The thickness and base elevation of each stratum from all the borings and CPTs are averaged and presented in Table 2.5.4-201. Note that the thicknesses and base elevations given in Table 2.5.4-201 are for all areas of the investigated site. Note that only data from borings, geophysical measurements, and CPTs that encounter and fully penetrate the strata are considered in evaluating the strata thickness and in selecting the strata base elevations in Table 2.5.4-201.

2.5.4.2.1.3.2 SPT N-Values

As noted in [Subsection 2.5.4.2.2.3](#), 88 geotechnical borings are performed for this subsurface investigation: 77 borings in the power block and 11 borings outside the power block. SPT samples are taken at approximately 2.5-foot intervals to 15 feet depth, at 5-foot intervals from 15 feet to 100 feet depth, at 10-foot intervals from greater than 100 feet to the maximum depth sampled using SPT equipment. Intact soil samples are obtained in selected borings.

Where rock is encountered, continuous coring is employed to obtain samples as presented in [Subsection 2.5.4.2.2.3](#).

2.5.4.2.1.3.2.1 Uncorrected N-Values

A summary of all N-values (inside and outside of the power block) measured in the field (uncorrected) is presented in [Figure 2.5.4-212](#) and [Table 2.5.4-202](#). Some very low N-values in the upper and lower Tamiami and Peace River Formations are questionable as described in [Subsection 2.5.4.8.2](#). The artesian groundwater conditions that resulted in soil disturbance are presumably the cause for N-values that are uncharacteristic of sediments at depths.

2.5.4.2.1.3.2.2 N-Value Correction

Field SPT N-values are adjusted for SPT hammer energy, borehole diameter (C_B), sampler (C_S) and rod length (C_R). This adjusted N-value, N_{60} , is determined using the following equation ([References 219](#) and [225](#)):

$$N_{60} = N C_E C_B C_S C_R \quad \text{Equation 2.5.4-2}$$

Where,

N = field measured SPT blow count

C_E = hammer energy correction factor

C_B = borehole diameter correction factor

C_S = sampler correction factor

C_R = rod length correction factor

The SPT N-value used in correlations with engineering properties is a value traditionally based on 60 percent hammer efficiency. All 10 of the drill rigs employed in this subsurface investigation for SPT sampling use automatic hammers, which typically have efficiencies greater than 60 percent. SPT hammer energy measurements are made for each drilling rig/hammer employed, in accordance with ASTM D 6066 ([Reference 220](#)), and the hammer energy

measurements (expressed as energy transfer ratios, or ETRs) are obtained. As shown in [Table 2.5.4-203](#), average ETRs range from 79.6 percent to 88.0 percent. The resulting energy correction factor, C_e (expressed as ETR/60%), ranges from 1.33 to 1.47, also as shown in [Table 2.5.4-203](#). N_{60} -values (from Equation 2.5.4-2) from each boring are corrected using the appropriate C_e value. Additional information on the correction factors for rod length, boring diameter, and soil sampler are provided in [References 219](#) and [225](#). The resulting SPT N-values are termed N_{60} . For the liquefaction analysis, additional correction factors for overburden pressure are applied.

A summary of all N_{60} values with depth is shown on [Figure 2.5.4-213](#) and in [Table 2.5.4-204](#).

2.5.4.2.1.3.2.3 Design N-Values

[Table 2.5.4-209](#) presents N_{60} values selected for design for each stratum, both within and outside the power block.

Note that as explained in [Subsection 2.5.4.2.1.3.3](#), four cone penetration tests (CPTs) were performed through the Tamiami Formation. The CPT corrected tip resistance (q_t) was then used to derive the N_{60} -values based on the best estimate relationship of q_t/N with increasing fines content from Kulhawy & Mayne (1990) ([Reference 282](#)). Using an average q_t of about 160 tsf and a q_t/N ratio of 4 for the Upper Tamiami, a N_{60} -value of 40 bpf is estimated. Similarly, using an average q_t of about 110 tsf and a q_t/N ratio of 3.5, a N_{60} -value of 32 bpf is estimated for the Lower Tamiami. Considering the substantial depth of the Tamiami Formation, these N_{60} -values derived from the CPT results provide a better representation of the subsurface conditions in comparison with the SPT N_{60} -values in [Table 2.5.4-204](#). However, considering the relatively high shear wave velocity values observed in these formations ([Figures 2.5.4-218](#) and [2.5.4-220](#)), even these N_{60} -values derived from the CPT results are probably conservative.

2.5.4.2.1.3.3 CPT Values

As noted in [Subsection 2.5.4.2.2.4](#), four CPTs are performed for this subsurface investigation with two each in each of the two power block areas. The CPTs are initiated at a depth of approximately 120 feet in a hole cored through the overlying rock. The CPTs are advanced through the upper and lower Tamiami Formation and into the Peace River Formation. One CPT extends as deep as 260 feet. These CPT results are used (among other results) to estimate the angle of internal friction of sand strata penetrated ([Subsection 2.5.4.2.1.3.8](#)).

CPT corrected (q_t) and normalized (q_{c1n}) tip resistance values are significant factors in liquefaction evaluation (refer to [Subsection 2.5.4.8.3](#)). Note that the terms “corrected” and “normalized” used here are as described in [Subsection 2.5.4.8.3](#). Summaries of all of the CPT tip resistance (q_t) values based on elevation, as well as the sleeve friction (f_s) and friction ratio (R_f) values, are shown in [Figure 2.5.4-214](#).

2.5.4.2.1.3.4 Rock Recovery and RQD

Rock is sampled using HQ3 and PQ3 core barrel equipment. The rock quality designation (RQD) is calculated based on the core runs sampled. In addition to recovery, the RQD provides an index of rock strength for general characterization of a rock mass. As shown on [Figure 2.5.4-215](#), the rock RQD is very inconsistent. In general rock quality appears to be at its maximum in the range from approximately El. -45 to El. -60 feet. A summary of recovery and RQD for the three rock strata cored is presented in [Table 2.5.4-206](#).

2.5.4.2.1.3.5 Natural Moisture Content and Atterberg Limits

The results of natural moisture content and Atterberg limits laboratory tests on samples from all of the soil strata tested are shown in [Table 2.5.4-205](#).

2.5.4.2.1.3.6 Grain Size Distribution

The results of grain size distribution tests performed on all of the samples tested are shown in [Table 2.5.4-205](#). This table shows the percentage (by dry weight) of gravel, sand, silt, and clay, and also the percentage fines, (i.e., the percentage passing the standard number 200 sieve). Specific gravity measurements are also included in this table. Average fines contents are summarized for each soil stratum graphically in [Figure 2.5.4-216](#). This figure clearly shows the marked difference in fines content between the upper Tamiami Formation (silty sand) and the lower Tamiami Formation (sandy silt).

2.5.4.2.1.3.7 Unit Weight

Unit weight is recorded for each rock sample tested for unconfined compressive strength and each soil sample tested for resonant column/torsional shear (RCTS) and triaxial shear strength in the laboratory. The results for all samples tested, expressed in terms of dry unit weight and natural moisture content, are included in [Table 2.5.4-205](#) (data from RCTS tests), [Table 2.5.4-207](#) (rock tests), and [Table 2.5.4-208](#) (static triaxial).

Total unit weights recommended for use in each stratum are summarized in [Table 2.5.4-209](#).

2.5.4.2.1.3.8 Angle of Internal Friction

The drained/effective angle of internal friction (ϕ') of each sand stratum is estimated using the data from corrected SPT N_{60} -values, CPT tip resistances (q_t), and laboratory consolidated undrained triaxial testing results.

Using [Reference 221](#), ϕ' is estimated from the best estimate corrected N_{60} -value.

The empirical correlation used to obtain ϕ' from CPT tip resistance ([Reference 222](#)) is:

$$\phi' = \arctangent [0.1 + 0.38 \cdot \log(q_t/\sigma_v')] \text{ (in degrees)} \quad \text{Equation 2.5.4-3}$$

Where,

q_t = the CPT corrected tip resistance

σ_v' = the effective overburden pressure at the depth of the CPT test interval

Recommended values of ϕ' derived from the different correlations/test methods (i.e., from SPT correlation, CPT correlation, and laboratory consolidated undrained triaxial testing), and for each stratum, are shown in [Table 2.5.4-209](#). An effective friction value (ϕ') of 20 degrees is measured in triaxial testing on one tube sample of the lower Tamiami Formation sandy silt (Stratum 6) as presented in [Table 2.5.4-208](#).

2.5.4.2.1.3.9 Undrained Shear Strength

Only one primarily fine-grained stratum is encountered in the subsurface investigation. The undrained shear strength (s_u) of this one soil stratum (Stratum 6, the lower Tamiami Formation) is estimated from corrected SPT N_{60} -values.

The empirical correlation used to obtain s_u from the N_{60} -value ([Reference 223](#)) is:

$$s_u = N_{60}/8 \text{ (in kips per square foot [ksf])} \quad \text{Equation 2.5.4-4}$$

2.5.4.2.1.3.10 Rock Unconfined Strength

Rock core samples from three of the rock strata cored (the Key Largo Limestone, Fort Thompson Formation, and Arcadia Formation) are tested for unconfined

compressive strength. Although the Miami Limestone is a rock, its texture does not lend itself to typical rock coring and the use of SPT to sample this formation is common in South Florida.

Results of the unconfined strength tests performed on 31 samples from the Key Largo Limestone, 46 samples from the Fort Thompson Formation, and three samples from the Arcadia Formation are summarized on [Table 2.5.4-207](#) and shown on [Figure 2.5.4-217](#).

2.5.4.2.1.3.11 Elastic Modulus and Shear Modulus (High Strain)

Elastic Modulus

For fine-grained soils, the high strain (static) elastic modulus (E or E_H) is evaluated using the following relationship ([Reference 224](#)):

$$E = 600 s_u \quad \text{Equation 2.5.4-5}$$

Where,

s_u = undrained shear strength

E for fine-grained soils can also be evaluated using the following equations ([Reference 225](#)):

$$E = 2 G (1 + \mu) \quad \text{Equation 2.5.4-6}$$

$$G_{0.0001\%} = \gamma/g (V_s)^2 \quad \text{Equation 2.5.4-7}$$

Where,

E = static (or high strain) elastic modulus

μ = Poisson's ratio

γ = total unit weight of soil

g = acceleration of gravity = 32.2 feet/second/second

V_s = shear wave velocity

G = static (or high strain) shear modulus

$G_{0.0001\%} = G_L$ = small strain shear modulus (i.e., strain in the range of 10^{-4} percent)

Relationships between high and low strain modulus are given in [Reference 226](#). High strain in this reference is typically taken as 0.25 percent to 0.5 percent. Shear modulus reduction curves can also be used, where available ([Subsection 2.5.4.2.1.3.16](#)).

For coarse-grained soils, E is evaluated using the following relationship ([Reference 224](#)):

$$E = 36 N \text{ (in ksf)} \quad \text{Equation 2.5.4-8}$$

Where,

N = average energy-corrected SPT blow count

Similarly to fine-grained soils, a second relationship pertaining to E for coarse-grained soils can also be evaluated using Equations 2.5.4-6 and 2.5.4-7, and the relationships between high and low strain modulus given in [Reference 226](#). Again, shear modulus reduction curves, where available, can be used to compute the high strain modulus.

[Table 2.5.4-209](#) gives high strain E values for each stratum, derived, in part, from s_u (Stratum 6), N_{60} (Strata 5 and 7), V_s (all strata).

Low strain modulus values are described further in [Subsection 2.5.4.2.1.3.15](#).

Shear Modulus and Poisson's Ratio

Shear modulus, G, is related to elastic modulus, E, as follows ([Reference 225](#)):

$$G = E / (2 [1 + \mu]) \quad \text{Equation 2.5.4-9}$$

with the terms as defined before.

Values of G for each stratum are calculated from the E values recommended for use in [Table 2.5.4-209](#). Poisson's ratio values of 0.37, 0.31, and 0.34 are used for rock strata (Strata 2, 3, and 4, respectively), and a Poisson's ratio of 0.35 is used for soil strata (Strata 5, 6, and 7). However, the saturated sand strata will have a higher Poisson's ratio (approaching 0.5) as indicated by the geophysical testing. A Poisson's ratio of 0.36 is recommended for Stratum 8. The resulting high strain G values are given in [Table 2.5.4-209](#) for the power block areas.

Typically, sound rock and even moderately weathered rock exhibit an elastic response to loading with little change, if any, in stiffness properties. For rocks, the elastic and shear modulus values generally remain constant at both small and large strains. Using Equations 2.5.4-6 and 2.5.4-5, E and G (same for high and low strain) can be computed from the shear wave velocities for the Key Largo Limestone and Fort Thompson and Arcadia Formations, see [Table 2.5.4-209](#).

However, at some stage of weathering, rock becomes sufficiently decomposed to exhibit modulus reduction. The Miami Limestone layer is considered to fall into a sufficiently weathered state for its modulus values to become strain dependent.

Note that the results of laboratory elastic modulus testing performed on one sample of the Key Largo Limestone and one sample of the Fort Thompson Formation are compared to the E and G values derived based on the average shear wave velocities measured, and they indicate E = 2700 kips per square inch (ksi) for the Key Largo Limestone and E = 2900 ksi for the Fort Thompson sample. The shear and elastic modulus values based on shear wave velocity are considered more representative because the laboratory results are derived from samples with higher than average RQD.

2.5.4.2.1.3.12 Static Earth Pressure Coefficients

Active, passive, and at-rest static earth pressure coefficients, K_a , K_p , and K_0 , are estimated assuming frictionless vertical walls and horizontal backfill using Rankine's theory, and are based on the following relationships ([Reference 225](#)):

$$K_a = \tan^2 (45 - \phi'/2) \quad \text{Equation 2.5.4-10}$$

$$K_p = \tan^2 (45 + \phi'/2) \quad \text{Equation 2.5.4-11}$$

$$K_0 = 1 - \sin (\phi') \quad \text{Equation 2.5.4-12}$$

Where,

ϕ' = drained/effective friction angle of the soil

Calculated static earth pressure coefficients are given in [Table 2.5.4-209](#).

Foundations are not constructed at depths below the Fort Thompson Formation (Stratum 4). Thus, earth pressure coefficients are not calculated below this stratum.

Coefficients used for seismic lateral earth pressure calculations are described in [Subsection 2.5.4.10.4.2](#).

2.5.4.2.1.3.13 Coefficient of Sliding

The coefficient of sliding is equal to tangent δ , where δ is the friction angle between the soil and the foundation material bearing against it, in this case concrete.

Based on [Reference 223](#), tangent $\delta = 0.6$ is selected for the Miami Limestone (Stratum 2), and tangent $\delta = 0.7$ is selected for the Key Largo Limestone and Fort Thompson Formation, Strata 3 and 4, respectively. Foundations are not constructed on materials deeper than the Fort Thompson Formation, Stratum 4.

2.5.4.2.1.3.14 Shear and Compression Wave Velocity

The measurement and interpretation of shear wave velocities are addressed in [Subsections 2.5.4.4](#) and [2.5.4.7](#), respectively, and are briefly summarized here. At both Unit 6 and 7, shear and compression wave velocities are measured with P-S suspension logging in five borings for each unit ([Subsection 2.5.4.4.2.1](#)) and with downhole velocity logging at one location for each unit ([Subsection 2.5.4.4.2.2](#)). [Figure 2.5.4-218](#) is a plot of all of the measured shear wave velocities to depths of 400 and 600 feet at Unit 6 and Unit 7, respectively. [Figure 2.5.4-219](#) is a plot of all the measured compression wave velocities to the same depths. A summary of the measurements with their calculated averages is presented in [Table 2.5.4-215](#). This table summarizes the measured shear and compressive wave velocities using P-S suspension logging with the average and standard deviation for each 10-foot interval investigated to a maximum depth of 610 feet. (El. -611 feet). The recommended values of shear wave velocity are shown versus depth in [Figure 2.5.4-220](#). A description of the data in these plots is given in [Subsection 2.5.4.7](#).

[Table 2.5.4-209](#) provides recommended shear wave velocity values for each stratum investigated.

2.5.4.2.1.3.15 Elastic Modulus and Shear Modulus (Low Strain)

The low strain shear modulus (G_L , normally assumed to be the shear modulus at 10^{-4} percent shear strain) is derived directly from the shear wave velocity using Equation 2.5.4-7. The value of low strain shear modulus for each stratum shown for the power block in [Table 2.5.4-209](#) is derived from the recommended shear wave velocity value (shown in [Table 2.5.4-209](#)). The low strain elastic modulus (E_L) is obtained from the low strain shear modulus (G_L) value using Equation 2.5.4-6 and applying the value of Poisson's ratio given in [Table 2.5.4-209](#).

2.5.4.2.1.3.16 Shear Modulus Degradation and Damping Ratio

Seven RCTS tests are performed on intact samples from Stratum 5 (upper Tamiami Formation) and Stratum 6 (lower Tamiami Formation). Each of these intact samples is from B-630, the Unit 6 boring in which thin-walled tube sampling is used as described in [Reference 257](#).

In each RCTS test, values of shear modulus (G) measured at increasing shear strain levels are obtained. These are compared to the value of G_{\max} , the shear modulus measured at 10^{-4} percent shear strain, and shown as the shear modulus degradation (ratio of G/G_{\max}) plotted against shear strain. A curve of G/G_{\max} from the literature that best fits the test data is selected. This is described further in [Subsection 2.5.4.7.3.1](#).

[Table 2.5.4-216](#) summarizes the selected values of G/G_{\max} versus shear strain for each stratum investigated. Each RCTS test also provides measured values of damping ratio (D) at increasing shear strain levels. The same procedure used for G/G_{\max} is employed to obtain a best-fit D versus shear strain curve from the literature. [Table 2.5.4-216](#) shows the selected values of D versus shear strain for each test. This is described further in [Subsection 2.5.4.7.3.2](#). RCTS test results are tabulated in Appendix F of [Reference 257](#).

2.5.4.2.1.4 Chemical Properties of Soil and Rock

An evaluation of the chemistry of the soil and rock strata is performed to consider possible corrosive effects on buried steel and aggressiveness towards buried concrete. For this evaluation, selected SPT samples are tested.

2.5.4.2.1.4.1 Laboratory Chemical Testing and Evaluation

Fifteen sets of chemical analysis, consisting of pH, chloride content, and sulfate content, are performed on samples from the power block areas. Depths range from ground surface to approximately 155 feet. Samples tested are from the Miami Limestone, Key Largo Limestone, Fort Thompson Formation, and upper Tamiami Formation. Test results are summarized in [Table 2.5.4-4.2 of Reference 257](#). As noted in [Subsection 2.5.4.5.1](#), the nuclear island is supported on lean concrete backfill and surrounded by limerock structural fill. Buried piping, duct banks, etc. are founded in limerock structural fill placed from about El. -5 feet (bottom of excavated muck) to El. +25.5 feet (final plant grade). Thus, the chemical properties of the in-situ soils discussed in the following paragraphs do not impact the nuclear island or buried utilities in the power block area.

Measured pH values range from 7.4 to 8.9, with an average of 8.4. The analytical results are indicative of mildly corrosive soils as indicated in the guidelines given in [Table 2.5.4-211](#). This table is a summary of guidelines presented in [References 227, 228, 229, and 230](#).

Measured chloride contents for the same soils are analyzed. The range for the chloride contents is from 2540 to 70,400 parts per million (ppm). These results indicate the soil is corrosive based on the [Table 2.5.4-211](#) guidelines. However, only one sample contains greater than 8830 ppm and it is a muck sample. Because this stratum is removed, the environment is considered corrosive but not as severely corrosive as indicated by the maximum measurement.

Measured sulfate contents for the same soils are analyzed. The range for the sulfate content is from 334 ppm to 7590 ppm (equivalent to 0.034 to 0.76 percent). Only one sample contains greater than 1190 ppm (0.119 percent). The sample with the highest sulfate is from the muck stratum (which is removed during construction). Thus, one sample from the muck stratum tested indicates severe aggression towards exposed concrete, but as noted above this stratum is removed. The sulfate content results from the Miami Limestone, Key Largo Limestone, Fort Thompson Formation, and upper Tamiami Formation indicate mild to moderate aggression toward concrete. Based on the guidance from applicable references summarized in [Table 2.5.4-211](#), Type II cement is considered acceptable for nonsafety-related structures that are in contact with these in-situ materials.

In addition to testing soil and rock samples for potential harmful behavior toward buried concrete and steel, selected samples are tested for calcium carbonate content to determine the degree to which the strata are primarily carbonate materials. [Table 2.5.4-210](#) summarizes the results in terms of Calcite Equivalent. The results indicate that the rock strata (Strata 2, 3, 4, and 8) generally have a higher Calcite Equivalent than the soil strata (Strata 5, 6, and 7). The differences in calcite content provide an indication that the soil strata (Strata 5, 6, and 7) underlying the upper rock strata (Strata 2, 3, and 4) are not merely decomposed rock but represent a distinctly different depositional environment. Additionally, the lower calcite composition of the soil strata indicates that the soil strata consist primarily of quartz and as such, no correction of N-values on the basis of calcium carbonate grains is warranted.

2.5.4.2.1.5 Field Testing Program

Field subsurface investigation activities were performed at the site from February 2008 through June 2008. The field testing program is addressed below in [Subsection 2.5.4.2.2](#).

2.5.4.2.1.6 Laboratory Testing Program

Laboratory tests are conducted on samples recovered during the field investigations following the retrieval of soil and rock samples.

The laboratory testing program is addressed in [Subsection 2.5.4.2.3](#).

2.5.4.2.2 Subsurface Investigation/Exploration

RG 1.132 provides guidance on conducting site investigations for nuclear power plants, and addresses the objectives of subsurface investigation with respect to the design of foundations and associated critical structures. Because subsurface investigations need to be site-specific, there is recognition in RG 1.132 that flexibility and adjustments to the overall program, applying sound engineering judgment, are necessary to tailor to site-specific conditions. Consequently, adjustments are made to the subsurface investigation (including adjustments to field testing locations and to the types, depths, and frequencies of sampling) during field operations, resulting in a more comprehensive subsurface investigation.

Subsurface investigation work at the site is performed under an approved quality assurance program with site-specific work procedures, including subsurface investigation work plans and a detailed technical specification. [Figure 2.5.4-202](#) shows the locations of field tests made for this subsurface investigation. The investigation activities at and near the site are conducted to develop a comprehensive characterization of subsurface conditions that influence the performance of safety-related structures, including the static and dynamic engineering properties of soil and rock in the site area. This subsection presents detailed descriptions of the type, quantity, extent, purpose, and results of the investigation activities at Units 6 & 7. Type, quantity, and depth of boreholes and in situ tests are selected to follow the guidance in the RG 1.132, and laboratory tests are performed to follow the guidance in RG 1.138.

Eighty-eight geotechnical borings, 22 groundwater wells, 4 cone penetrometer tests (CPTs), and 2 test pits comprise part of the subsurface investigation. The coordinates and elevations associated with each of the boring and CPT locations

are shown in [Table 2.5.4-212](#). The coordinates and elevations of the exploratory test pits are presented in [Table 2.5.4-213](#). Profile plots from site explorations are provided in [Figures 2.5.4-203](#) through [2.5.4-208](#). [Figure 2.5.4-209](#) shows the locations of these profiles. Properties of soils and rocks used in evaluations are summarized in [Table 2.5.4-209](#). The complete results of this subsurface investigation are presented in [Reference 257](#).

Eleven drill rigs and one CPT rig are used on the site. Ten drill rigs are used for SPT sampling. The types of drilling and CPT equipment used during the subsurface exploration investigation include:

- CME 45, tracked rig (1)
- CME 55, ATV and marsh buggy (2)
- CME 75, truck-mounted rig (1)
- CME 550, ATV and marsh buggy (5)
- CME 750, ATV (1)
- Gus Pech Sonic rig (not used for SPT)
- Fugro CPT rig (not used for SPT)

Due to the soft surface soil conditions, a geotextile reinforced, crushed limestone gravel roadway along the centerline of the power block provides access to the exploration locations for the site drilling equipment and support vehicles. Timber mats provide access to exploration locations away from the gravel road.

An onsite storage facility for soil sample and rock core retention is established before the start of the subsurface investigation. Each sample is logged into an inventory system, and samples removed from the facility are noted in an inventory logbook. A chain-of-custody form is also completed for all samples removed from the facility. Material storage and handling is in accordance with ASTM D 4220 ([Reference 234](#)). Complete results of this subsurface investigation are presented in [Reference 257](#). A summary of field test activities follows.

2.5.4.2.2.1 Planning the Field Testing Program

RG 1.132 provides guidance on spacing and depth of borings, sampling procedures, in situ testing procedures, and geophysical investigation methods.

This guidance is employed in preparing the technical specification for the project and addressing the bases for the site-specific subsurface investigation.

For the power block, the quantities of borings and CPTs for major structures (including Seismic Category I structures) are based on a minimum of one boring or one CPT per structure and one boring or one CPT per 10,000 square feet of structure plan area. RG 1.132 also includes a recommendation that borings for Seismic Category I structures extend to a depth approximately equal to the width of the structure below the planned foundation level. The sampling intervals employed in borings made for this subsurface investigation vary slightly from RG 1.132, but are in accordance with the technical specification, and are reasonable for characterizing site subsurface conditions.

Information from the previous Turkey Point subsurface investigation program for Units 3 & 4 ([Reference 231](#)) indicates that the site is underlain by the Miami Limestone and the Fort Thompson Formation to a depth of approximately 70 feet. Below this is the Tamiami Formation, a clayey and calcareous marl locally indurated to limestone. Based on this information, borings that extend to a depth of 125 feet are placed beneath each building. Borings beneath the reactor and other key structures are extended up to approximately 250 feet, and one boring beneath each reactor extends to at least 400 feet. The deepest boring, B-701 (DH), extends to a maximum depth of 616 feet.

2.5.4.2.2.2 Planning the Laboratory Testing Program

The laboratory testing for this site subsurface investigation is planned according to guidance provided in RG 1.138. Laboratory testing details and results are contained in [Reference 257](#).

Soil samples assigned for laboratory testing are transported by van under chain-of-custody from the onsite storage area to the testing laboratories. Geotechnical laboratory testing for this site subsurface investigation is performed at multiple laboratories including:

- MACTEC Engineering and Consulting, Inc. (MACTEC) (Atlanta, Georgia)
- MACTEC (Raleigh, North Carolina)
- Severn Trent Laboratories (STL) (part of Test America, St. Louis, Missouri)
- Fugro Consultants, Inc. (Houston, Texas)

Both the Fugro and the University of Texas–Austin laboratories perform specialty RCTS testing. Fugro also performs a consolidated-undrained triaxial test. STL performs chemical testing (pH, chloride, and sulfate). The remainder of the testing is performed by MACTEC.

2.5.4.2.2.3 Boring and Sampling

The rock core descriptions on the boring logs in [Reference 257](#) are based on the classification system commonly used in Florida. The carbonate rock encountered at the site is classified according to Dunham ([Reference 215](#)). The geologic formations encountered in the geotechnical exploration are identified in the field. This preliminary classification is later confirmed or modified by senior geologists based on examination of samples and cores, and the results of laboratory testing.

Of the 88 geotechnical borings drilled and sampled as part of the site investigations, one (B-701 DH) has a depth of 616 feet in the Unit 7 power block and one (B-601 DH) has a depth of 420 feet in the Unit 6 power block. The remaining 86 borings range in depth from 100 to 290 feet, with a median depth of approximately 125 feet. This subsurface investigation is used to obtain detailed information about the near-surface geologic characteristics and composition of sediments underlying the site.

Borings are advanced from the ground surface using mud rotary drilling techniques until encountering SPT refusal (defined as 50 blows for 0.5 feet or less of penetration) or to an approximate depth of 35 feet, whichever occurs first. SPT soil samples at these upper depths from the geotechnical borings are obtained at approximate 2.5-foot and 5-foot intervals depending on sample depth.

Once SPT refusal is encountered or an approximate depth of 35 feet is reached, a steel casing is set, and holes are advanced using triple tube wire-line rock coring equipment and procedures described in ASTM D 2113 ([Reference 232](#)). Rock coring is accomplished utilizing HQ3- or PQ3-sized core barrels with split inner-barrel liners. Three-, four-, and/or six-inch diameter casings are used to stabilize the upper portions of borings as necessary. Multiple-sized casings are typically set in borings advanced to more than 100 feet depth. Borings are advanced to a predetermined termination depth. In many of the borings, rock coring is terminated in favor of drilling and SPT sampling (at 10-foot intervals) as the subsurface materials change from the Fort Thompson Formation limestone to the upper Tamiami Formation sand. The sampling method changes at a greater depth as the stratum changes from the Peace River Formation to the Arcadia Formation, where rock coring recommences in B-701 (DH).

To collect intact samples for testing, thin-walled tube samples are collected at various depths in one boring (B-630) in general accordance with ASTM D 1587 (Reference 233). Specifically, samples are collected with Shelby tubes, Osterberg sampler, and Pitcher barrel sampler equipment. The samples are handled and transported in accordance with ASTM D 4220 (Reference 234).

All rigs utilized on this project for the collection of SPT soil samples use automatic hammers. Energy measurements, in accordance with ASTM D 4633 (Reference 235), are made on the SPT hammer-rod systems on each of the drilling rigs, as presented in Subsection 2.5.4.2.1.3.2. A summary of rig information is presented in Table 2.5.4-203.

Geotechnical field data including boring logs, core photographs, and test pit logs are included in Appendix B of Reference 257.

The groundwater levels in the borings monitored during drilling operations are generally near or above the existing ground surface. Due to the use of drilling fluid additives, the groundwater conditions observed in the geotechnical borings do not truly reflect the groundwater conditions at the project site. Reliance for determining groundwater level is placed on measurements from the observation wells, as described in Subsection 2.5.4.2.2.6.

Circulation of drill fluids is typically lost at the start of coring operations due to the porosity of the limestone formations encountered at the site. As a result, large amounts of water are used to complete the borings. In borings that terminate at depths below the limestone units, circulation of drill fluids is typically regained by advancing steel casing through the limestone formations. Standard bentonite based drilling additives are used in borings not associated with observation well clusters.

At selected locations and following review of the adjacent geotechnical borings, groundwater observation wells are installed by rotary wash drilling methods, rotosonic drilling methods, or in previously drilled PQ3 size core holes as described in Subsection 2.5.4.2.2.6. The borings not used for observation wells are filled using a cement-bentonite grout prior to demobilizing from the site.

2.5.4.2.2.4 Cone Penetration Testing

Four cone penetrometer tests (CPTs) are conducted in the unconsolidated Tamiami and Peace River Formations at the site. Two CPTs are performed in the Unit 6 power block, and two are performed in the Unit 7 power block. A purpose-built approximately 20-ton capacity track-mounted cone penetration unit is used to

perform the work. Each probe is advanced beginning at a depth of approximately 120 feet to the assigned termination depth or to cone refusal, which marks the limit of the pushing capacity of the rig. CPT soundings are initially advanced through HQ3-size core holes predrilled through the upper limestone layers to about 120-foot depth as described in Appendix B of [Reference 257](#). At one location, an ATV drill rig is used to advance casing through hard zones (El. –230 to El. –250), allowing the CPT to be performed to a depth of approximately 290 feet. Selected CPTs are also used for conducting 24 pore pressure dissipation tests. The tests are performed at varying depth intervals ranging from approximately 5 to 50 feet based on encountered stratum.

Seismic shear wave testing is attempted during the first CPT sounding at C-702. However, due to the soft surficial muck layer, it is not possible to generate a shear wave to the depth of the cone tip. CPT locations are filled using a cement-bentonite grout prior to demobilizing from the site.

Results for all CPT testing are included in Appendix C of [Reference 257](#).

2.5.4.2.2.5 Test Pits

Exploratory test pits are excavated at two locations using a rubber-tired backhoe. After removing 3 to 5 feet of muck, the test pits are excavated 2 feet into rock (Miami Limestone). The field representative selects the materials to be sampled, and a rig geologist collects the bulk samples. These bulk samples are placed in new 5-gallon plastic buckets with handles for carrying. Selected portions of the samples are tested in the laboratory for laboratory compaction, California Bearing Ratio (CBR), and Limerock Bearing Ratio (LBR) tests. The rig geologist prepares a Geotechnical Test Pit Log based on visual description of the excavated materials according to ASTM D 2488 ([Reference 214](#)). The surveyed locations of the test pits and the Geotechnical Test Pit Logs are included in Appendix B of [Reference 257](#).

2.5.4.2.2.6 Groundwater Observation Wells and Field Testing

A detailed description of groundwater well installation, observations, and testing is contained in [Subsection 2.4.12](#). A summary is given below.

2.5.4.2.2.6.1 Well Installation

Ten observation well pairs are installed within the power block and surrounding areas of the site as part of this project. With two additional deeper wells installed near well clusters 606 and 706, a total of 22 observation wells are installed during

this project. The well-construction details are shown in “Observation Well Installation Records” in Appendix G of [Reference 257](#).

The observation well depths and screen intervals are specified by a hydrogeologist after review of borehole records and geophysical logs where appropriate. Borings for the observation wells are advanced through soil using mud rotary drilling techniques with a nominal 6-inch outside diameter, and through rock using PQ3 wire-line coring techniques with a nominal 5-inch outside diameter. Borehole depths shown on the borehole logs indicate the total depth drilled and sampled. Due to small amounts of drill spoil at the base of the drill bit or due to the sampler advancing beyond the drilled depth, the total depth shown on the borehole log may be slightly greater than the well depth reported on the companion well installation record.

Upon reaching the designated depth for a well, machine-slotted PVC casing connected to solid walled PVC casing is set, and a 12/20 silica sand pack and bentonite seal placed in the wells. A cement/bentonite grout mixture is placed from the top of the bentonite seal to the ground surface in each borehole by the tremie method.

2.5.4.2.2.6.2 Water-Level Measurements

The depth to the water table in each well is measured at various times related to development, in situ testing, and water quality sampling using an electric water-level meter. Depth measurements are referenced to the marked top of the PVC casing. These measurements and initial water levels are shown on the various field forms in Appendix G of [Reference 257](#). Water levels are measured for the two deep wells, 606D and 706D, separately. Additionally, data loggers and telemetry units are installed at each of the observation well locations. Water level measurements are included in [Subsection 2.4.12](#).

2.5.4.2.2.6.3 Well Development

After well installation is complete, each well is developed using a submersible pump. A minimum of 10 saturated borehole volumes is removed from each well during the development process. During this process, the pump is cycled off and on to create a surge effect in the well. The wells are considered developed when the pumped water is relatively clear and free of suspended sediment. Field indicator parameters are measured during well development and noted on well development records. Copies of the well development records are included in Appendix G of [Reference 257](#).

2.5.4.2.2.6.4 Well Purging and Sampling

Observation wells OW-606L, OW-606U, OW-621L, OW-621U, OW-706L, OW-706U, OW-721L, OW-721U, OW-735U, OW-802U, OW-805U, and OW-809U are purged and sampled using a submersible pump. The final field-indicator parameter readings are summarized in Table 5.2 in Volume 1 of [Reference 257](#). Well sampling record sheets are included in Appendix G of [Reference 257](#).

The laboratory-provided sample containers are filled with groundwater directly from the tubing attached to the pump. The containers are placed in a cooler with ice, and the cooler is delivered by overnight courier to the Test America Laboratories, Inc., in Earth City, Missouri, under chain-of-custody. Selected samples are tested for a variety of cations and anions as shown in Table 5.3 of [Reference 257](#).

2.5.4.2.2.6.5 In Situ Hydraulic Conductivity Testing

In situ hydraulic conductivity testing is described in [Subsection 2.4.12](#).

2.5.4.2.3 Laboratory Testing

Soil laboratory testing is conducted on approximately 178 disturbed (split-spoon), 7 intact (tube), and 2 bulk samples (from test pits) obtained during the subsurface investigation. In addition, 88 selected rock core samples are tested for unconfined compressive strength, and two of these are tested with stress-strain measurements. A summary of the testing performed is provided in Table 4.3 of [Reference 257](#). The testing is performed in accordance with the current respective ASTM standards, other standards, or documented test procedures where applicable. Sampling, handling, and transportation of samples are further described in [Reference 257](#).

If the quantity of material is insufficient to perform the assigned testing, either a replacement sample is assigned or the testing is cancelled.

Because of the generally weak character of the rock, preparation of the rock cores for unconfined compressive strength testing requires special considerations. Based on initial experience with sample handling, it is observed that attempting to trim the ends and sides to meet the dimensional tolerance requirements of ASTM D 4543 ([Reference 236](#)) has a high potential risk of sample damage. The rock cores are trimmed close to the required length and then capped for testing. The actual dimensions are recorded on laboratory test forms.

Due to the fragility of the rock and the porosity of the limestone, attaching strain gages for determination of stress-strain characteristics is not possible for most samples. Of the 88 rock samples tested for compressive strength, strain gages could be attached to only two samples. Strength test results for rock cores are presented in Appendix E2 of [Reference 257](#).

Except as described in the following paragraphs, the laboratory testing is conducted in MACTEC's laboratories in Raleigh, North Carolina; Charlotte, North Carolina; and Atlanta, Georgia. Soil index tests are conducted in the Raleigh laboratory, carbonate content tests are performed in the Atlanta laboratory, and rock strength tests are conducted in the Charlotte laboratory.

Chemical testing for pH, sulfates, and chlorides on selected soil samples is performed by Severn Trent (Test America) in Earth City, Missouri. In all, 15 soil samples are identified for soil chemical testing, and a portion of each jar sample is divided and submitted to Test America for the appropriate testing.

Resonant column torsional shear (RCTS) testing of seven selected intact soil samples from B-630 is conducted by Fugro Consultants, Inc., in Houston, Texas, under the technical direction of Dr. K.H. Stokoe of the University of Texas. Intact sample tubes are X-rayed prior to testing to evaluate sample integrity.

Consolidated undrained (CU) triaxial shear testing of an intact soil sample from Boring B-630 is also performed by Fugro Consultants, Inc., in Houston, Texas.

Particle size distribution tests are performed on samples of the Miami Limestone (Stratum 2) as obtained from the test pit excavations for TP-601 and TP-701. The results of the particle size distribution tests are presented in Appendix E1 of [Reference 257](#).

The assigned tests are performed in accordance with the following ASTM standard or other procedure:

Identification Tests

- Laboratory Determination of Water (Moisture) Content of Soil and Rock by Mass — ASTM D 2216 ([Reference 237](#))
- Specific Gravity of Soil Solids by Water Pycnometer — ASTM D 854 ([Reference 238](#))

Turkey Point Units 6 & 7
COL Application
Part 2 — FSAR

- Particle-Size Analysis of Soils — ASTM D 422 (for analysis including hydrometer) ([Reference 239](#))
- Particle-Size Distribution (Gradation) of Soils Using Sieve Analysis — ASTM D 6913 (for analysis not including hydrometer) ([Reference 240](#))
- Liquid Limit, Plastic Limit, and Plasticity Index of Soils — ASTM D 4318 ([Reference 241](#))
- Moisture, Ash, and Organic Matter of Peat and Other Organic Soils — ASTM D 2974 ([Reference 242](#))
- Unit Weight (Sections 5.7-5.9, and 8.1, and Subsection 11.3.2 of ASTM D 5084) ([Reference 243](#))
- Classification of Soils for Engineering Purposes (Unified Soil Classification System) — ASTM D 2487 ([Reference 213](#))
- Description and Identification of Soils (Visual-Manual Procedure) — ASTM D 2488 ([Reference 214](#))
- Rapid Determination of Carbonate Content of Soils — ASTM D 4373 ([Reference 244](#))

Note that grain size distribution data for specimens tested in accordance with ASTM D 6913 ([Reference 240](#)) are reported to the nearest whole number, whereas those with assigned hydrometer tests performed in accordance with ASTM D 422 ([Reference 239](#)) are reported to one decimal place.

Compaction Tests

- Laboratory Compaction Characteristics of Soil Using Modified Effort — ASTM D 1557 ([Reference 245](#))
- CBR (California Bearing Ratio) of Laboratory-Compacted Soils — ASTM D 1883 ([Reference 246](#))
- LBR (Florida Lime Rock Bearing Ratio) of Laboratory-Compacted Soils — Florida Method FM-5-515 ([Reference 247](#))

Shear Strength Tests

- Unconfined Compressive Strength Testing of Intact Rock Core Samples — ASTM D 7012 ([Reference 248](#))
- Consolidated Undrained Triaxial Shear Testing of Undisturbed Soil Samples — ASTM D 4767 ([Reference 249](#))

Modulus and Damping Tests (RCTS)

- Test Procedures and Calibration Documentation Associated with the RCTS Tests at the University of Texas at Austin, and at the Furgo Laboratory: UTSD RCTS GR06-4, April 25, 2006, Geotechnical Engineering Center, University of Texas, Austin, Texas.

Chemical Testing of Soil

- pH — EPA Standard SW 846 9045C ([Reference 250](#))
- Chloride — EPA Standard Method MCAWW 300.0A ([Reference 251](#))
- Sulfate — EPA Standard Method MCAWW 300.0A ([Reference 251](#))

Reporting of Laboratory Test Data

Except for the RCTS tests, the geotechnical laboratory test reports, consisting of individual test data as required by the testing standard, are contained in Appendix E of [Reference 257](#). Summaries of the test results are shown in Tables 4.1 through 4.3 of Appendix E of [Reference 257](#).

2.5.4.3 Foundation Interfaces

PTN COL 2.5-5
PTN COL 2.5-6

Subsurface profiles depicting inferred stratigraphy at each power block are presented in [Figures 2.5.4-203 through 2.5.4-208](#). A plan showing the subsurface profile locations is provided in [Figure 2.5.4-209](#). Note that subsurface profiles shown on [Figures 2.5.4-203 through 2.5.4-205](#) illustrate typical conditions at Unit 6, and subsurface profiles shown on [Figures 2.5.4-206 through 2.5.4-208](#) illustrate typical conditions at Unit 7.

The final plant grade is shown in [Figure 2.5.4-201](#). The grade in profile is shown in [Figure 2.5.4-221](#). Seismic Category I structures bear on sub-basemat concrete placed on this stratum as described in [Subsection 2.5.4.5](#). A plan and profiles

illustrating power block foundation excavation geometries and the locations and depths of Units 6 & 7 Seismic Category I structures are shown on [Figure 2.5.4-222](#), as well as the relationship of structure foundations to the various subsurface strata. These are addressed further in [Subsection 2.5.4.5](#).

2.5.4.4 Geophysical Surveys

PTN COL 2.5-6

This subsection provides a summary of the geophysical survey methods and analysis undertaken for this subsurface investigation. Refer to [Subsection 2.5.4.7](#) for a description of selected results. Detailed descriptions of methods and results are presented in Appendix D of [Reference 257](#).

The geophysical investigation to detect possible solution features is presented in [Subsection 2.5.4.4.5](#).

Downhole geophysical testing and logging is performed in 12 borings in the power block areas: B-601(DH), B-604(DH), B-608(DH), B-610(DH), B-620(DH), B-640DHT, B-701(DH), B-704G(DH), B-708(DH), B-710G(DH), B-720G(DH), and B-740DHT. Borings designated as “G” on the boring location plan ([Figure 2.5.4-202](#)), for example “B-704G(DH),” are offset borings drilled adjacent to the original staked geotechnical boring for geophysical testing. The suite of tests listed below is performed in each boring in accordance with the procedures listed below.

Borings B-640DHT and B-740DHT are used only for downhole velocity testing. (The location designated B-640DHT is the same location that was previously used for the CPT designated as C-602A.) A downhole seismic velocity logging system is used in the two PVC cased borings to validate the suspension velocity data collected at this site. This method is described in [Subsection 2.5.4.4.2.2](#).

All the collected data are presented in Appendix D of [Reference 257](#).

2.5.4.4.1 Geophysical Borehole Logging

2.5.4.4.1.1 Natural Gamma

Gamma logs record the amount of natural gamma radiation emitted by the soil and rocks surrounding the boring. Natural gamma is recorded using two probes, one combined with the three-arm caliper and one combined with the electrical logging tool. The dual measurements provide a quality check. The natural gamma

data are qualitative and provide assistance in identifying strata changes. Natural gamma testing is performed in accordance with ASTM D 6274 ([Reference 252](#)). Natural gamma data are collected using a Model 3ACS three-leg caliper probe, serial number 5368, manufactured by Robertson Geologging, Ltd. With this tool, caliper measurements are collected concurrent with measurement of natural gamma emission from the boring walls. Natural gamma data are also collected using a Model ELXG electric log probe, *S/N* 5490, manufactured by Robertson Geologging, Ltd. This probe measures natural gamma along with Single Point Resistance (SPR), short-normal (16-inch) resistivity, long normal (64-inch) resistivity, and spontaneous potential (SP).

Natural gamma measurements rely upon trace amounts of uranium and thorium that are present in potassium-bearing minerals such as feldspar, mica, and clays that contain a radioactive isotope of potassium. The measurement is useful because the radioactive elements are concentrated in certain soil and rock types (e.g., clay or shale) and depleted in others (e.g., sandstone or coal).

Measurements follow ASTM D 6167 ([Reference 253](#)). No analysis is required with the natural gamma logs; however, depths to identifiable boring features are compared to verify compatible depth readings on all logs. Natural gamma data are collected using both the caliper probe system as well as with the ELOG probe. A comparison between the two data sets provides an almost exact match, verifying the performance of the natural gamma measuring systems.

2.5.4.4.1.2 Long and Short Normal Resistivity/Spontaneous Potential

Normal-resistivity logs record the electrical resistivity of the borehole environment and surrounding soil and water as measured by variably spaced potential electrodes on the logging probe. Spacing for potential electrodes is 16 inches for short-normal resistivity and 64 inches for long normal resistivity. Normal resistivity logs are affected by bed thickness, borehole diameter, and borehole fluid, and can only be collected in water or mud filled open holes. Long and short-normal resistivity/spontaneous potential testing are performed in accordance with ASTM D 5753 ([Reference 254](#)).

No analysis is required with the resistivity or spontaneous potential data; however, depths to identifiable boring features are compared to verify compatible depth readings in all logs. Using Robertson Geologging Winlogger software version 1.5, build 4011, these data are combined with the caliper and natural gamma logs and converted to LAS 2.0 and PDF formats.

These electrical methods provide poor demarcation of different lithologic units at this site due to the influence of saltwater intrusion. Several of the borings exhibit artesian flow, and the composition of the boring fluid changed significantly during the collection of field data, with the drilling mud being displaced by clear water. The electrical data are not valid above a depth of 40 feet because the upper yoke electrode moves out of the boring fluid at that depth. There may also be differences in the electrical data at the same depth from different logging runs due to changes in the salinity of the boring fluid. In addition, the upper 40 feet of many of the deeper logs are affected by the movement of the yoke electrode into the steel surface casing.

2.5.4.4.1.3 Three-Arm Caliper

Caliper logs record borehole diameter with depth. Changes in borehole diameter are related to boring construction, such as casing or drilling bit size, and to fracturing or caving along the borehole wall. Because borehole diameter commonly affects log response, the caliper log can be useful in the analysis of other geophysical logs. Caliper with gamma logging is used to assist in the identification of strata changes. Three-Arm Caliper testing is performed in accordance with ASTM D 6167 ([Reference 253](#)).

Caliper data are collected using a Model 3ACS three-leg caliper probe, serial number 5368, manufactured by Robertson Geologging, Ltd. With the short arm configuration used in these surveys, the probe permits measurement of boring diameters between 1.6 and 16 inches. With this tool, caliper measurements are collected concurrently with measurements of natural gamma emissions from the boring walls.

No analysis is required with the caliper; however, depths to identifiable boring features are compared to verify compatible depth readings on all logs. Using Robertson Geologging Winlogger software version 1.5, build 4011, these data are combined with the resistivity, natural gamma, and spontaneous potential (SP) logs and converted to LAS 2.0 and PDF formats.

The caliper logs for these borings generally show diameters of less than 6 inches below 30 feet. There may be differences in the boring diameters at the same depth from different logging runs due to reaming of the boring, or erosion by the drilling fluid between logging runs.

2.5.4.4.2 Shear Wave Velocity Measurements

2.5.4.4.2.1 Suspension P-S Velocity Logging

Suspension P-S velocity logging is conducted in accordance with GEOVision procedure for OYO P-S Suspension Seismic Velocity Logging, Rev. 1.31. Measurements of compression (P) and shear (S_H) wave velocity are made at 1.6-foot intervals.

Suspension velocity measurements are performed in 10 uncased nominal 3.88- to 5.0-inch diameter borings using the suspension P-S logging system, manufactured by OYO Corporation, and their subsidiary, Robertson Geologging. Components used for these measurements are listed in Appendix D of [Reference 257](#). This system directly determines the average velocity of a 3.3-foot-high segment of the soil column surrounding the boring of interest by measuring the elapsed time between arrivals of a wave propagating upward through the soil column. The receivers that detect the wave, and the source that generates the wave, are moved as a unit in the boring producing relatively constant amplitude signals at all depths.

An ASTM standard is not available for the suspension P-S velocity logging method; therefore, measurements follow the “GEOVision Procedure for P-S Suspension Seismic Velocity Logging,” as presented in Appendix D of [Reference 257](#) and summarized below.

Ten borings are filled with bentonite or polymer based drilling mud. Four- or six-inch diameter steel surface casing is used to maintain an open hole through loose soils, necessitating multiple logging runs to access different portions of the borings. Using the proprietary OYO program PSLOG.EXE version 1.0, the recorded digital waveforms are analyzed to locate the most prominent first minima, first maxima, or first break on the vertical axis records, indicating the arrival of P-wave energy. The difference in travel time between receiver 1 and receiver 2 arrivals is used to calculate the P-wave velocity for the 3-foot segment of the soil column. The recorded digital waveforms are analyzed to locate clear S_H -wave (horizontal shear wave) pulses.

The P-wave and S_H -wave velocities are also calculated and plotted from the travel time over the 6.3-foot interval from source to receiver.

The borings at this site are well suited for collection of suspension P-S velocity data, although there are some regions prone to squeezing and washouts, particularly just below the upper limestone layer, between depths of approximately

115 and 120 feet. All of these data show excellent correlation between source and receiver data, as well as excellent correlation between P-wave and S_H -wave velocities. P-wave and S_H -wave onsets are very clear, and later oscillations are well damped. There is variation between the profiles from all these borings above 115 feet depth, due to different degrees of degradation of the limestone, but the general velocity trends are similar. Below 115 feet, the profiles are very similar, with slight variation of the harder layers between 120 to 150 feet and 210 to 260 feet depth.

Figure 2.5.4-218 shows the measured shear wave velocity profile (receiver to receiver), and Figure 2.5.4-219 shows the corresponding compression wave velocity profile. Subsection 2.5.4.7 contains a description of results.

2.5.4.4.2.2 Downhole Velocity Logging

Downhole velocity logging to measure shear wave velocity is performed in B-640(DHT) and B-740(DHT) using methods described in “GeoVision Procedure for Downhole Seismic Velocity Logging,” as presented in Appendix D of Reference 257. (An ASTM standard is not available for the downhole velocity logging method.) The tests are performed to provide a second method of shear wave velocity measurement to compare to the P-S suspension logging results. Downhole velocity testing is conducted in a borehole that has PVC casing installed with a grouted annulus. Logging was planned to be conducted to 150 feet bgs; however, in B-640DHT, curvature of the installed casing prevented passage of the probe beyond approximately 125 feet. The lesser depth is determined acceptable.

There are consistent waveforms between adjacent depth stations, and good consistency in the relationship between P- and S_H -waves. Also there is good consistency between profiles of adjacent borings. P-wave velocities in the fast layer are slower than measured by the suspension method. In order to properly image this fast layer, higher frequency waves are needed from the source. However, these are filtered out by the fill layer at the top of the borehole. Except for the layers near the surface, comparison with suspension velocities is within 10 percent.

Subsection 2.5.4.7 contains a description of results.

2.5.4.4.3 Borehole Acoustic Televiewer Logging

Acoustic image and boring deviation data are collected using a High Resolution Acoustic Televiewer probe (HiRAT), serial number 5174, manufactured by

Robertson Geologging, Ltd. The probe is 7.58 feet long, and 1.9 inches in diameter, and is fitted with upper and lower fourband centralizers.

This system produces images of the boring wall based upon the amplitude and travel time of an ultrasonic beam reflected from the formation wall.

The acoustic televiewer data quality in all 10 borings are very good, providing clear images of a number of vugs and eroded zones. Many of the borings exhibit diagonal banding (zebra striping) caused by rapid reaming down the boring with new core bits. This alters the characteristic smooth surface of diamond cored borings. This wear pattern can have a significant impact on acoustic televiewer image quality, and in these borings may conceal small dikes, but does not conceal fractures. No large vugs or cavities are observed in the logs. Location of vuggy and weathered zones on the televiewer logs correspond with increases in caliper log diameter and suspension P-S velocity drops.

2.5.4.4.4 S-Wave and P-Wave Velocity Profile Selection

Suspension P-S velocity logging results summarized in [Table 2.5.4-215](#) are used to develop the recommended V_s velocity profiles shown in [Figure 2.5.4-220](#). The data collected at individual suspension P-S velocity logging borings and at individual seismic CPTs are sorted by stratum and averaged, and presented in [Table 2.5.4-209](#). In this table, the measured V_c values in the saturated sand strata (Strata 5, 6, and 7) are adjusted to account for the high readings due to measuring the V_c of water. The average thickness and elevation of each stratum is also determined at each of the boring test locations, and averaged. The V_s profiles given in [Figure 2.5.4-218](#) plot measured shear wave versus depth, and indicate strata thicknesses and depths. [Figure 2.5.4-220](#) illustrates the design V_s profile (average) for materials at the site from ground surface to approximately 600 feet depth. As previously noted, Unit 7 V_s data are collected to a depth of approximately 600 feet, while at Unit 6 V_s data are collected to a depth of approximately 400 feet.

2.5.4.4.5 Geophysical Exploration for Possible Dissolution Features

An integrated geophysical survey that focused on the Units 6 & 7 power block area was conducted to evaluate the potential for carbonate dissolution features, including sinkholes, at the site (see [Subsections 2.5.1.1.1.1.1](#) and [2.5.1.2.4](#) for a discussion of the types of sinkholes occurring in Florida). The geophysical survey encompasses an approximately 39-acre area of the site. The survey consists of 11 survey lines that covered over 12,000 linear feet ([Figure 2.5.4-223](#)). Lines 1

Turkey Point Units 6 & 7
COL Application
Part 2 — FSAR

through 7 extend through and beyond the locations of Category 1 structures associated with Units 6 & 7. Lines 8 through 11 were added during the investigation to further characterize geophysical anomalies located near surface depressions that were filled with water and/or vegetation. Each survey line is composed of stations spaced 20 feet apart. Each station is located horizontally using a Trimble Ag-132 differential GPS with an accuracy of three feet and referenced in feet from the southernmost or westernmost end of the corresponding survey line. The horizontal coordinates are in Florida State Plane East using the North American Datum of 1983 (NAD 83). Elevations for each station were subsequently obtained using a Topcon DL-102 digital level, and tied to an existing benchmark. The elevations are relative to the North American Vertical Datum of 1988 (NAVD 88) and have a loop closure accuracy within 0.06 feet per linear mile.

The investigation consists of three non-invasive geophysical techniques:

- Microgravity to develop profiles that identify lateral variation in subsurface density caused by paleosinkholes, variations in the top of rock, and/or weak zones that may contain cavities.
- Seismic refraction to develop compression wave velocity cross sections that aid in delineating stratigraphic variations in the subsurface and soft zones conducive to the development of karst features.
- Multi-channel analysis of surface waves (MASW) to develop shear-wave velocity cross sections that delineate the top of rock and identify weak zones within the rock.

2.5.4.4.5.1 Microgravity Survey

At least one microgravity measurement is taken at each station along the 11 survey lines using a gravimeter (excluding stations between 500 and 640 along Line 2 where a data gap exists due to localized flooding). Measurements are made at a base station at the start and end of each day to allow corrections related to instrument drift to be made to the survey data. After corrections for other factors (e.g., tide, latitude, free air, and gravimeter height) are applied to the measured gravity data, a planar trend representing the background gravity at the site is subtracted from the Bouguer values to obtain the residual gravity value for each station.

The magnitude of gravity anomalies at the site is dependent on the depth, size, and density contrast of a subsurface feature. Subsurface density variations must be large enough or shallow enough to produce an anomaly above the noise threshold. With repeated measurements at 22 percent (135) of the stations at the site showing an average deviation of approximately ± 3 microgals (μGals), anomalies $\geq 10 \mu\text{Gals}$ should be routinely detectable. [Figure 2.5.4-224](#) shows the magnitude of a low gravity anomaly as a function of depth for the case of various size water-filled spherical cavities in limestone. [Figure 2.5.4-224](#) also illustrates what the measured gravity anomaly would look like for selected diameters and depths. As the figure shows, an isolated spherical void 25 feet in diameter or larger would theoretically be detectable if centered within the Key Largo Limestone at a depth of 40 feet. In general, subsurface structures approximated as spherical in shape can be detected at a depth to their center of approximately two times their effective diameter at the $10 \mu\text{Gal}$ detection threshold. However, if a spherical void were to develop due to dissolution in limestone, it would need to have at least one input and one output tunnel. Thus, it is appropriate to use a more geologically plausible water-filled horizontal conduit scenario, such as the one shown in [Figure 2.5.4-225](#), to guide interpretation when characterizing low density karst features at the site. [Figure 2.5.4-225](#) indicates that a water-filled horizontal conduit 10 feet in diameter would theoretically be near the conservatively chosen detection threshold of $-10 \mu\text{Gals}$ if centered within the Key Largo Limestone at a depth of 40 feet. The magnitude of such a low gravity anomaly would in reality likely be larger for a given diameter due to the dissolution of fracture zones and bedding planes above such a conduit. Therefore, low-density features with a large lateral extent should be detectable at depths of up to 5 to 10 times their thickness at the site. Both [Figure 2.5.4-224](#) and [Figure 2.5.4-225](#) illustrate that for a gravity anomaly of a particular size and density contrast, as the depth to the center of the anomaly increases, the overall magnitude measured at the ground surface will decrease and the width of the anomaly when shown in profile view will increase ([Reference 257](#)).

The microgravity profiles for Line 5 and Line 9 are included in [Figures 2.5.4-226](#) and [2.5.4-227](#), respectively. For the overall residual gravity dataset, the median value is $0 \mu\text{Gals}$ with individual measurements ranging from $-108 \mu\text{Gals}$ to $+37 \mu\text{Gals}$. Those segments of each profile that are $10 \mu\text{Gals}$ or more below the median value are shaded blue and delineate low-density zones in the subsurface that have the potential to correlate with karst features. [Figure 2.5.4-228](#) depicts the microgravity data contoured across the survey area to assess spatial trends in the data. Comparison of [Figure 2.5.4-223](#) to [Figure 2.5.4-228](#) illustrates that the

three largest (both in magnitude and lateral extent) low gravity anomalies at the site are centered on the surface depressions containing vegetation.

2.5.4.4.5.2 Seismic Refraction Survey

For the seismic refraction survey conducted at the site, compression waves (P-waves) are produced at the ground surface by striking an aluminum plate with a sledgehammer. The P-waves transmitted through the soil and rock are recorded by 24 geophones pushed down into the ground surface at known distances from where the waves were generated. A seismograph is used to record the travel-times of the first arriving energy, from which P-wave velocities were derived.

The maximum depth to which a seismic refraction survey is effective is controlled by a number of factors, including the geophone spread length, the shot offset distance, the P-wave velocity contrast between geologic layers, the thickness of individual layers, and the assumption that velocity increases with depth. Spacing between geophones in each seismic array is 10 feet, resulting in a total spread length of 230 feet. In general, P-waves are generated at five locations for each spread, consisting of shots located in the center, at 20 feet from each end, and at 100 feet from each end of the spreads. The seismic arrays are moved down the survey lines at 200-foot increments, thus providing 30 feet of overlap between spreads. For this survey, the overriding limiting factor on the depth of the investigation is a velocity inversion occurring at an elevation of approximately –50 feet at the interface between the Key Largo Limestone and the Fort Thompson Formation.

Two-dimensional cross sections are developed by processing the seismic refraction data that model P-wave velocity along each survey line. The P-wave models for Line 5 and Line 9 are included in [Figures 2.5.4-226](#) and [2.5.4-227](#), respectively. Each cross section contains the modeled average P-wave velocity contour for the contact between the muck and Miami Limestone (4280 feet/second) and for the contact between the Miami Limestone and Key Largo Limestone (9570 feet/second). Existing borings located on or near each survey line along with the elevation of subsurface contacts derived from the corresponding boring logs are shown on each P-wave velocity model for comparison. Because seismic P-wave velocities are affected by the presence of the water table, which is close to ground surface at the site, the estimated elevation of the muck/Miami Limestone contact is likely better estimated from the average shear wave (S-wave) velocity contour derived from MASW data collected at the site ([Subsection 2.5.4.4.5.3](#)). Vertical resolution of seismic refraction data is a complex function of the geophone spacing, the depth to subsurface refractors,

the seismic velocity contrasts, and site-specific near surface conditions (Reference 255). For this survey, vertical resolution is approximately 20 percent. Thus, if a subsurface feature such as a void existed at a depth of 30 feet at the site, it would be averaged over a thickness of about six feet in the P-wave velocity models. Lateral resolution of a seismic refraction survey is dependent upon geophone spacing and shot-point spacing. For this survey, lateral resolution falls in the range of one to two geophone spacings (10 to 20 feet), with a conservative estimate being 20 feet (Reference 280).

2.5.4.4.5.3 MASW Survey

This technique utilizes seismic noise generated at the ground surface by striking an aluminum plate with a sledgehammer. This action produces Raleigh surface waves, along with other types of seismic waves. Raleigh waves have velocities that depend on their wavelength, with short wavelengths (high frequencies) sampling shallow depths and long wavelengths (low frequencies) sampling to greater depths. Data are collected along each of the 11 survey lines, with a data gap existing along Line 2 between stations 460 and 640 due to localized flooding. Data are recorded using a seismograph and 24 geophones with an inter-geophone spacing of four feet, resulting in a total length of 92 feet for each geophone spread. The 24 geophones are mounted in a land-streamer configuration that allows the 92-foot spread to be pulled from one measurement location to another using a tracked vehicle. Measurements are made at intervals of 20 feet along each of the survey lines. A constant 12-foot distance is maintained between the sledgehammer shot point and the first geophone in each spread during testing.

As Raleigh waves propagate outward along the ground surface at the site, they undergo dispersion due to heterogeneous conditions within the subsurface. After the data are collected, dispersion curves showing the velocity of the surface waves as a function of frequency are calculated from the data. By applying the ratio of Raleigh wave velocity to S-wave velocity (approximately 0.9 to 1) to these calculated dispersion curves, S-wave velocity is estimated. Dispersion curves are manually selected for input into an inversion program by analyzing the phase-velocity power spectra of the surface waves. Shot point records that do not yield coherent dispersion curves are discarded. The resulting one-dimensional models from multiple locations along a survey line are combined and contoured to produce two-dimensional cross sections of S-wave velocity along the 11 survey lines. The S-wave model for Line 5 and Line 9 are included in Figures 2.5.4-226 and 2.5.4-227, respectively. Each cross section contains the modeled average S-wave velocity contour for the contact between the muck and Miami Limestone

(440 feet/second) and for the contact between the Miami Limestone and Key Largo Limestone (3660 feet/second). Existing borings located on or near each survey line along with the elevation of subsurface contacts shown on the corresponding boring logs are provided on the cross sections for comparison. For sites with high S-wave velocity disparities in the subsurface at shallow depths, such as that which exists between the muck and underlying limestone, MASW surveys may not succeed in accurately capturing the absolute S-wave velocity of the rock. While S-wave velocities for limestone in the models are likely underestimated, the modeled depths to limestone as well as the relative changes in velocity within the limestone are considered to be valid.

As indicated above, the depth of investigation for a MASW survey is primarily controlled by the frequency of the surface waves. Because the amplitude of surface waves decreases exponentially with depth, heavier (lower frequency) sources are necessary to penetrate deeper. Due to the relatively high frequencies produced in the soft muck by sledgehammer impacts during the site survey, interpretation of subsurface conditions using the resulting S-wave velocity models should be restricted to shallow depths. While the velocity models show S-wave velocity data down to El. -50 feet at the site, the models should be constrained to the uppermost 35 feet. Vertical resolution of the MASW data is around 20 percent of the depth. Thus, if a subsurface feature such as a void exists at a depth of 30 feet at the site, it would be averaged over a thickness of about six feet in the S-wave velocity models. Because lateral resolution for MASW is approximately 25 percent of the total seismic array length, lateral variations in the subsurface are averaged over a length of approximately 23 feet for this survey. Studies comparing MASW measurements to borehole measurements indicate that MASW velocity models are typically accurate to within 15 percent of actual values.

2.5.4.4.5.4 Results

A comparison of [Figures 2.5.4-223](#) to [2.5.4-228](#) indicates that the three largest low gravity anomalies, both in magnitude and lateral extent, are centered on the surface depressions containing vegetation located outside the Units 6 & 7 power block areas. The gravitational response to subsurface density variations was modeled along Line 9 to assess the potential subsurface causes for the microgravity lows associated with the vegetation filled surface depressions ([Figure 2.5.4-229](#)). This model is calculated based on the estimated wet density values for the subsurface strata shown in the table below combined with stratigraphic boundaries estimated from the corresponding S-wave and P-wave velocity models ([Figure 2.5.4-227](#)).

Turkey Point Units 6 & 7
COL Application
Part 2 — FSAR

Material	Wet Density (g/cc)	Reference
Water	1.0	Telford et al. (Reference 278)
Muck	1.1 – 1.3	Measured from onsite samples
Miami Limestone	2.0	Telford et al. (Reference 278)
Key Largo Formation	2.2	<i>Geotechnical Exploration and Testing in Reference 257</i>

The model shows that a thick zone of muck centered within the surface depressions containing vegetation traversed by Line 9 is responsible for approximately 60 percent of the large microgravity low. The other 40 percent of the anomaly is most likely the result of a lower density zone in the upper Miami Limestone coupled with deeper and/or softer Key Largo Limestone in this area.

Significantly smaller magnitude microgravity lows are present at a number of locations outside the surface depressions containing vegetation at the site, such as the –20 μGal anomaly found between stations 400 and 500 along survey Line 5 (Figures 2.5.4-226 and 2.5.4-228). A model of the gravitational response to subsurface density variations is produced for this anomaly using the same methodology discussed above (Figure 2.5.4-230). The model indicates that this small magnitude low-gravity anomaly is caused by a wedge of soft Miami Limestone with a bulk density 0.2 to 0.3 grams per cubic centimeter (g/cc) lower than the surrounding Miami Limestone. This model correlates well with data collected from boring B-728, where SPT sample refusal occurred at El. –28.7 feet as compared to El. –18.1 feet for nearby boring B-710.

The gravitational effects due to thickness variations of the muck across the site are stripped from the residual gravity dataset using the following approximation from Telford et al. (Reference 278):

$$\Delta g = (12.77) \Delta \rho D \quad \text{Equation 2.5.4-13}$$

Where,

Δg = gravity anomaly in μGals

$\Delta \rho$ = density contrast (–0.7 g/cc) between the muck and underlying limestone

D = thickness of the muck (estimated from MASW data)

Figure 2.5.4-231 shows a contour map of microgravity at the site with residual gravity values corrected for muck thickness variations using the relationship defined above. Once this muck thickness correction is applied to the microgravity

dataset for the site, all low gravity anomalies can be explained by softer zones within the Miami Limestone having a density 0.2 to 0.3 g/cc lower than 2.0 g/cc. This statement is supported by an evaluation of the magnitude and width of low gravity anomalies (excluding those found on and around the surface depressions filled with vegetation) at the site, which are conducive to soft zones in the Miami Limestone. It is also supported by SPT N-values obtained within the Miami Limestone across the site, which indicate the presence of very soft to hard soils. Existing borings associated with low gravity anomalies generally have lower SPT N-values when compared to SPT N-values from borings associated with relatively higher microgravity values.

2.5.4.4.5.5 Summary and Commitment

Based on geophysical site characterization data, there is no apparent indication that sinkhole hazards exist at the site. There is also no apparent evidence for the presence of underground openings within the survey area that could result in surface collapse. Large low gravity anomalies with magnitudes less than $-30 \mu\text{Gals}$ are only detected outside the power block areas, primarily in areas associated with surface depressions containing vegetation. Once the effects of variations in muck thickness are removed from the residual gravity data, all the remaining low gravity anomalies can be explained by density variations within the Miami Limestone. The results of the drilling program and borehole geophysical data (Subsections 2.5.1.2.4 and 2.5.4.1.2.1) indicate the existence of two preferential secondary porosity flow zones. The extent of rod drops in six of the 88 borings (approximately 9000 feet of rock cores) integrated with the field geophysical data supports the interpretation that large voids are absent beneath the footprints of the Units 6 & 7 nuclear islands. However, considering the uncertainties related to resolution in the geophysical data at depth and away from survey lines, a microgravity survey will be performed on the excavation surface to detect the presence, or verify the absence, of potential water-filled dissolution features beneath the power block. The microgravity survey will be designed to detect 25-foot diameter spherical voids and cylindrical voids as small as 12 feet in diameter at the base of the 25-foot-thick grout plug at an elevation of approximately -60 feet NAVD 88. If present, microgravity anomalies may be further investigated by drilling and sampling to determine their origin.

Turkey Point Units 6 & 7
COL Application
Part 2 — FSAR

PTN COL 2.5-7

2.5.4.5 Excavations and Backfill

PTN COL 2.5-13

2.5.4.5.1 Source and Quantity of Backfill and Borrow

Significant earthwork is required to establish finish grades at the Units 6 & 7 project area, especially to raise the power block to finish grade (as high as El. +25.5 feet at the center of the power block area) and to provide for backfilling around the embedded major power block structures including Seismic Category I structures. The grade change is achieved by constructing a mechanically stabilized earth (MSE) retaining wall around the perimeter of the plant area. The MSE wall will be constructed around the perimeter of the Units 6 & 7 plant area, excluding the south side of the plant area where the makeup water reservoir would provide the plant area exterior wall. The construction of the MSE wall will be standard for this type of retaining wall, with successive lifts of compacted, controlled fill reinforced with either strip- or grid-type reinforcement between lifts. The finished height of the MSE wall will range from 20 to 21.5 feet. From the MSE wall, the finished grade would slope upward for some distance towards Units 6 & 7 to an elevation approximately 5 feet higher than the top of the retaining wall. Modular facing panels will form the outside face of the MSE wall. The MSE wall will be designed to retain the soil mass and resist loading resulting from the probable maximum hurricane.

The deepest excavation is approximately El. –35 feet. Structural fill is placed around but not below the power block structures extending to as deep as El. –14 feet. Lean concrete fill is placed between El. –14 feet and the bottom of excavation. The final grade is shown on [Figure 2.5.4-201](#). The grade in profile is shown in [Figure 2.5.4-221](#).

2.5.4.5.1.1 Replacement of Stratum 1 with Compacted Limerock Fill

Due to the poor soil properties of Stratum 1 (muck), Stratum 1 is removed in its entirety prior to commencing the major earthwork and grading operations. After removing the muck, the grade is raised to approximately El. +0 feet through placement and compaction of Miami Limestone fill material and limerock material from other sources.

The evaluation of the Miami Limestone (Stratum 2) for construction purposes involves the excavation of two exploratory test pits at the power block, located as shown on [Figure 2.5.4-202](#). The maximum depth of each test pit is 5 feet bgs. The results of laboratory testing on bulk samples collected from the test pits for moisture-density (modified Proctor compaction), CBR, and LBR are summarized in [Table 2.5.4-214](#). These tests show that, when excavated with construction

equipment and not crushed, Miami Limestone-derived materials are gravel-sand mixtures with fines contents of 12 percent to 17 percent. The grain size distribution of actual fill material is expected to vary based on the degree of cementation of the native material in excavated areas and the methods of excavation, handling, and crushing (if performed).

The most likely offsite structural fill sources are identified, as follows:

- SDI Quarry (Florida City, Florida)
- CEMEX/Florida Rock (Card Sound Road, Homestead, Florida)
- White Rock South (Miami, Florida)

Each of these sources, as well as onsite material excavated from the power block excavations, offers Miami Limestone (Stratum 2) material and other limestone-derived materials in granular form. This material is locally known as limerock. Limerock can be graded into a variety of grain size distributions ranging from gravel to sand-sized particles.

The results of laboratory index tests (natural moisture content, gradation), chemical tests (pH, sulphate content, chloride content), moisture-density relationship tests (modified Proctor compaction), and strength tests (LBR and CBR) for these materials are contained in Appendix E.1 of [Reference 257](#). Once the final backfill source(s) for structural fill is determined, additional material testing is required to verify the design properties.

2.5.4.5.1.2 Power Block and Site Grade Raising

Approximately 10 million cubic yards of structural fill are required to fill the site to finish grade. The fill material is from identified offsite sources as well as the power block excavation for each unit.

Power block area materials excavated during site grading consist of fill material derived from onsite and local limerock sources with the proposed sources identified in [Subsection 2.5.4.5.1.1](#).

Structural fill consisting of excavated fill material is placed around but not below any nuclear island structure. Replacement material below the nuclear islands consists of lean concrete fill. The selection of lean concrete mix design is made at project detailed design. The compressive strength of 1.5 ksi is estimated for lean concrete fill.

DCD Subsection 2.5.4.1.3 requires that the compressive strength of the mudmat (located beneath the NI foundation) have a minimum compressive strength of 2500 psi. The mudmat used at this site consists of approximately 1-foot-thick upper and lower concrete layers with waterproofing membrane sandwiched between them. The mudmat will be approximately 2 feet thick from El. –16 to El. –14 NAVD 88. The 1500 psi lean concrete fill is placed directly beneath the mudmat from El. –35 to El. –16 and is used for filling purposes to replace in situ limestone material with best estimate unconfined compressive strengths of 200 and 1500 psi, as noted in Table 2.5.4-209. It provides a uniform base with well-defined material properties.

The lower strength of 1500 psi for the concrete fill will require less cement and thus reduce the heat of hydration found in stronger mixes. Uncontrolled heat of hydration is the cause of thermal cracking and thus minimizing the heat of hydration for this mass concrete will reduce the possibility of such cracking. ACI 207 (Reference 281) will be used for guidance in developing a thermal control plan to reduce thermal cracking of the lean concrete as noted in Subsection 2.5.4.12.

2.5.4.5.1.3 Makeup Water Reservoir

The base of the makeup water reservoir is set at El. –2 feet. To construct the subgrade and mat for the base of the reservoir, the excavation bottom is approximately El. –4 feet. The exact final subgrade elevation is determined during final design.

2.5.4.5.2 Extent of Excavations, Fills, and Slopes

The plan arrangement of the power block, including major structure footprints, is shown on Figure 2.5.4-201. The existing natural ground surface elevation at the power block is generally level at approximately El. –0.5 feet. The power block finish grade elevation is raised approximately 26 feet to El. +25.5 feet using compacted structural fill as shown on Figure 2.5.4-221. Structural fill is used to backfill against the nuclear island, and nonsafety-related (Category II) structural fill (also termed general fill) is used below shallower nonsafety-related structures as shown in Figure 2.5.4-222. Structural fill is further described below in this subsection.

Turkey Point Units 6 & 7
COL Application
Part 2 — FSAR

The approximate foundation dimensions, foundation elevation, and predominant soil strata at the foundation elevation of the nuclear island buildings are as follows:

Structure	Approximate Foundation Dimensions (feet)	Approximate Foundation El. (feet) ^(a)	Predominant Soil Stratum at Foundation
Reactor & auxiliary building (nuclear island)	88 to 159 by 254	–14 (–35)	Lean concrete fill over Key Largo Limestone

(a) The foundation elevation shown in “()” symbols denotes the elevation and soil stratum at the base of significant over-excavation (to reach a suitable bearing stratum) at the particular structure (e.g., at the nuclear island buildings). Strata 1, 2, and 3 are over-excavated to approximately El. –35 feet or suitable subgrade of Stratum 3. The over-excavation is replaced by lean concrete.

To achieve the anticipated excavation level for each nuclear island, foundation excavations require removing approximately 100,000 cubic yards of soil and rock at each location. The extent of excavation, filling, and the approximate limits of temporary ground support for major structures are shown in plan and profile on [Figure 2.5.4-222](#). This figure shows that the excavations for foundations result in the nuclear islands being founded directly onto lean concrete above the competent rock of Stratum 3 (Key Largo Limestone).

The deepest excavation at the power block (i.e., the bottom of over-excavation for the nuclear island foundations) is approximately 35 feet below existing ground surface and 60 feet below finish grade (El. –35 feet) as shown on [Figure 2.5.4-222](#). The profiles from the power block subsurface investigation (refer to [Figures 2.5.4-203](#) through [2.5.4-208](#)) show that the subsurface strata to support foundations are relatively horizontal. However, it should be noted that the extent of excavation to final subgrade and/or to final over-excavation level is determined during construction. This determination is based on observation of actual subsurface conditions encountered, and their suitability for foundation support. Once subgrade suitability at the proposed bearing stratum is confirmed, nuclear island excavations are backfilled with lean concrete fill up to the foundation level of the structures. Structural fill used as backfill against the nuclear island is controlled and placed in accordance with a quality program per Appendix B of 10 CFR Part 50. General fill is compacted in accordance with standard construction practices, including applicable standards of the Florida Department of Transportation. Nonsafety-related power block structures are founded on general fill above the Miami Limestone. Compaction and quality control/quality assurance programs for filling are addressed in [Subsection 2.5.4.5.3](#).

There is no permanent or temporary safety-related excavation or fill slopes created by power block site grading as described in [Subsection 2.5.5](#).

2.5.4.5.3 Compaction of Backfill

Prior to earthwork operations, borrow sources for various required fill materials (i.e., power block structural fill and general fill) are qualified by testing for index properties, chemical properties, and engineering properties, especially: grain size and plasticity characteristics; soil pH, sulfate content, chloride content characteristics; and moisture-density relationships. The following compaction criteria apply:

- Structural fill used as backfill around the nuclear island structures and beneath nonsafety-related power block structures is compacted to a minimum of 95 percent of modified Proctor ([Reference 245](#)) maximum dry density.
- At power block non-structure areas, general fill is compacted to a minimum of 92 percent of modified Proctor ([Reference 245](#)) maximum dry density.

Fill placement and compaction control procedures are addressed in a technical specification prepared at project detailed design. The specification includes requirements for suitability of the various required fill materials, sufficient testing to address potential material variations, and in-place density and moisture content testing frequency (e.g., typically a minimum of one test per 10,000 square feet of fill placed per lift). The specification also includes requirements for an onsite testing firm for quality control, especially to ensure specified material gradation and plasticity characteristics, the achievement of specified moisture-density criteria, earthwork equipment, maximum lift thickness, and other requirements to ensure that fill operations conform to a high standard of practice. The onsite testing firm is required to be independent of the earthwork contractor and to have an approved quality assurance/quality control program. A sufficient number of laboratory tests are required to ensure that any variations in the various required fill materials are accounted for. A materials-testing laboratory is established onsite to exclusively serve the project site work.

2.5.4.5.4 Dewatering and Excavation Methods

Groundwater control in major power block structure excavations is required during construction. With the deepest excavation level at approximately El. –35 feet, i.e., extending approximately 35 feet below the groundwater level, a complete construction dewatering system is required. Power block groundwater conditions and construction dewatering requirements are addressed in more detail in [Subsection 2.5.4.6](#).

Turkey Point Units 6 & 7
COL Application
Part 2 — FSAR

Power block excavations are primarily open cuts, with temporary ground support provided by a reinforced concrete diaphragm wall surrounding each power block excavation area. Excavation is performed with standard excavation equipment, but may be supplemented with other methods. The reinforced diaphragm walls resist lateral earth and hydrostatic pressures while providing a barrier to groundwater flow. The reinforced diaphragm walls are seated at approximately El. -60 feet, just below the most competent portion of the Fort Thompson Formation. Tiebacks to provide resistance to the lateral earth and hydraulic pressures are installed based on the final design that includes embedment, spacing and other details, as applicable. The completed reinforced diaphragm walls effectively impede any overturning or sliding from the lean concrete fill, provided as a sub-basemat for Category I seismic structures, confined within the walls.

Predicted pumping rates to enable the required dewatering for each unit are given in [Subsection 2.5.4.6.2](#). That subsection also describes how these rates can be reduced significantly by installing a grout plug between approximately El. -35 feet and the bottom of the diaphragm wall at approximately El. -60 feet. With the grout plug installed, the seepage can be controlled during excavation using sumps and discharge pumps.

Final subgrades are inspected and approved prior to placement of lean concrete. Safety-related concrete placement is conducted under a quality program in accordance with Appendix B of 10 CFR 50. Inspection and approval procedures are addressed in the foundation and earthwork technical specifications developed at project detailed design. These specifications include, among other things, measures such as over-excavation and replacement of unsuitable rock (if encountered) and protection of surfaces from deterioration. Unsuitable rock includes soft, highly fractured, and highly porous materials. Excavations additionally comply with applicable OSHA regulations ([Reference 256](#)).

Foundation subgrade rebound (or heave) is monitored in excavations for each nuclear island. Subgrade rebound is not anticipated at the site based on the competency of the Key Largo Limestone at the base of the excavation and the underlying Fort Thompson Formation. The nuclear island is monitored during construction for:

- Groundwater levels, both interior and exterior to temporary excavations
- Horizontal and vertical movement of temporary slopes
- Loads in temporary ground support anchorages and/or struts

- Earth pressures acting on underground structures
- Foundation settlements

An instrumentation and monitoring technical specification is developed during project detailed design. The specification addresses issues such as the proper installation of a sufficient number of instruments to measure the parameters of interest, monitoring and recording frequency, and reporting requirements.

PTN COL 2.5-6
PTN COL 2.5-8

2.5.4.6 Groundwater Conditions

Groundwater conditions for the site are established by periodic measurements of groundwater levels following observation well installation in 2008, as discussed in [Subsection 2.4.12.1.4](#). Evaluation of these measurements provide a basis for engineering design and for the conceptual construction dewatering discussion provided in [Subsection 2.5.4.6.2](#).

2.5.4.6.1 Site-Specific Data Collection and Monitoring

Groundwater conditions at the site are summarized in [Subsection 2.5.4.2.2.6](#). In order to more accurately define aquifer parameters, four pumping wells and 50 observation wells were installed for the performance of aquifer pumping tests. Two pumping wells were installed at each reactor site. One well was open from depths of 22 to 45 feet to test the Key Largo Limestone and the second well was open from depths of 66 to 105 feet to test the Fort Thompson Formation. In addition to the pumping wells, each reactor site included 5 well clusters of 5 observation wells each, installed in the following zones:

- Upper aquitard (Miami Limestone)
- Upper Biscayne aquifer test zone (Key Largo Limestone)
- Middle aquitard (freshwater limestone unit)
- Lower Biscayne aquifer test zone (Fort Thompson Formation)
- Lower aquitard (Upper Tamiami Formation)

Descriptions and locations of the aquifer pumping test wells and observation wells are presented in [Subsection 2.4.12.2.4.1](#) and [Appendix 2BB](#), along with the results of the aquifer pumping tests.

2.5.4.6.1.1 Groundwater Elevations

Site groundwater elevations are discussed in [Subsection 2.4.12.2.2](#).

2.5.4.6.1.2 Hydraulic Conductivity Tests

Twenty groundwater observation wells are installed at the site to monitor seasonal fluctuations in groundwater elevations and to evaluate the hydraulic conductivity of the soil and rock strata. Further investigation in the form of aquifer pumping tests was conducted to better define site-specific aquifer parameters. The results of these investigations are described in [Subsection 2.4.12](#). The locations of the observation wells are shown on [Figure 2.4.12-209](#). The groundwater elevations, gradients, and hydraulic conductivity results are discussed in [Subsection 2.4.12.2](#).

2.5.4.6.2 Construction Dewatering

The excavation for each new unit will be surrounded by a reinforced concrete diaphragm wall that will act as a cut-off for horizontal groundwater flow into the excavation. Conceptual plans indicate each excavation will have dimensions of approximately 210 feet by 310 feet. The planned bottom of the wall is at El. -60 feet, i.e., just below a layer of limestone situated between the Key Largo Limestone ([Subsection 2.5.4.2.1.3](#)) and the Fort Thompson Formation ([Subsection 2.5.4.2.1.2.4](#)) that is considerably less permeable than either of these strata. This is referred to as the Freshwater Limestone in [Appendix 2BB](#) and [Appendix 2CC](#). The layer has a lower permeability and thus reduces the amount of vertical inflow into the bottom of the excavation during dewatering.

The existing groundwater elevation in the power block areas is dependent on tidal variations, but averages close to El. 0 feet. The base of the excavation for the nuclear island is approximately El. -35 feet. Thus, temporary construction dewatering is needed down to at least El. -35 feet. The pumping test program described in [Subsection 2.4.12.1.4](#) resulted in the development of estimates of the hydraulic conductivity of the Freshwater Limestone and the underlying Fort Thompson Formation. Freshwater Limestone used in the groundwater model described in [Appendix 2CC](#) is assumed to have a vertical hydraulic conductivity of approximately $2.3\text{E-}06$ cm/sec, compared to approximately $1.7\text{E-}01$ cm/sec for the Fort Thompson Formation. In the groundwater model, the Freshwater Limestone is assumed to be absent if the available information (from borings, etc.) indicates a thickness of less than 1.5 feet.

An option for construction-related groundwater control is to form a grout plug between the bottom of the excavation at approximately El. -35 feet and the bottom

of the diaphragm wall at approximately El. -60 feet. Grout is injected in a series of primary grout holes until minimal grout take is achieved. Secondary grout holes are then drilled between the primary grout holes and grout is injected until minimal grout take again occurs. Tertiary grout holes are probably required. Quarternary grout holes may be needed at some locations but probably only where excessive seepage is observed as the excavation progresses. The groundwater model simulation ([Appendix 2CC](#)) assumes hydraulic conductivity of the grout plug is $1.0\text{E-}04$ cm/sec. The corresponding predicted groundwater extraction rate is 96 gpm per unit. In addition to using this value of hydraulic conductivity, a series of sensitivity analyses using a range of hydraulic conductivities ($1.0\text{E-}03$, $1.0\text{E-}05$ and $1.0\text{E-}06$ cm/sec) is conducted to determine the feasible range of dewatering discharge rates, which range from approximately 1000 to 1 gpm per unit. These values demonstrate that grouting can significantly reduce the quantity of discharge water generated during excavation dewatering activities.

2.5.4.6.3 Seepage or Potential Piping Conditions During Construction

No earthwork structures are used during construction of Units 6 & 7 to retain water. Therefore, no adverse conditions due to seepage or piping through such structures are anticipated.

2.5.4.6.4 Permeability Testing

Permeability (or hydraulic conductivity) testing is described in [Subsection 2.5.4.6.1.2](#).

2.5.4.7 Response of Soil and Rock to Dynamic Loading

PTN COL 2.5-2
PTN COL 2.5-6

The site subsurface profile is characterized with respect to the properties of strata pertinent for dynamic loading. Detailed descriptions of the development of the GMRS and the associated probabilistic seismic hazard assessment (PSHA), as well as the geologic characteristics of the site, are addressed in [Subsection 2.5.2](#). Refer also to [Subsection 2.5.4.4](#) for additional description on site-specific geophysical methods and results.

2.5.4.7.1 Site Seismic History

The seismic history of the area and of the site, including any prior history of seismicity and any historical evidence of liquefaction or boiling, is addressed in [Subsection 2.5.2](#).

2.5.4.7.2 P- and S-Wave Velocity Profiles

Because of the significant depth of unconsolidated sediments at the site (refer to [Subsection 2.5.4.1](#)) compared to the depth of compression and shear wave velocity measurements made during this subsurface investigation (i.e., to approximately 600 feet depth), additional information is required to complete the velocity profile for the site for use in seismic ground response analyses. Velocities in the upper 600 feet are measured at the site, and velocities deeper than 600 feet are obtained from available references as described in [Subsection 2.5.4.7.2.2](#).

2.5.4.7.2.1 Seismic Velocities in the Upper 600 Feet

Geophysical measurements in the upper 600 feet of site soils are obtained by suspension P-S velocity logging methods and by downhole geophysical methods, as presented in [Subsections 2.5.4.4.2.1](#) and [2.5.4.4.2.2](#), respectively.

Recommended shear wave velocity profiles for the upper 600 feet of site soils at the power block are shown on [Figure 2.5.4-220](#). Average shear wave velocities (V_s) are summarized in [Table 2.5.4-215](#).

A significant range of shear and compression wave velocities within Strata 2, 3, and 4 with a peak near the top of Stratum 4 is observed. This variation is due to the different degrees of degradation of these materials. The velocities measured in soil Strata 5, 6, and 7 are observed to be appreciably more consistent.

Suspension P-S velocity logging is performed in 10 dedicated borings (five borings in each of the two power blocks), with depths ranging from 150 feet to 600 feet, and at the locations shown on [Figure 2.5.4-202](#). Downhole geophysical testing including gamma, caliper, resistivity, spontaneous potential, and caliper measurements extend as deep as 400 feet bgs. The suspension P-S logging data and the downhole geophysical data are contained in Appendix B of [Reference 257](#).

Comparison of measured V_s results between the two power block areas indicates similar velocities.

The design/average V_s is summarized in [Subsection 2.5.4.4.4](#).

2.5.4.7.2.2 Seismic Velocities Deeper than 600 Feet

Refer to [Subsection 2.5.4.2.1.1](#) for a brief description of geologic conditions at depths greater than 600 feet. Cenozoic bedrock (“basement rock”) occurs at a depth of at least 15,000 feet ([Reference 209](#)). Additional subsurface data, in the

form of sonic logs performed for oil field exploration borings and installation of exploratory well EW-1 supplement the site data to characterize conditions below 615.5 feet depth explored in the present investigation. Eight sonic logs, taken at borings drilled within the site region, (Figure 2.5.4-210) have sonic data ranging in elevation from approximately –500 feet to approximately –11,900 feet (References 209 and 211). Sonic data obtained from EW-1 (Figure 2.5.4-243) ranges in elevation from approximately –1078 feet to approximately –3226 feet NAVD 88 (Reference 287).

Shear wave velocities are derived from the sonic log data using the relationship given in Subsection 2.5.4.2.1.2.10 (Equation 2.5.4-1). Average shear wave velocities are calculated for all eight sonic logs. These average shear wave velocity values are presented on Figures 2.5.4-211 and 2.5.4-243.

These figures also include profiles of average V_s values plus or minus one standard deviation. Note that sonic data from the eight sonic logs show shear wave velocities of strata deeper than 600 feet below finished site grade to increase from approximately 4000 feet/second at 600 feet to approximately 8500 to 10,000 feet/second below 10,000 feet.

2.5.4.7.3 Static and Dynamic Laboratory Testing

Static laboratory testing of representative soil samples obtained from this subsurface investigation are conducted, with results summarized on Table 2.5.4-209 and in Subsection 2.5.4.2.1.3.

Dynamic laboratory RCTS tests obtain data on shear modulus degradation and damping characteristics of site soils over a wide range of strains and are performed on seven samples recovered in this subsurface investigation. Samples tested for RCTS ranged in depth from 129.5 to 294 feet. The samples are all from the upper and lower Tamiami and Peace River Formations (Strata 5, 6, and 7). The results of these tests are described briefly below in Subsections 2.5.4.7.3.1 and 2.5.4.7.3.2.

2.5.4.7.3.1 Selected Shear Modulus Degradation Curves for Site Strata

As described in Subsection 2.5.4.2.1.3.16, seven RCTS tests are performed on intact samples collected from Strata 5, 6, and 7. Each of these intact samples is from the power block area. In each RCTS test, values of shear modulus (G) measured at increasing strain levels are obtained. These values are compared to the value of G_{\max} , the shear modulus measured at 10^{-4} percent shear strain. The shear modulus degradation (ratio of G/G_{\max}) is plotted against shear strain, and a

curve of G/G_{\max} from the literature that best fits the test data is selected. Literature curves are used rather than an actual best-fit curve through the test data because the literature curves typically extend over a greater range of shear strain than the test data. Curves recommended by the Electric Power Research Institute (EPRI) for non-cohesive soils are employed ([Reference 258](#)).

The modulus degradation curves (plots of G/G_{\max} versus shear strain) from actual RCTS tests are presented on [Figure 2.5.4-232](#). [Figure 2.5.4-233](#) shows the selected values of G/G_{\max} versus shear strain for the two strata tested in the power block in addition to the other site strata addressed in this evaluation. The selected G/G_{\max} versus strain values for each stratum are also presented in [Table 2.5.4-216](#).

Stratum 1 is removed from the site so the shear modulus degradation properties of that stratum are not relevant.

Stratum 2 is a weak rock stratum described in [Subsection 2.5.4.7.3.3](#).

Due to the similarity of the grain size distribution and the materials, the recommended shear modulus degradation for Stratum 7 is the same as for Stratum 6, i.e., natural soil deeper than 159 feet depth in [Figure 2.5.4-233](#). This modulus degradation curve is also selected for Stratum 8 which consists of very weak rock and is part of the same geological formation (Hawthorn Group) as Stratum 7.

Rock Strata 3 and 4 are considered not subject to modulus degradation, as described in [Subsection 2.5.4.7.3.3](#).

Dynamic properties of compacted structural fill are described in [Subsection 2.5.4.7.3.4](#).

For soil/rock beneath 600 feet, strain levels are so small that it can be reasonably assumed that there is no shear modulus degradation.

2.5.4.7.3.2 Selected Damping Curves for Soils

Each RCTS test also provides measured values of damping ratio (D) at increasing shear strain levels. The damping data for tests performed are shown on [Figure 2.5.4-234](#). The same procedure used for shear modulus degradation (G/G_{\max} versus shear strain) is employed to obtain a best-fit D versus shear strain curve from the literature. [Figure 2.5.4-235](#) shows the selected values of D versus

shear strain for tested Strata 5, 6, and 7, i.e., the natural soil curve used for all three soil strata. This D versus shear strain curve is also selected for Stratum 8.

2.5.4.7.3.3 Shear Modulus and Damping for Rock

Rock strata are encountered at several depths at the site. For Strata 3 and 4, the shear modulus is considered non-strain dependent based upon the competency of the rock. For the Miami Limestone (Stratum 2), the limestone is considered sufficiently weak as to have a strain-dependent shear modulus. A recommended shear modulus degradation for this stratum based on literature ([Reference 259](#)) for mudstones/shales is provided in [Figure 2.5.4-233](#). Similarly, a recommended damping curve for Stratum 2 is provided in [Figure 2.5.4-235](#).

See [Subsection 2.5.4.1](#) for a brief description of geologic conditions at depths greater than 600 feet based upon regional data. See [Subsection 2.5.4.7.2.2](#) for a description of deep shear wave velocity profiles pertinent to the site derived from sonic logging data.

It should be noted that hard rock is considered to have damping, but is not strain dependent. For site-specific work, damping of 1 percent is adopted for Strata 3 and 4, and bedrock shear modulus is considered to remain constant (i.e., no degradation) in the shear strain range of 10^{-4} percent to 1 percent.

2.5.4.7.3.4 Dynamic Properties of Structural Fill

The muck layer underneath the power block area at Units 6 & 7 is removed and replaced with compacted limerock fill from onsite excavated Miami Limestone and offsite sources, with fill placement starting from El. -5 feet and building up to El. +25.5 feet. Non-Category I structures are supported on compacted structural limerock fill.

Estimated shear wave velocity for structural limerock fill with upper and lower boundary estimates using a coefficient of variation (COV) of 1.5 applied to the shear modulus is shown on [Figure 2.5.4-236](#). This relatively large COV is selected because of uncertainty about the degree of cementation of the limerock fill that could occur after placement. There is evidence of such cementation in the shear wave velocity measurements made at two locations within the existing Unit 5 at Turkey Point during a non-safety related investigation of the compacted limerock fill. Measured shear wave velocity values in the top 12 feet or so of the fill average between 1450 and 1500 feet/second, close to the upper boundary value shown in [Figure 2.5.4-236](#) between 10 and 15 feet depth. It is noted that increase in shear wave velocity due to cementation of the fill is more pronounced close to the

surface. The confining pressure increase with increasing depth in the fill results in higher shear wave velocities with depth, as shown in [Figure 2.5.4-236](#), while the cementation effects with depth remain relatively constant.

The large particle sizes of the gravel/sand structural fill preclude RCTS testing of this material. Therefore, modulus degradation and damping ratio versus strain are estimated based on applicable literature ([Reference 260](#)). The adopted shear modulus degradation and damping ratio curves for compacted structural fill are presented in [Figures 2.5.4-233](#) and [2.5.4-235](#), respectively, and [Table 2.5.4-216](#). Refer to [Subsection 2.5.4.5.1](#) for structural fill and general fill requirements.

2.5.4.7.4 Small Strain Shear Modulus Estimation

With shear wave velocity and other parameters established, small strain shear modulus values can be calculated from Equation 2.5.4-7. Note that shear wave velocity and unit weight values for use in the equation are given in [Table 2.5.4-209](#). Refer to [Subsection 2.5.4.2](#) for a stratum-by-stratum description of the derivation of shear modulus (G) and other geotechnical engineering parameters for use in design.

2.5.4.7.5 Seismic Parameters for Liquefaction Evaluation

The site-specific soil column extending to the proposed ground surface is developed for evaluation of liquefaction potential. The development of the design response spectra (DRS) calculated based on consideration of the design earthquake and the soil column dynamic properties is described [Subsection 2.5.2](#). The seismic acceleration as a function of elevation is used to develop the Cyclic Stress Ratio (CSR). The CSR is used to evaluate liquefaction potential as described in [Subsection 2.5.4.8](#).

2.5.4.8 Liquefaction Potential

PTN COL 2.5-9

The potential for soil liquefaction at the site is evaluated following guidance given in RG 1.198. Current state-of-the-art deterministic methods, outlined in [Reference 219](#), are followed. The subsurface conditions and soil properties considered are those described in [Subsection 2.5.4.2.1](#).

Liquefaction can only occur where the stratum is saturated. The shallowest saturated stratum is the proposed compacted limerock fill layer that is only saturated for the lowest approximately 5 feet of section. This material (exact

composition to be determined at final design phase) consists of a granular mixture including fines compacted to at least 95 percent maximum dry density in accordance with structural fill requirements. Typically, a compacted fill of similar material under the approximately 20 feet of overburden has a sufficiently high shear wave velocity and strength, as determined from the corrected N-values, to provide more than adequate resistance to liquefaction. As such, it is not prone to liquefaction and the factor of safety for liquefaction resistance of this stratum is not calculated.

As described in [Subsection 2.5.1](#), the site rock strata (Strata 2, 3, 4, and 8) have sufficiently high shear wave velocities and cementation to avoid liquefaction. Thus, only the soil strata of the upper and lower Tamiami and Peace River Formations (Strata 5, 6, and 7) are considered for liquefaction potential analysis.

The Tamiami and Peace River Formations are attributed to the Pliocene and Miocene ages, respectively. Conventionally, only younger deposits, especially Holocene age and, to a lesser extent, Pleistocene age deposits, are considered potentially liquefiable. Accepted practice for the investigation and mapping of areas with seismic liquefaction potential is limited to soils younger than middle Pleistocene (700,000 years ago). Publications on liquefaction cite the assessments presented by [Reference 261](#) that relate liquefaction susceptibility to the age of the soil deposit. These publications cover liquefaction studies from the east coast as well as the central and western United States (i.e., [References 262, 263, 264, 265, and 266](#)). An analysis of paleoliquefaction features along the Atlantic seaboard in [Reference 267](#) for the Nuclear Regulatory Commission states that “no liquefaction sites were found in materials older than about 700,000 years.” RG 1.198 also notes the low probability of liquefaction of sediments older than late Pleistocene.

Unconsolidated soil deposits at the site are Pliocene (at least 1.6 million years old) or older. Additionally, the overburden of rock from Strata 2, 3, and 4 should preclude development of liquefaction-induced features, such as lateral spreading and settlement, from propagation to the ground surface. To be complete and conservative, a comprehensive liquefaction analysis for all CPT and shear wave velocity data is made. SPT results are also considered, but are discounted due to artesian conditions causing inconsistent and some unrealistically low SPT N-values.

2.5.4.8.1 Liquefaction Evaluation Methodology

Liquefaction is the transformation of a granular soil material from a solid to a liquefied state as a consequence of increased pore water pressure and reduced effective stress. Soil liquefaction occurrence (or lack thereof) depends on geologic age, state of soil saturation, density, gradation, plasticity, and earthquake intensity and duration. The liquefaction analysis presented here employs state-of-the-art deterministic methods ([References 219](#) and [268](#)).

As noted in [Subsection 2.5.4.6.1](#), groundwater levels selected as representative of the conditions at the time of the site-specific subsurface investigation (i.e., prior to the conditions expected during operation) are assumed at El. 0.

The natural soil at the power block is found mainly in muck, the upper and lower Tamiami Formation (Strata 5 and 6), and the Peace River Formation (Stratum 7).

There are several key aspects of liquefaction potential of Strata 5, 6, and 7 that should be considered prior to numerical evaluation. These aspects are age, depth, and rock overburden.

As addressed above, only the soil strata of the upper and lower Tamiami Formation and Peace River Formation (Strata 5, 6, and 7) are considered for liquefaction potential analysis. As noted above, the Tamiami and Peace River Formations are attributed to the Pliocene and Miocene ages, respectively. Conventionally, only younger deposits, especially Holocene age and, to a lesser extent, Pleistocene age deposits, are considered potentially liquefiable. As the unconsolidated soil deposits at the site below rock are Pliocene (at least 1.6 million years old) or older, the probability of liquefaction is considered extremely low. [Reference 269](#) proposes an age correction factor, C_A , that accounts for the low probability of liquefaction of older deposits. Although this factor is not applied in this calculation, it would be approximately 2 to 2.5; therefore, use of this factor would increase the calculated factors of safety against liquefaction by 2 to 2.5.

The depth of the unconsolidated deposits of Strata 5, 6, and 7 makes liquefaction very unlikely. Although liquefaction has reportedly been observed in soils greater than 50 feet deep, a maximum depth of 50 feet may be adequate for evaluation of liquefaction potential in most cases ([Reference 270](#)). Because data on liquefaction are very sparse for depths greater than approximately 50 feet, calculation results for greater depths have a lower degree of certainty ([Reference 219](#)).

Liquefaction potential and the potential damage associated with liquefaction of loose sands under a stiff “crust” is considered in [Reference 270](#). The overlying rock of Strata 2, 3, and 4 and the proposed limerock fill at the ground surface can be considered such a crust. Ishihara ([Reference 271](#)) considers thickness of a crust layer as deep as 26 feet and predicts that for a similar thickness of liquefiable strata, a maximum ground acceleration of greater than approximately 0.5 g is required to induce ground damage. The estimated peak ground acceleration at the proposed Units 6 & 7 is approximately 0.1g. For liquefaction to develop ground damage, the crust has to shear. This is extremely unlikely in the case of Strata 2, 3, and 4, which are approximately 100 feet thick in total and have reasonable shear strength (using rock criteria). Therefore, even if liquefaction occurs at depth, no effects at or near the ground surface are experienced.

For completeness, calculations to evaluate the factor of safety (FOS) against liquefaction are performed. The measured CPT values, and the shear wave velocity, V_s , are used for liquefaction analysis. These evaluations are performed separately, using the state-of-art approaches summarized in [References 219](#) and [268](#). SPT results are not used in the liquefaction calculations, as explained in the following subsection.

2.5.4.8.2 Liquefaction Resistance Based on SPT Data

As indicated on [Figures 2.5.4-212](#) and [2.5.4-213](#), there is a very wide scatter of uncorrected and corrected N-values. The N_{60} -values vary from 0 to 100 blows/foot in the upper Tamiami Formation and from 3 to around 100 blows/foot in the lower Tamiami Formation. Where SPT sampling encountered refusal, the N-value is capped at 100, so the actual range of penetration resistance is higher than these values indicate. There is no obvious correlation between N-value and elevation in these strata. Silty sands and sandy silts that range in depth from 120 to 220 feet would normally be dense to very dense with consistently high N_{60} -values. Blow counts of less than 20 blows/foot and particularly less than 5 blows/foot (including the zero values) are most probably due to sample disturbance. [Subsection 2.4.12](#) describes the upward vertical hydraulic gradient observed in the water level measurements. It seems likely that this hydraulic gradient has contributed to at least partial blowout of the bottom of the hole prior to/during SPT sampling on many if not most of the samples. To evaluate where N-values are not representative of actual in situ density conditions, the corrected N-values are compared to the CPT corrected tip resistance. The ratio of q_{c1}/N_1 for clean sands is typically 4 to 5 and for silty sands 3.5 to 4.5 based on the work presented in [Reference 282](#). [Figure 2.5.4-237](#) indicates the N-values relative to the predicted range based on the ratio of q_{c1}/N_1 . As can be seen in the figure, very few of the N-

values fall into the predicted range, supporting the theory that these blow counts are significantly affected by the hydraulic gradient. Therefore, the measured N-values are not used in the calculation of liquefaction potential in favor of the measured CPT and V_s results that are more consistent with each other and with expected values for deposits of similar age, depth, and overburden.

2.5.4.8.3 FOS Against Liquefaction Based on CPT and V_s Data

The CPT measurements are much less susceptible to soil disturbance from hydraulic gradients, and V_s measurements are not affected at all. The CPT measurements are taken at approximately 0.07 foot depth intervals, where CPT could be probed (no rock coring), from approximately 120 to 290 feet depth. Considering a total of 7304 points, a FOS is calculated if the material is considered potentially liquefiable based on tip resistance and fines content. The V_s measurements, taken at depth intervals generally 1.6 to 1.7 feet, are used for the FOS against liquefaction with a total of 878 points considered.

Table 2.5.4-218 is a summary of the results of the calculations. The native soils that indicate the lowest FOS values are those in the upper Tamiami Formation. However, the FOS values calculated indicate adequate resistance to liquefaction based on published criteria ($FOS > 1.25$). The FOS as a function of elevation for the CPT-based calculations is presented in Figure 2.5.4-238. As described above, even if liquefaction occurs, the thickness and stiffness of the overlying rock, lean concrete fill, and compacted limerock fill precludes the effects of liquefaction from reaching near the ground surface.

2.5.4.9 Earthquake Site Characteristics

PTN COL 2.5-2 The consideration of possible earthquake site characteristics is described in Subsection 2.5.2.

2.5.4.10 Static Stability

PTN COL 2.5-10 As noted earlier, finish grade at the power block is approximately El. +25.5 feet. Also as noted, the reactor and auxiliary buildings (nuclear island) are Seismic Category I structures. This subsection addresses the stability of foundation soils for these structures, the locations of which are shown on Figure 2.5.4-201. Other major structures, including the turbine buildings, the radwaste buildings, and the

Turkey Point Units 6 & 7
COL Application
Part 2 — FSAR

annex buildings, although not Seismic Category I structures, are considered in the settlement analysis.

2.5.4.10.1 Units 6 & 7 Foundations and Subsurface Conditions

Approximate foundation dimensions, foundation elevations, and required foundation-bearing capacities for the site Seismic Category I structures are indicated in the following table.

Structure	Approximate Foundation Dimensions (feet)	Approximate Foundation El. (feet)	Average Required Bearing Capacity (Static) (ksf) ^(a)	Maximum Required Dynamic Bearing Capacity (ksf) ^(b)
Reactor and auxiliary buildings (Units 6 & 7)	88 to 159 by 254 (irregular)	-14.0	8.9	35

(a) This pressure is the required design pressure required per the DCD.

(b) This pressure is the total pressure considering all static and short-term loads required per the DCD.

Power block subsurface conditions are described in detail in [Subsection 2.5.4.2](#). Geotechnical engineering parameters selected for design for each of the various soil strata occurring at the site are also described in [Subsection 2.5.4.2](#) and are summarized in [Table 2.5.4-209](#). The parameters contained in this table are used as the basis for foundation analyses presented here.

For foundation analysis purposes, the specific subsurface conditions/profiles associated with each of the Seismic Category I structures at both Unit 6 and Unit 7 are developed as shown on [Figures 2.5.4-203 through 2.5.4-208](#). Associated strata depths and elevations for each of these structure-specific conditions/profiles are shown in [Table 2.5.4-201](#). As can be seen from these profiles and additional information in [Subsection 2.5.4.2](#), the subsurface conditions in the upper 120 feet can be considered uniform in accordance with RG 1.132, therefore, there is no extreme lateral variability in the subgrade stiffness.

As noted in [Subsection 2.5.4.6.1](#), based on groundwater observation well measurements, the current (preconstruction) groundwater level at the power block is El. 0 feet, very close to the existing ground surface. The estimated post-construction depth to groundwater at the power block is 25.5 feet. The actual groundwater level fluctuates due to changes in the tidal and cooling water canal levels. The groundwater level (El. 0 feet) used in foundation analyses is considered conservative but representative based on groundwater measurements presented in [Subsection 2.4.12.2.2](#). Due to positive surface gradients away from

the nuclear islands, the potential for infiltration of groundwater to raise the ground water level to within 2 feet of the finished grade is considered negligible.

2.5.4.10.2 Units 6 & 7 Bearing Capacity Evaluation

The ultimate bearing capacity, q_{ult} , of a foundation is calculated using

Reference 225:

$$q_{ult} = c N_c \zeta_c + q N_q \zeta_q + 0.5 \gamma' B N_\gamma \zeta_\gamma \quad \text{Equation 2.5.4-14}$$

Category I seismic structures bear on lean concrete placed on the rock of Key Largo Limestone (Stratum 3). For foundations bearing on rock, **Reference 272** is used to calculate bearing capacity.

Using **Reference 272**, the ultimate bearing capacity (q_{ult}) formula for a footing on weak rocks with little fracturing is calculated as:

$$q_{ult} = c N_c C_{f1} + \gamma D_f N_q + 0.5 \gamma B N_\gamma C_{f2} \quad \text{Equation 2.5.4-15}$$

Where,

c = rock mass cohesion

γD_f = effective overburden pressure at base of foundation

γ = effective unit weight of rock

D_f = depth from ground surface to base of foundation

B = width of foundation

N_c , N_q , and N_γ are bearing capacity factors for rock

C_{f1} and C_{f2} are shape factors that replace the ζ shape factor in Equation 2.5.4-14.

From Table 5.4 of **Reference 272**,

$$C_{f1} = C_{f2} = 1.0 \text{ for } L/B > 6 \text{ strip foundation} \quad \text{Equation 2.5.4-16a}$$

$$C_{f1} = 1.12, C_{f2} = 0.9 \text{ for } L/B = 2 \quad \text{Equation 2.5.4-16b}$$

$$C_{f1} = 1.05, C_{f2} = 0.95 \text{ for } L/B = 5 \quad \text{Equation 2.5.4-16c}$$

$$C_{f1} = 1.25, C_{f2} = 0.85 \text{ for square foundation} \quad \text{Equation 2.5.4-16d}$$

$$C_{f1} = 1.2, \quad C_{f2} = 0.7 \text{ for circular foundation} \quad \text{Equation 2.5.4-16e}$$

Where,

L = length of footing.

From Equation 5.8 of [Reference 272](#),

$$N_{\phi} = \tan^2(45 + \phi/2) \quad \text{Equation 2.5.4-17}$$

$$N_c = 2 N_{\phi}^{0.5} (N_{\phi} + 1) \quad \text{Equation 2.5.4-18}$$

$$N_{\gamma} = 0.5 N_{\phi}^{0.5} (N_{\phi}^2 - 1) \quad \text{Equation 2.5.4-19}$$

$$N_q = N_{\phi}^2 \quad \text{Equation 2.5.4-20}$$

Equation 2.5.4-15 can be simplified to:

$$q_{ult} = c N_c C_{f1} \quad \text{Equation 2.5.4-15a}$$

This simplification is conservative because it neglects the contribution of the second two terms.

Since there were no laboratory test results available to derive rock mass cohesion or friction angle for Miami Limestone, a generic value was used from [Reference 272](#). For limestones with 10 to 20 mm clay infillings, $c = 2.3$ ksf and $\phi = 14^\circ$. Using Equation 2.5.4-215a gives an allowable bearing capacity of 5.8 ksf, including a factor of safety of 3.

Alternatively, an allowable bearing capacity of not more than 20 percent of the unconfined compressive strength (U) of the rock can be used, according to [Reference 221](#). For the Miami Limestone, a U of 200 psi is given in [Table 2.5.4-209](#). Twenty percent of this strength is 40 psi (5.76 ksf). The results of the two methods compare favorably.

The foundation bearing capacities of the Category 1 seismic structures are considered similarly. The design U for the Key Largo Limestone is 1.5 ksi from [Table 2.5.4-209](#) with 20 percent of 1.5 ksi = 300 psi ~ 43 ksf. This allowable capacity compares favorably to the value of 54.5 ksf which is calculated using Equation 2.5.4-15a (conservatively assuming a friction angle that is the same as for the Miami Limestone = 14° and a cohesion of 10 percent of the U, i.e., 21.6 ksf); the lower value of 43 ksf is recommended.

Foundation bearing capacities are calculated using the average material properties in [Table 2.5.4-209](#) and Equations 2.5.4-14 through 2.5.4-20. A summary of the allowable bearing capacities (using FOS = 3.0) of Seismic Category I structures (nuclear island) is given in [Table 2.5.4-217](#). Analysis results show that for the Seismic Category I structures (including both units), the allowable static bearing capacity is 43 ksf, which greatly exceeds the anticipated average required bearing capacity of 8.9 ksf specified in the DCD.

The above bearing capacity formulation is based on the assumption that the strata within the zone of foundation deformation are uniform with depth in terms of shear strength properties. While recognizing that the site strata are interlayered, the properties of the soil and rock are conservatively selected to provide for a representative bearing capacity.

2.5.4.10.2.1 Dynamic Bearing Capacity

The maximum dynamic bearing capacity required is 35 ksf (DCD). This total load includes normal loading plus seismic conditions with a 0.3g peak ground acceleration, which greatly exceeds the seismicity in Florida. Using the calculated allowable bearing capacity of 43 ksf for rock and lean concrete overlying the rock, this condition is satisfied even with the 0.3g peak ground acceleration.

Note that for concrete, no guidance is given in ACI 349-06 ([Reference 273](#)) for increasing or decreasing the design bearing strength for dynamic loading.

2.5.4.10.3 Settlement

PTN COL 2.5-12
PTN COL 2.5-16

Foundation settlements are estimated using pseudo-elastic compression methods. Based on a stress-strain model that computes settlement in discrete layers, the settlement of shallow foundations due to elastic compression of subsurface materials is estimated as:

$$\delta = \sum (\Delta p_i h_i) / E_i \quad \text{Equation 2.5.4-21}$$

Where,

δ = settlement

i = 1 to n , where n is the number of layers

Δp_i = vertical applied pressure at the center of layer i

h_i = thickness of layer i

E_i = elastic modulus of layer i

The stress distribution below the corner of a rectangular flexible foundation is based on a Boussinesq-type distribution ([Reference 225](#)):

$$\sigma_z = (p/2\pi) \{ \tan^{-1} [l b / (z R_3)] + (l b z / R_3) (1/R_1^2 + 1/R_2^2) \} \quad \text{Equation 2.5.4-22}$$

Where,

l = length of the footing

b = width of footing

z = depth below footing at which pressure is computed

$$R_1 = (l^2 + z^2)^{0.5}$$

$$R_2 = (b^2 + z^2)^{0.5}$$

$$R_3 = (l^2 + b^2 + z^2)^{0.5}$$

Note that to calculate σ_z values below the midpoint of an edge and below the center of a rectangular foundation, the values of σ_z calculated from Equation 2.5.4-22 above are multiplied by two and four, respectively, to obtain p_i , the vertical applied pressure at the center of layer i for use in Equation 2.5.4-21.

The containment and auxiliary buildings (nuclear island) share the same mat foundation and are founded on lean concrete placed above rock of the Key Largo Limestone. Therefore, for settlement computations, the bottom of the foundation is taken at El. -14 feet on lean concrete. Settlement of the rock strata is computed using the elastic modulus values tabulated in [Table 2.5.4-209](#). Settlement of the soil strata is evaluated using the strain compatible elastic moduli of the Tamiami and Peace River Formations with corresponding axial strains, as discussed later in this section. The elastic modulus for the lean concrete used for settlement estimates is derived as follows:

The thickest part of lean concrete is between El. -14 feet and El. -35 ft, i.e., 21 feet thick (see [Figure 2.5.4-222](#)). The elastic modulus of lean concrete with a unit weight of 145 pcf can be calculated using the following equation ([Reference 274](#)).

$$E_c = 1820 \cdot f'_c{}^{0.5} \text{ (ksi)} \quad \text{Equation 2.5.4-23}$$

where,

f'_c = specified compressive strength of concrete (ksi)

The lean concrete placed on rock is expected to have a minimum compressive strength of 1.5 ksi.

$$f'_c = 1.5 \text{ ksi, then } E_c = 1820 \cdot 1.5^{0.5} = 2229 \text{ ksi} \approx 321,000 \text{ ksf}$$

The settlements under the nuclear island foundation with plan dimensions of 88 feet by 254 feet and 159 feet by 254 feet are calculated with an applied pressure of 8.9 ksf. The estimated total settlements at the center and at midpoints of the sides are largely impacted by the large foundation size and loading, and by the elastic modulus values of the soil strata. The preconsolidated soils of the Tamiami and Peace River Formations are confined below an 80-foot-thick stratum of rock, and thus a relatively low settlement estimate is expected from these dense granular and stiff fine-grained layers. Settlements at the center of the mat foundations are evaluated using the strain-compatible elastic moduli of the Tamiami and Peace River Formations with corresponding axial strains. The strain-compatible evaluation is performed only for the soil strata, i.e., the Tamiami and Peace River Formations where there is a difference between the high and low strain moduli. In order to apply the elastic moduli in Equation 2.5.4-21, their values need to be equated with strain level. In this case, the modulus degradation with increasing strain is based on the recommended curves in [Figure 2.5.4-233](#) after converting shear strain to axial strain.

For calculating settlement of structures using the elastic method, the maximum principal strain is the vertical strain (i.e., $\epsilon_1 = \epsilon_v$), while the minimum principal strain is assumed to be zero (i.e., $\epsilon_3 = 0$). Because the maximum shear strain $\gamma_{\max} = \epsilon_1 - \epsilon_3 = \epsilon_1$ ([Reference 275](#)) and $E/E_{\max} = G/G_{\max}$, the elastic modulus reduction curves with respect to vertical strain should be the same as the shear modulus reduction curves with respect to the shear strain. Therefore, the strain levels in degradation curves ([Figure 2.5.4-233](#)) are interchangeable between the shear strain and axial strain without any need of correction. Thus, the same degradation curve in [Figure 2.5.4-233](#) with G/G_{\max} on the vertical axis and percent shear strain on the horizontal axis can be used to determine appropriate values of E for settlement calculations. The ratio of E/E_{\max} is equivalent to G/G_{\max} and the computed percent axial strain corresponds to the percent shear strain using [Figure 2.5.4-233](#).

A trial process is followed for soil Strata 5, 6, and 7 using the degradation curves to arrive at a compatible axial strain, such that the strain for the adopted modulus and the calculated strain converge. For rock and concrete strata, the settlements computed are based on a constant (not strain dependent) elastic modulus. The results of the settlement analysis on [Table 2.5.4-219](#) show the computed

settlements at the center and edge of the nuclear island foundations with dimensions of 88 feet by 254 feet and 159 feet by 254 feet, under loading of 8.9 ksf. (Two sets of plan dimensions are used because of the irregular shape of the foundation.) Similar settlement calculations are made for the turbine, annex and radwaste buildings, and the results are presented in [Table 2.5.4-219](#). As with the nuclear island, settlements of the annex building are analyzed for two sets of foundation dimensions.

As noted earlier, Equation 2.5.4-22 computes the stress distribution beneath a flexible foundation, which accounts for the sometimes significant difference in computed settlement between the center of the foundation and the mid-point of the side of the foundation. In fact, the foundations of the structures listed in [Table 2.5.4-219](#) are thick, reinforced concrete mats with appreciable structural stiffness. Thus the mean settlements listed in [Table 2.5.4-219](#) more closely reflect the actual anticipated settlements across the whole foundation. [Table 2.0-201](#) lists the DCD limits of acceptable settlement without need for additional evaluation. Limits for the nuclear island are 6 inches total settlement and a differential settlement across the nuclear island foundation mat of one-half inch in 50 feet. The [Table 2.5.4-219](#) values are within the limits for total settlement. The values for differential settlement are within the limits for Case I and outside the limits for Case II. However, as noted above, the [Table 2.5.4-219](#) values assume a flexible foundation, and the actual differential settlement across the thick, reinforced mat foundation is negligible.

[Table 2.0-201](#) also lists limits of differential settlement between the nuclear island and surrounding structures as 3 inches. The difference between the estimated settlement of the nuclear island and the settlement of the surrounding structures in [Table 2.5.4-219](#), i.e., the differential settlement, is within the limits. As noted below, because of the nature of the soils and rock underlying the new units, post-construction settlement will be negligible.

Because the construction of each unit is over a period of greater than five years, the elastic settlement estimated in [Table 2.5.4-219](#) is essentially complete prior to the start of operation of the unit. No time-dependent consolidation settlement is anticipated. Any additional settlement after completion is considered not significant.

2.5.4.10.4 Earth Pressures

PTN COL 2.5-7
PTN COL 2.5-11

The static and seismic active and at-rest lateral earth pressures acting on underground structure below-grade walls are addressed in this subsection. The analysis of seismic earth pressure is addressed generically. Note that active earth pressures apply to yielding walls such as steel sheet pile walls, MSE walls, and, to a lesser extent, more rigid concrete slurry (diaphragm) walls, which are used primarily as temporary ground support in construction. At-rest earth pressures occur in the case of non-yielding walls, such as the rigid, below-grade walls of underground structures (e.g., for the containment/auxiliary buildings, control buildings, etc.).

Increases in lateral earth pressures resulting from compaction close-in to below-grade structures are not considered here. These increases are controlled at the construction stage by limiting the size of compaction equipment and its proximity to below-grade walls. Note that the magnitude of compaction-induced earth pressure increases can only be assessed once a range of allowable equipment sizes and types are selected/specified.

For the seismic active and at-rest earth pressure cases, earthquake-induced horizontal ground accelerations are accounted for by employing the factor $k_h g$. Here, $k_h = 0.1$ is used. Vertical ground accelerations ($k_v g$) are considered negligible ([Reference 276](#)).

2.5.4.10.4.1 Static Lateral Earth Pressures

The static active earth pressure, p_{AS} , is calculated using [Reference 225](#):

$$p_{AS} = K_{AS} \cdot \gamma \cdot z \quad \text{Equation 2.5.4-24}$$

Where,

K_{AS} = Rankine coefficient of static active lateral earth pressure

γ = unit weight of the structural fill and general fill (γ' , effective unit weight when below the groundwater level)

z = depth bgs

The Rankine coefficient, K_{AS} , is calculated from:

$$K_{AS} = \tan^2 (45 - \phi'/2) \quad \text{Equation 2.5.4-25}$$

Where,

ϕ' = effective friction angle of the structural fill and general fill, in degrees

The static at-rest earth pressure, p_{0S} , is calculated using [Reference 225](#):

$$p_{0S} = K_{0S} \cdot \gamma \cdot z \quad \text{Equation 2.5.4-26}$$

Where,

K_{0S} = coefficient of at-rest static lateral earth pressure

The coefficient, K_{0S} , is calculated from:

$$K_{0S} = 1 - \sin(\phi') \quad \text{Equation 2.5.4-27}$$

Hydrostatic groundwater pressure is considered for both the active and the at-rest static conditions, calculated by:

$$p_w = \gamma_w \cdot z_w \quad \text{Equation 2.5.4-28}$$

Where,

p_w = hydrostatic pressure

z_w = depth below the groundwater level

γ_w = unit weight of water = 62.4 pcf

2.5.4.10.4.2 Seismic Lateral Earth Pressures

The active seismic pressure, p_{AE} , is given by the Mononobe-Okabe equation ([Reference 276](#)), represented by:

$$p_{AE} = \Delta K_{AE} \cdot \gamma \cdot (H - z) \quad \text{Equation 2.5.4-29}$$

Where,

ΔK_{AE} = coefficient of active seismic earth pressure = $K_{AE} - K_{AS}$

K_{AE} = Mononobe-Okabe coefficient of active seismic earth thrust

H = below-grade height of the wall

The coefficient K_{AE} is calculated from:

$$K_{AE} = \cos^2 (\phi' - \theta) / \{ \cos^2 \theta \cdot [1 + (\sin \phi' \sin (\phi' - \theta) / \cos (\theta))^{0.5}]^2 \} \quad \text{Equation 2.5.4-30}$$

Where,

$$\theta = \tan^{-1} (k_h)$$

k_h = horizontal earthquake acceleration, as in [Subsection 2.5.4.10.4](#).

Using the ASCE 4-98 method ([Reference 277](#)), the design ground motion is used to calculate a seismic at-rest pressure as a function of depth for below-grade walls.

2.5.4.10.4.3 Lateral Earth Pressures Due to Surcharge

Lateral earth pressure resulting from surcharge applied at the ground surface alongside a below-grade structure wall, p_{sur} , is calculated using:

$$p_{sur} = K q \quad \text{Equation 2.5.4-31}$$

Where,

K = earth pressure coefficient; K_{AS} for active, K_0 for at-rest, ΔK_{AE} or ΔK_{OE} for seismic loading, depending on the nature of the loading (ΔK_{OE} = seismic at-rest coefficient)

q = uniform surcharge pressure

Note that a surcharge pressure of 500 psf is included in the earth pressure calculations summarized here. The validity of this pressure is reviewed during the detailed design phase.

2.5.4.10.4.4 Lateral Earth Pressure Diagrams

Using the relationships outlined above and the compacted limerock fill properties summarized in [Table 2.5.4-209](#), sample earth pressure diagrams are developed. Compacted limerock fill properties (granular soils) used have a unit weight (γ_t) of 130 pcf and a drained friction angle (ϕ') of 33 degrees (refer to [Table 2.5.4-209](#)). These values apply to both structural and general fill. A uniform surcharge load of 500 psf is included.

2.5.4.10.5 Sample Earth Pressure Diagrams

Recommended diagrams for use in calculating lateral earth pressures against walls are developed based on strata thicknesses and lateral earth pressure

coefficients. **Figure 2.5.4-239** shows the diagram for above grade walls where the walls can rotate or deflect away from the soil mass, known as the active case. This case considered walls extending from the highest finish grade (El. +25.5 feet) to a depth of El. -35 feet, and models active earth pressures on the diaphragm wall during the construction period.

Figure 2.5.4-240 shows the pressure diagram for below grade walls where no rotation is possible (at-rest case). This case considers walls from El. +25.5 feet to El. -14 feet, the base of the deepest structure wall.

2.5.4.10.6 Selected Design Parameters and Results Overview

The results of the investigation indicate that the site is underlain by rock overlying unconsolidated deposits. The risk of subsidence due to karst is not considered significant. The risk associated with settlement is considered insignificant. A summary of the parameters recommended for geotechnical design is presented in **Table 2.5.4-209**.

2.5.4.11 Design Criteria and References

PTN COL 2.5-3

The design criteria summarized below are geotechnical design criteria and/or geotechnical-related design criteria that pertain to structural design. Refer to the respective subsections above for additional details.

Under “Factor of Safety Against Liquefaction,” RG 1.198 indicates that $FOS < 1.10$ is generally considered a trigger value. The $FOS = 1.25$ selected for the analysis of site soils is considered appropriate and conservative, especially when also considering the conservatism employed in ignoring the rock overburden, the depth, and the geologic age of the deposits.

Subsection 2.5.4.10 describes allowable bearing capacities and estimated settlement values for plant structures, and compares them to threshold values published in the DCD.

Table 2.5.4-217 contains calculated bearing capacities, both static and dynamic, for Units 6 & 7 Seismic Category I structures. In the case of static bearing capacity, a minimum $FOS = 3.0$ is applied against the calculated ultimate bearing capacity in evaluating the static bearing capacity of a structure. In the case of dynamic bearing capacity, the calculated ultimate bearing capacity is typically compared directly against the required dynamic bearing capacity of a structure

(i.e., the calculated allowable bearing capacity of subsurface materials for normal loads plus the SSE as per the DCD). (Because the SSE in the DCD has a 0.3g peak ground acceleration that is much higher than that anticipated for South Florida, the dynamic bearing capacity in the DCD is substantially higher than the maximum dynamic loading that would be realized at the site). For the Units 6 & 7 Category I structures, the computed allowable bearing capacity (including FOS = 3.0) of 43 ksf exceeds the DCD maximum dynamic loading of 35 ksf.

Table 2.5.4-219 contains estimated settlements of Units 6 & 7 Seismic Category I structures and other structures under design foundation loads. The calculated total settlements are less than the threshold described in Table 2.5-1 of the DCD.

Subsection 2.5.4.10 also addresses criteria for static and seismic earth pressure estimation. The calculated lateral earth pressure diagrams shown on Figures 2.5.4-239 and 2.5.4-240 are best estimates, and thus contain a FOS = 1.0. In the analyses of sliding and overturning due to these lateral loads when the seismic component is included, a FOS = 1.10 is recommended.

PTN COL 2.5-7 2.5.4.12 Techniques to Improve Subsurface Conditions

Given the depths of structure foundations and the subsurface conditions that occur at those depths, as shown in part on Figures 2.5.4-221 and 2.5.4-222, special ground improvement measures are not warranted. Ground treatment is limited to over-excavation of unsuitable materials, such as zones of less competent materials occurring at foundation subgrades, and their replacement with lean concrete fill. Groundwater control is required as part of this over-excavation as described in Subsections 2.5.4.5 and 2.5.4.6.

Over-excavation of approximately 21 feet at the reactor/auxiliary building is designed to replace soils and weak rock that are not adequate to directly support the high foundation loads of these structures, with the required FOS. For all affected structures, compacted limerock fill and lean concrete fill are placed according to engineering specifications and quality control/quality assurance testing procedures established during detailed design phase.

According to ACI 207 (Reference 281), the lean concrete fill under the Nuclear Island is defined as mass concrete. A thermal control plan considering the geometry of the fill concrete, the proposed 1,500 psi strength, total volume of fill

concrete placement, and rate of concrete production, will be prepared to minimize thermal cracking in accordance with ACI 207 guidelines.

Across the entire plant area, the muck of Stratum 1 is removed and replaced with compacted limerock fill as described in [Subsection 2.5.4.5.1.1](#).

2.5.4.13 References

201. Not Used. |
202. Sinclair, W., and J. Stewart, *Sinkhole Type, Development, and Distribution in Florida*, U.S. Geological Survey, Map Series No. 110, 1985.
203. Lane, E., *Karst in Florida*, Special Publication 29, Florida Geological Survey, 1986.
204. Renken, R., J. Dixon, J. Koehmstedt, S. Ishman, A. Lietz, R. Marella, P. Telis, J. Rogers, and S. Memberg, *Impact of Anthropogenic Development on Coastal Ground-Water Hydrology in Southeastern Florida, 1900–2000*, U.S. Geological Survey, Circular 1275, 2005.
205. Vanlier, K., J. Armbruster, Z. Altschuler, and H. Mattraw, *Natural Hazards in Resource and Land Information for South Dade County*, U.S. Geological Survey, Florida Geological Survey Investigation I-850, 1973.
206. Parker, G., G. Ferguson, S. Love, et al., *Water Resources of Southeastern Florida*, U.S. Geological Survey, Water Supply Paper 1255, 1955.
207. Cunningham, K., J. Carlson, G. Wingard, E. Robinson, and M. Wacker, *Characterization of Aquifer Heterogeneity Using Cyclostratigraphy and Geophysical Methods in the Upper Part of the Karstic Biscayne Aquifer, Southeastern Florida*, U.S. Geological Survey, Water-Resources Investigations Report 2003-4208, 2004.
208. Lane, E., *Florida's Geological History and Geological Resources*, Florida Geological Survey, Special Publication 35, 1994.
209. Arthur, J., *Petrogenesis of Early Mesozoic Tholeiite in the Florida Basement and an Overview of Florida Basement Geology*, Florida Geological Survey, Report of Investigations 97, 1988.

Turkey Point Units 6 & 7
COL Application
Part 2 — FSAR

- 210. Salvador, A., *Origin and Development of the Gulf of Mexico Basin*, The Geology of North America, Vol. J, The Gulf of Mexico Basin, Geological Society of America, 1991.
- 211. Reese, R. and E. Richardson, *Synthesis of the Hydrogeologic Framework of the Floridan Aquifer System and Delineation of a Major Avon Park Permeable Zone in Central and Southern Florida*, U.S. Geological Survey, Scientific Investigations Report 2007-5207, 2008.
- 212. Pollastro, R., *1995 USGS National Oil and Gas Play-Based Assessment of the South Florida Basin, Florida Peninsula Province*, National Assessment of Oil and Gas Project: Petroleum Systems and Assessment of the South Florida Basin, U.S. Geological Survey, Digital Data Series 69-A, 2001.
- 213. ASTM International, *Standard Practice for Classification of Soils for Engineering Purposes (Unified Soil Classification System)*, ASTM D 2487-06, Conshohocken, Pennsylvania, 2006.
- 214. ASTM International, *Standard Practice for Description and Identification of Soils (Visual-Manual Procedure)*, ASTM D 2488-06 Conshohocken, Pennsylvania, 2006.
- 215. Dunham, R., *Classification of Carbonate Rocks According to Depositional Texture, Classification of Carbonate Rocks: A Symposium*, American Association of Petroleum Geologists, AAPG Memoir 1, 1962.
- 216. U.S. Department of the Interior Bureau of Reclamation, *Engineering Geology Field Manual*, 2001.
- 217. Bowles, J., *Foundation Analysis and Design*, 5th ed., McGraw-Hill Companies Inc., New York, 1996.
- 218. Schlumberger, *Poisson's Ratio, Oilfield Glossary*. Available at <http://www.glossary.oilfield.slb.com/Display.cfm?Term=Poisson%27s%20ratio>, accessed July 28, 2008.
- 219. Youd, T. et al., *Liquefaction Resistance of Soils: Summary Report from the 1996 National Center for Earthquake Engineering Research (NCEER) and 1998 NCEER/National Science Foundation (NSF) Workshops on Evaluation of Liquefaction of Soils*, ASCE Journal of Geotechnical and

Turkey Point Units 6 & 7
COL Application
Part 2 — FSAR

Environmental Engineering, Vol. 127, No. 10, American Society of Civil Engineers, October 2001.

- 220. ASTM International, *Standard Practice for Determining the Normalized Penetration Resistance of Sands for Evaluation of Liquefaction Potential*, ASTM D 6066-96, Conshohocken, Pennsylvania, 2004.
- 221. Winterkorn, H. and H. Fang, *Soil Technology and Engineering Properties of Soils*, Foundation Engineering Handbook, Van Nostrand Reinhold Co., New York, 1975.
- 222. Robertson, P. and R. Campanella, *Interpretation of Cone Penetration Tests: Part I Sands*, Canadian Geotechnical Journal, Vol. 20(4), pp. 718–733, 1983.
- 223. Naval Facilities Engineering Command, *Foundations & Earth Structures*, Design Manual 7.02, Alexandria, Virginia, 1986.
- 224. Davie, J. and M. Lewis, *Settlement of Two Tall Chimney Foundations*, *Proceedings*, 2nd International Conference on Case Histories in Geotechnical Engineering, St. Louis, Missouri, June 1988.
- 225. Coduto, D., *Foundation Design Principles and Practices*, 2d ed., Prentice Hall, New Jersey, 2001.
- 226. Senapathy, H., J. Clemente, and J. Davie, *Estimating Dynamic Shear Modulus in Cohesive Soils*, XVth International Conference on Soil Mechanics and Geotechnical Engineering, Istanbul, Turkey, 2001.
- 227. American Petroleum Institute, *Cathodic Protection of Aboveground Petroleum Storage Tanks*, API Recommended Practice 651, 3d ed., Washington, D.C., 2007.
- 228. STS Consultants Inc., *Reinforced Soil Structures*, Vol. 1, Design and Construction Guidelines, FHWA Report No. FHWA-RD-89-043, McLean, Virginia., 1990.
- 229. Federal Highway Administration, *Corrosion/Degradation of Soil Reinforcements for Mechanically Stabilized Earth Walls and Reinforced Soil Slopes*, FHWA Publication FHWA-NHI-00-044, 2000.

Turkey Point Units 6 & 7
COL Application
Part 2 — FSAR

- 230. American Concrete Institute, *Manual of Concrete Practice, Part 1, Materials and General Properties of Concrete*, Detroit, Michigan, 1994.
- 231. Florida Power & Light Company, *Updated Final Safety Analysis Report, Turkey Point Nuclear Units 3 & 4*, Miami-Dade County, Florida, Docket Nos. 50-250 and 50-251, 1992.
- 232. ASTM International, *Standard Practice for Rock Core Drilling and Sampling for Site Investigation*, ASTM D 2113-08, Conshohocken, Pennsylvania, 2005.
- 233. ASTM International, *Standard Practice for Thin-Walled Tube Sampling of Undisturbed Soils for Geotechnical Purposes*, ASTM D 1587, Conshohocken, Pennsylvania, 2008.
- 234. ASTM International, *Standard Practices for Preserving and Transporting Soil Samples*, ASTM D 4220-95, Conshohocken, Pennsylvania, 2007.
- 235. ASTM International, *Standard Test Method for Energy Measurement for Dynamic Penetrometers*, ASTM D 4633-05, Conshohocken, Pennsylvania, 2005.
- 236. ASTM International, *Standard Practices for Preparing Rock Core as Cylindrical Test Specimens and Verifying Conformance to Dimensional and Shape Tolerances*, ASTM D 4543-08, Conshohocken, Pennsylvania, 2008.
- 237. ASTM International, *Standard Test Methods Laboratory Determination of Water (Moisture) Content of Soil and Rock by Mass*, ASTM D 2216-05, Conshohocken, Pennsylvania, 2005.
- 238. ASTM International, *Standard Test Methods Specific Gravity of Soil Solids by Water Pycnometer*, ASTM D 854-06, Conshohocken, Pennsylvania, 2006.
- 239. ASTM International, *Standard Test Method for Particle-Size Analysis of Soils*, ASTM D 422-63, for Analysis Including Hydrometer, Conshohocken, Pennsylvania, 2007.
- 240. ASTM International, *Standard Test Methods for Particle-Size Distribution (Gradation) of Soils Using Sieve Analysis*, ASTM D 6913-04, for analysis not including hydrometer, Conshohocken, Pennsylvania, 2004.

Turkey Point Units 6 & 7
COL Application
Part 2 — FSAR

- 241. ASTM International, *Standard Test Methods for Liquid Limit, Plastic Limit, and Plasticity Index of Soils*, ASTM D 4318-05, Conshohocken, Pennsylvania, 2005.
- 242. ASTM International, *Standard Test Methods for Moisture, Ash, and Organic Matter of Peat and Other Organic Soils*, ASTM D 2974-07a, Conshohocken, Pennsylvania, 2007.
- 243. ASTM International, *Standard Test Methods for Measurement of Hydraulic Conductivity of Saturated Porous Materials Using a Flexible Wall Permeameter*, ASTM D 5084-03, Conshohocken, Pennsylvania, 2003.
- 244. ASTM International, *Standard Test Method for Rapid Determination of Carbonate Content of Soils*, ASTM D 4373-02, Conshohocken, Pennsylvania, 2007.
- 245. ASTM International, *Standard Test Methods for Laboratory Compaction Characteristics of Soil Using Modified Effort*, ASTM D 1557-07, Conshohocken, Pennsylvania, 2007.
- 246. ASTM International, *Standard Test Method for CBR (California Bearing Ratio) of Laboratory-Compacted Soils*, ASTM D 1883-07, Conshohocken, Pennsylvania, 2007.
- 247. Florida Department of Transportation, *Florida Method of Test for Limerock Bearing Ratio*, FDOT FM-5-515, 2000.
- 248. ASTM International, *Standard Test Method for Compressive Strength and Elastic Moduli of Intact Rock Core Specimens Under Varying States of Stress and Temperatures*, ASTM D 7012-07, Conshohocken, Pennsylvania, 2007.
- 249. ASTM International, *Standard Test Method for Consolidated Undrained Triaxial Compression Test for Cohesive Soils*, ASTM D 4767-04, Conshohocken, Pennsylvania, 2004.
- 250. U.S. Environmental Protection Agency, *Soil and Waste pH*, Method SW 846 9045D, last updated September 17, 2008.
- 251. U.S. Environmental Protection Agency, *Methods for Chemical Analysis of Water and Wastes*, EPA-600/4-79-020, March 1983 and subsequent revisions.

Turkey Point Units 6 & 7
COL Application
Part 2 — FSAR

- 252. ASTM International, *Standard Guide for Conducting Borehole Geophysical Logging — Gamma*, ASTM D6274-98(04), Conshohocken, Pennsylvania, reapproved 2004.
- 253. ASTM International, *Standard Guide for Conducting Borehole Geophysical Logging in Mechanical Caliper*, ASTM D 6167-97(04), Conshohocken, Pennsylvania, 2004.
- 254. ASTM International, *Standard Guide for Planning and Conducting Borehole Geophysical Logging*, ASTM D 5753-05, Conshohocken, Pennsylvania, 2005.
- 255. ASTM International, *Standard Guide for Using the Seismic Refraction Method for Subsurface Investigation*, ASTM D 5777-00, Conshohocken, Pennsylvania, 2000.
- 256. Occupational Safety and Health Administration, *Safety and Health Regulations for Construction*, 29 CFR Part 1926, 2000.
- 257. MACTEC Engineering and Consulting, Inc., *Final Data Report—Geotechnical Exploration and Testing: Turkey Point COL Project Florida City, Florida*, Rev. 2, included in COL Application Part 11, October 6, 2008.
- 258. Electric Power Research Institute, *Guidelines for Determining Design Basis Ground Motions*, Vol. 1-5, EPRI Report TR-102293, Palo Alto, California, 1993.
- 259. Sun, J., R. Golesorkhi, and H. Seed, *Dynamic Moduli and Damping Ratios for Cohesive Soils*, Earthquake Engineering Research Center, Report 88/15, University of California, Berkeley, 1988.
- 260. Seed, H., R. Wong, I. Idriss, and K. Tokimatsu, *Moduli and Damping Factors for Dynamic Analyses of Cohesionless Soils*, Earthquake Engineering Research Center, Report EERC 84/14, University of California, Berkeley, 1984.
- 261. Youd, T. and D. Perkins, *Mapping Liquefaction-Induced Ground Failure Potential*, ASCE Journal of the Geotechnical Engineering Division, Vol. 104, No. GT4, 1978.
- 262. Amick, D., G. Maurath, and R. Gelinas, *Characteristics of Seismically Induced Liquefaction Sites and Features Located in the Vicinity of the*

Turkey Point Units 6 & 7
COL Application
Part 2 — FSAR

1886 Charleston, South Carolina Earthquake, Seismological Research Letters, Vol. 61, No. 2, pp. 117–130, 1990.

- 263. Palmer, S., S. Magsino, E. Bilderback, J. Poelstra, D. Folger, and R. Niggemann, *Liquefaction Susceptibility and Site Class Maps of Washington State, by County*, Open-File Report 2004-20, Washington Division of Geology and Earth Resources, September 2004.
- 264. Rauch, A., *EPOLLS: An Empirical Method for Predicting Surface Displacements Due to Liquefaction-Induced Lateral Spreading in Earthquakes*, doctoral dissertation, Virginia Polytechnic Institute and State University, May 5, 1997.
- 265. California Geological Survey, *Guidelines for Evaluating and Mitigating Seismic Hazards in California*, Special Publication 117, updated 2008.
- 266. Sykora, D. and D. Yule, *Reassessment of Liquefaction Potential and Estimation of Earthquake-Induced Settlements at Paducah Gaseous Diffusion Plant, Paducah, Kentucky*, U.S. Army Corps of Engineers, April 1996.
- 267. Amick, D., R. Gelinas, G. Maurath, R. Cannon, D. Moore, E. Billington, and H. Kemppinen, *Paleoliquefaction Features Along the Atlantic Seaboard*, U.S. NRC Report NUREG/CR-5613, 1990.
- 268. Idriss, I., and R. Boulanger, *Soil Liquefaction During Earthquakes*, Earthquake Engineering Research Institute Engineering Monograph MNO-12, Oakland, California, 2008.
- 269. Lewis, M. I. Arango, and M. McHood, *Site Characterization Philosophy and Liquefaction Evaluation of Aged Sands — A Savannah River Site and Bechtel Perspective*, J. Laier, D. Crapps, and H. Mohamad (eds.) From Research to Practice in Geotechnical Engineering, ASCE Geotechnical Special Publication 180, 2008.
- 270. Southern California Earthquake Center of University of Southern California, *Recommended Procedures for Implementation of DMG Special Publication 117*, Guidelines for Analyzing and Mitigating Liquefaction Hazards in California, 1999.

Turkey Point Units 6 & 7
COL Application
Part 2 — FSAR

- 271. Ishihara, K., *Stability of Natural Deposits During Earthquakes*, Proceedings, 11th International Conference on Soil Mechanics and Foundation Engineering, Vol. 1, Balkema, Rotterdam, The Netherlands, pp. 321–376, 1985.
- 272. Wyllie, D., *Foundations on Rock*, 2d ed., E&FN SPON, New York, 1999.
- 273. American Concrete Institute, *Code Requirements for Nuclear Safety-Related Concrete Structures* (ACI 349-06) and Commentary, Detroit, Michigan, 2006.
- 274. American Association of State Highway and Transportation Officials, *LRFD Bridge Design Specification*, 2d ed., Washington, D.C., 1998.
- 275. Poulos, H. and E. Davis, *Elastic Solutions for Soil and Rock Mechanics*, John Wiley & Sons, New York, 1974.
- 276. Seed, H. and R. Whitman, *Design of Earth Retaining Structures for Dynamic Loads, Proceeding of the Specialty Conference on Lateral Stresses in the Ground and Design of Earth-Retaining Structures*, American Society of Civil Engineers, New York, 1970.
- 277. American Society of Civil Engineers, *Seismic Analysis of Safety-Related Nuclear Structures and Commentary*, Standard 4-98, ASCE, Reston, Virginia, 1998.
- 278. Telford, W. L. Geldart, R. Sheriff, and D. Keys, *Applied Geophysics*, Cambridge University Press, 1976.
- 279. Not Used.
- 280. Not Used.
- 281. American Concrete Institute, *Guide to Mass Concrete* (ACI 207), Detroit, Michigan, 2006.
- 282. Kulhawy, F. and P. Mayne, *Manual on Estimating Soil Properties for Foundation Design*, Report No. EL-6800, EPRI, August 1990.
- 283. Not Used.
- 284. Not Used.

Turkey Point Units 6 & 7
COL Application
Part 2 — FSAR

285. Not Used.
286. Technos, Inc., *Geophysical Survey for Karst Characterization at Proposed Units 6 and 7 Turkey Point Nuclear Plant, Miami-Dade County, Florida*, prepared for MACTEC Engineering and Consulting, Inc., Project No. 08-148, March 27, 2009.
287. McNabb Hydrogeologic Consulting, Inc., *Report on the Construction and Testing of Class V Exploratory Well EW-1 at the Florida Power & Light Company Turkey Point Units 6 & 7*, Vol. 1, in Turkey Point Units 6 & 7 Site Certification Application Amendment Rev. 2, September 2012. Available at http://publicfiles.dep.state.fl.us/Siting/Outgoing/FPL_Turkey_Point/Units_6_7/Amendment_Application_Rev2/08_APPENDIX%2010.2.8.pdf, accessed January 10, 2013.
288. South Carolina Electric & Gas Company, *Final Safety Analysis Report*, V.C. Summer Nuclear Units 2 & 3, Figure 2.5.4- 224, Docket Nos. 52-027 and 52-028, South Carolina, August 17, 2011.
289. Tennessee Valley Authority, *Final Safety Analysis Report, Bellefonte Nuclear Units 3 & 4*, Figure 2.5.4-331, Docket Nos. 52-014 and 52-015, Alabama, January 21, 2009.

Turkey Point Units 6 & 7
COL Application
Part 2 — FSAR

PTN COL 2.5-1
PTN COL 2.5-5
PTN COL 2.5-6
PTN COL 2.5-10

Table 2.5.4-201
Summary of Layer Thicknesses

ALL AREAS INVESTIGATED									For Use	
Stratum	Layer Thickness				El. of Bottom of Layer				Top	Bottom
	Min	Max	Average	Median	Min	Max	Average	Median	El.	El.
	(ft)	(ft)	(ft)	(ft)	(ft)	(ft)	(ft)	(ft)	(ft)	(ft)
Muck	2.0	7.0	3.4	3.2	-8.2	-3.3	-4.6	-4.5	-1.2	-4.5
Miami Limestone	17.2	30.3	22.6	22.0	-35.3	-24.1	-27.2	-26.3	-4.5	-26.7
Key Largo Limestone	13.5	28.0	22.3	23.0	-53.4	-44.1	-49.5	-49.4	-26.7	-49.4
Fort Thompson Formation	60.0	68.4	65.6	65.7	-117.7	-108.3	-115.1	-115.1	-49.4	-115.1
Tamiami Formation	98.5	215.0	116.9	101.0	-217.5	-213.1	-215.5	-214.9	-115.1	-215.2
Peace River Formation	239.0	239.0	239.0	239.0	-452.1	-452.1	-452.1	-452.1	-215.2	-452.1
Arcadia Formation	—	—	>164.5	—	—	—	<-616.6	—	-452.1	<-616.6

Data from [Reference 257](#)

Turkey Point Units 6 & 7
COL Application
Part 2 — FSAR

PTN COL 2.5-6

Table 2.5.4-202
Summary of Uncorrected N-Values

Stratum	Muck	Miami Limestone	Key Largo Limestone	Fort Thompson Formation	Upper Tamiami Formation	Lower Tamiami Formation	Peace River Formation	Arcadia Formation
Number of Tests	106	619	110	35	253	72	64	2
Minimum N	0	0	2	0	0	2	2	42
Maximum N	7	100	100	100	100	100	100	100
Average N ^(a)	0	25	71	51	18	16	60	71

(a) Averaged to nearest whole number

Data from [Reference 257](#)

Turkey Point Units 6 & 7
COL Application
Part 2 — FSAR

PTN COL 2.5-6

Table 2.5.4-203
SPT Hammer Efficiency Corrections

Drill Rig	Rods	Number of Measurements	Min. ETR ^(a) (%)	Max. ETR (%)	Avg. ETR (%)	C _e (Avg. ETR%/60%)
MACTEC Atlanta CME 55LC (Hammer Serial No. MEC-02)	AW-J	3	81.7	86.6	83.7	1.40
MACTEC Atlanta CME 550 Marsh Buggy (Hammer Serial No. 893)	AW-J	8	84.6	94.0	88.0	1.47
MACTEC Atlanta CME 550 ATV (Hammer Serial No. MEC-03)	AW-J	3	77.1	82.3	79.6	1.33
MACTEC Atlanta CME 550 ATV (Hammer Serial No. MEC-04)	AW-J	4	79.4	83.1	80.4	1.34
MACTEC Atlanta 550 Track Rig (Hammer Serial No. MEC-05) ^(b)	AW-J NW-J	6	80.0	88.0	83.6	1.39
Miller Drilling CME 550 ATV (Hammer Serial No. M06)	AW-J	4	81.1	84.9	83.6	1.39
Miller Drilling CME 750 ATV (Hammer Serial No. 07) ^(c)	AW-J NW-J	9	79.7	89.4	83.4	1.45
MACTEC Charlotte CME 75 (Hammer Serial No. MEC-09)	NW-J	3	77.1	84.3	82.8	1.38
MACTEC Atlanta (Raleigh) CME 45C (Hammer Serial No. MEC-12)	AW-J	6	79.4	89.7	83.2	1.39
MACTEC Atlanta CME 55 ATV (Hammer Serial No. MEC-425)	NW-J	4	76.0	91.4	87.4	1.46

- (a) ETR = energy transfer ratio = the percent of measured SPT hammer energy versus the theoretical SPT hammer energy (350 ft-pounds).
- (b) Both AW-J and NW-J rods were used with this rig. The average for the AW-J rods was 82.2 percent. The average for the NW-J rods was 86.3 percent.
- (c) Both AW-J and NW-J rods were used with this rig. The average for the AW-J rods was 81.8 percent. The average for the NW-J rods was 88.9 percent.

Turkey Point Units 6 & 7
COL Application
Part 2 — FSAR

PTN COL 2.5-6

Table 2.5.4-204
Summary of Corrected N-Values (N₆₀)

Stratum	Muck	Miami Limestone	Key Largo Limestone	Fort Thompson Formation	Upper Tamiami Formation	Lower Tamiami Formation	Peace River Formation	Arcadia Formation
Number of Tests	106	619	110	35	253	72	64	2
Minimum N	0	0	3	0	0	3	3	68
Maximum N	8	100	100	100	100	100	100	100
Average N ^(a)	0	29	78	60	27	23	72	84

(a) Averaged to nearest whole number

Data from [Reference 257](#)

Turkey Point Units 6 & 7
COL Application
Part 2 — FSAR

PTN COL 2.5-6

Table 2.5.4-205 (Sheet 1 of 2)
Summary of General Physical and Chemical Properties Test Results

Stratum	Description of Value	SIEVE ANALYSIS					Specific Gravity G_s	Dry Unit Weight γ (pcf)	Natural Moisture Content w (%)	ATTERBERG LIMITS			CHEMICAL TESTS			
		Gravel (%)	Sand (%)	Fines (%)	Silt (%)	Clay (%)				LL (%)	PL (%)	PI (%)	Calcite (%)	pH	Chloride (ppm)	Sulfate (ppm)
Muck	Number of Tests	1	1	1	—	—	—	—	—	—	—	—	—	1	1	1
	Minimum	0	55	45	—	—	—	—	—	—	—	—	—	7.4	70,400	7,590
	Maximum	0	55	45	—	—	—	—	—	—	—	—	—	7.4	70,400	7,590
	Average	0	55	45	—	—	—	—	—	—	—	—	—	7.4	70,400	7,590
Miami Limestone	Number of Tests	61	61	61	7	7	2	—	—	—	—	—	15	5	5	5
	Minimum	0	18	1	6	6	2.73	—	—	—	—	—	86	8.3	3,250	334
	Maximum	71	92	49	23	26	2.73	—	—	—	—	—	95	8.9	8,830	1,190
	Average	39	43	18	11	12	2.73	—	—	—	—	—	91	8.6	5,870	762
Key Largo Limestone	Number of Tests	5	5	5	—	—	1	32	32	—	—	—	—	1	1	1
	Minimum	14	24	9	—	—	2.65	103.9	3.3	—	—	—	—	8.7	2,540	461
	Maximum	59	69	40	—	—	2.65	151.4	20.6	—	—	—	—	8.7	2,540	461
	Average	37	45	18	—	—	2.65	123.9	10.3	—	—	—	—	8.7	2,540	461
Upper Tamiami Formation	Number of Tests	74	74	74	37	37	4	1	1	5	5	5	17	8	8	8
	Minimum	0	31	8	2	5	2.66	120.1	32.5	18	14	1	11	8.3	4,290	560
	Maximum	57	92	61	49	15	2.67	120.1	32.5	25	24	10	40	8.7	7,020	1,180
	Average	6	66	29	18	10	2.66	120.1	32.5	23	19	4	20	8.4	5,400	941

Turkey Point Units 6 & 7
COL Application
Part 2 — FSAR

PTN COL 2.5-6

Table 2.5.4-205 (Sheet 2 of 2)
Summary of General Physical and Chemical Properties Test Results

Stratum	Description of Value	SIEVE ANALYSIS					Specific Gravity G _s	Dry Unit Weight γ (pcf)	Natural Moisture Content w (%)	ATTERBERG LIMITS			CHEMICAL TESTS			
		Gravel (%)	Sand (%)	Fines (%)	Silt (%)	Clay (%)				LL (%)	PL (%)	PI (%)	Calcite (%)	pH	Chloride (ppm)	Sulfate (ppm)
Lower Tamiami Formation	Number of Tests	26	26	26	11	11	—	3	4	13	13	13	5	—	—	—
	Minimum	0	21	26	44	8	—	116.3	29.8	21	12	1	22	—	—	—
	Maximum	1	74	79	61	18	—	118.7	31.4	34	24	13	29	—	—	—
	Average	0	38	62	53	12	—	117.4	30.7	26	21	5	25	—	—	—
Peace River Formation	Number of Tests	19	19	19	7	7	2	3	3	6	6	6	3	—	—	—
	Minimum	0	28	6	5	5	2.68	121.3	22.1	20	4	2	20	—	—	—
	Maximum	0	94	72	48	9	2.70	121.9	23.6	24	21	17	34	—	—	—
	Average	0	77	23	16	7	2.69	121.5	22.8	22	16	6	25	—	—	—

Data from [Reference 257](#)

Notes:

LL = Liquid Limit

PL = Plastic Limit

PI = Plasticity Index

PPM = Parts Per Million (equivalent to milligrams per kilogram)

Turkey Point Units 6 & 7
COL Application
Part 2 — FSAR

PTN COL 2.5-6

Table 2.5.4-206
Summary of Recovery and RQD Values for Rock Strata

Stratum	Description of Value	Recovery (%)	RQD (%)	No. of Samples	
				Recovery	RQD
Key Largo	Minimum	0	0	333	333
	Maximum	100	100		
	Average	86	65		
Fort Thompson	Minimum	0	0	1099	1098
	Maximum	100	100		
	Average	68	40		
Arcadia	Minimum	18	0	34	34
	Maximum	100	100		
	Average	82	57		

Data from [Reference 257](#)

Turkey Point Units 6 & 7
COL Application
Part 2 — FSAR

PTN COL 2.5-6

Table 2.5.4-207
Summary of Unconfined Strength Testing of Rock

Stratum	Number of Tests		Description of Value	Unconfined Compressive Strength (psi)	Unit Weight (psf)
	For Unconfined Compressive Strength	For Unit Weight			
Key Largo	31	32	Minimum	309	114.9
			Maximum	7800	156.4
			Average	2729	136.2
Fort Thompson	46	56	Minimum	172	109.7
			Maximum	5031	153.2
			Average	2269	135.5
Arcadia	3	5	Minimum	18	124.3
			Maximum	310	133.9
			Average	141	129.0

Data from [Reference 257](#)

psi = pounds per square inch

psf = pounds per square foot

Turkey Point Units 6 & 7
COL Application
Part 2 — FSAR

PTN COL 2.5-6

Table 2.5.4-208
Summary of Triaxial Testing Results

Borehole B-630		
Sample No.		UD 12
Sample Depth (ft)		178.9
USCS		ML
Gradation	Sand (%)	33.0
	Silt (%)	55.7
	Clay (%)	11.3
Atterberg Limits	LL (%)	21
	PI (%)	1
Triaxial Test Data	c (ksf)	1.88
	ϕ (°)	14
	c' (ksf)	1.7
	ϕ' (°)	20
Total Unit Weight (3 subsamples)	γ_t (pcf)	115.41
		115.27
		115.80
Moisture Content (3 subsamples)	w (%)	30.13
		32.21
		31.75
Dry Unit Weight (pcf) (3 subsamples)	γ_d (pcf)	88.69
		87.19
		87.89

Data from [Reference 257](#)

Turkey Point Units 6 & 7
COL Application
Part 2 — FSAR

PTN COL 2.5-6
PTN COL 2.5-7
PTN COL 2.5-10
PTN COL 2.5-11
PTN COL 2.5-12
PTN COL 2.5-16

Table 2.5.4-209 (Sheet 1 of 2)
Summary of Recommended Geotechnical Engineering Parameters

Stratum ^(a)	1 ^(a)	2	3	4	5	6	7	8	Fill
Description	Muck	Miami	Key Largo	Ft. Thompson	Upper Tamiami	Lower Tamiami	Peace River	Arcadia	—
Elevation of top of layer (ft)	−1.2	−4.5	−26.7	−49.4	−115.1	−159.0	−215.2	−452.1	—
USCS symbol	ML, MH	GM, GP-GM, SM, SW-SM, SW, SP-SM	Limestone	Limestone	SM, SP-SM	ML	SM	Limestone	—
Total unit weight, γ (pcf)	80	125	136	139	120	120	120	130	130
Natural water content, w , (%)	>80	—	—	—	—	30	—	—	33
Fines content (%)	>60	18	—	—	28	62	16	—	15
Atterberg limits									
Liquid limit, LL	—	—	—	—	—	24	—	—	—
Plastic limit, PL	—	—	—	—	—	20	—	—	—
Plasticity index, PI	—	—	—	—	—	4	—	—	—
SPT N_{60} -value (blows/ft)	~0	20	—	—	40	32	75	—	30
Undrained properties									
Undrained shear strength, s_u (ksf)	—	—	—	—	—	4.0	—	—	—
Internal friction angle, ϕ , (deg)	—	—	—	—	—	—	—	—	—
Drained properties									
Effective cohesion, c' (ksf)	—	—	—	—	0	1.7	0	—	—
Effective friction angle, ϕ' (deg)	—	—	—	—	35	20	40	—	33
Average Rock core recovery (%)	—	—	83 to 96	41 to 98	—	—	—	63 to 100	—
Average RQD (%)	—	—	54 to 81	16 to 91	—	—	—	32 to 90	—
Unconfined compressive strength, U (psi)	—	200	1,500	2,000	—	—	—	100	—
Elastic modulus (high strain), E_H	—	630 ksi	2,600 ksi	1,500 ksi	1,500 ksf	2,500 ksf	2,700 ksf	980 ksi	1,100 ksf
Elastic modulus (low strain), E_L	—	950 ksi	2,600 ksi	1,500 ksi	19,700 ksf	25,750 ksf	27,400 ksf	980 ksi	9,100 ksf
Shear modulus (high strain), G_H	—	230 ksi	1,000 ksi	550 ksi	550 ksf	900 ksf	1,000 ksf	360 ksi	420 ksf
Shear modulus (low strain), G_L	—	350 ksi	1,000 ksi	550 ksi	7,300 ksf	9,500 ksf	10,150 ksf	360 ksi	3,500 ksf
Shear wave velocity, V_s , (ft/sec)	—	3,600	5,800	4,250	1,400	1,600	1,650	3,600	860
Compression wave velocity, V_c , (ft/sec)	—	8,000	11,000	8,700	2,900	3,300	3,450	7,850	1,600
Coefficient of sliding	—	0.6	0.7	0.7	0.4	0.3	—	—	0.5
Poisson's ratio, μ	—	0.37	0.31	0.34	0.35	0.35	0.35	0.36	0.3
Static earth pressure coefficients									

Turkey Point Units 6 & 7
COL Application
Part 2 — FSAR

Table 2.5.4-209 (Sheet 2 of 2)
Summary of Recommended Geotechnical Engineering Parameters

Stratum^(a)	1^(a)	2	3	4	5	6	7	8	Fill
Active, K_a	—	0.3	—	—	0.27	0.5	—	—	0.3
At-rest, K_o	—	0.5	—	—	0.5	0.66	—	—	0.5

(a) Properties of Stratum 1 (muck) are not provided as this stratum was removed prior to construction.

The values tabulated for use as design guideline only. Refer to specific boring logs, CPT logs, and laboratory test results for appropriate modifications at specific design locations.

USCS = Unified Soil Classification System (ML = silt; MH = silt of high plasticity; GM = silty gravel; GP = poorly graded gravel; SM = silty sand; SW = well graded sand; SP = poorly graded sand)

Turkey Point Units 6 & 7
COL Application
Part 2 — FSAR

PTN COL 2.5-6

Table 2.5.4-210
Summary of Calcite Content Testing Results

Stratum	Description of Value	Calcite Equivalent (%)
Miami Limestone	Number of Tests	17
	Minimum	86
	Maximum	95
	Average	91
Key Largo Limestone	Number of Tests	4
	Minimum	78
	Maximum	93
	Average	89
Fort Thompson Formation	Number of Tests	4
	Minimum	68
	Maximum	95
	Average	87
Tamiami Formation	Number of Tests	22
	Minimum	11
	Maximum	40
	Average	21
Peace River Formation	Number of Tests	3
	Minimum	20
	Maximum	34
	Average	25
Arcadia Formation	Number of Tests	3
	Minimum	78
	Maximum	93
	Average	86

Data from [Reference 257](#)

Turkey Point Units 6 & 7
COL Application
Part 2 — FSAR

PTN COL 2.5-6

Table 2.5.4-211
Guidelines for the Evaluation of Soil Chemistry

Potential for Attack on Buried Steel (Corrosiveness/Chlorides)					
Parameter	Range For Steel Corrosiveness				
	Noncorrosive	Mildly Corrosive	Moderately Corrosive	Corrosive	Very Corrosive
Resistivity (ohm-meters)	>100 ^{(a),(b)}	20–100 ^(a) 50–100 ^(b) >30 ^{(b),(c)}	10–20 ^(a) 20–50 ^(b)	5–10 ^(a) 7–20 ^(b)	<5 ^(a) <7 ^(b)
pH	—	>5 and <10 ^(b)	—	5–6.5 ^(a)	<5 ^(a)
Chlorides (ppm)	—	<200 ^(b)	—	300–1,000 ^(a)	>1,000 ^(a)
Potential for Attack on Concrete in Contact with the Ground (Aggressiveness/Sulphates)					
Recommendations For Normal Weight Concrete Subject To Sulfate Attack ^(d)					
Concrete Exposure	Water Soluble Sulfate (SO ₄) in Soil, %		Cement Type	Maximum Water/Cement Ratio	
Mild	0.00–0.10		—	—	
Moderate	0.10–0.20		II, IP(MS), IS(MS)	0.5	
Severe	0.20–2.00		V ^(e)	0.45	
Very Severe	Over 2.00		V with pozzolan	0.45	

- (a) **Reference 226**
100 ohm – cm = 1 ohm – m
PPM = parts per million (weight) and is equivalent to milligrams/kilograms
- (b) **Reference 227**
% (percent by weight) is converted to ppm(w) or milligrams/kilograms per kilogram with the equivalence
1% = 10,000 ppm
- (c) **Reference 228**
- (d) **Reference 229**
- (e) Alternatively, a blend of Type II cement and a ground granulated blast furnace slag or a pozzolan that gives equivalent sulfate resistance, can be considered

Turkey Point Units 6 & 7
COL Application
Part 2 — FSAR

PTN COL 2.5-6

Table 2.5.4-212 (Sheet 1 of 2)
As-built Boring and CPT Probe Information

Depth (ft)	Boring/CPT/TP Number	Northing (U.S. ft) ^(a)	Easting (U.S. ft) ^(a)	Ground Surface El. (ft) ^(b)	Boring/CPT/TP Number	Northing (US ft) ^(a)	Easting (US ft) ^(a)	Ground Surface El. (ft) ^(b)	Depth (ft)
419.2	B-601(DH)	396,967.9	876,642.9	-1.4	B-710(DH)R	397,087.2	875,781.9	-1.3	15.0
204.1	B-602	397,019.6	876,594.1	-1.4	B-710G(DH)	397,075.1	875,792.2	-1.4	273.5
151.2	B-603	397,018.4	876,697.0	-1.4	B-711	397,085.6	875,884.8	-1.1	151.7
165.0	B-604(DH)	396,915.9	876,591.6	-1.5	B-712	397,082.1	876,022.1	-1.1	128.3
201.0	B-605	396,916.8	876,694.1	-1.7	B-713	397,179.3	875,959.0	-1.1	152.5
151.2	B-606	396,958.9	876,738.0	-1.4	B-714	397,258.7	876,020.6	-1.0	125.6
152.5	B-607	396,830.0	876,644.2	-1.5	B-715	397,259.2	875,908.5	-0.9	150.1
265.4	B-608(DH)	396,829.5	876,735.9	-1.5	B-716	397,214.3	875,872.7	-1.1	126.6
150.7	B-609	396,762.5	876,689.0	-1.5	B-717	397,287.0	875,873.1	-1.1	127.2
269.0	B-610(DH)	397,084.2	876,644.4	-1.4	B-718	397,190.9	875,792.6	-1.2	150.8
151.5	B-611	397,086.7	876,735.0	-1.5	B-719	397,293.2	875,791.3	-1.1	126.7
125.1	B-612	397,085.5	876,869.1	-1.5	B-720(DH)	397,396.7	875,791.1	-0.9	204.9
150.2	B-613	397,162.2	876,809.4	-1.4	B-720G(DH)	397,385.2	875,794.0	-1.1	220.8
128.0	B-614	397,204.1	876,870.7	-1.5	B-721	397,338.0	876,120.1	-1.5	127.4
150.6	B-615	397,167.4	876,761.8	-1.5	B-722	397,434.2	875,979.6	-1.0	103.2
125.0	B-616	397,207.9	876,723.7	-1.2	B-723	397,421.2	875,675.4	-1.0	100.6
126.1	B-617	397,288.1	876,721.7	-1.4	B-724	397,325.5	875,663.2	-0.7	100.0
154.7	B-618	397,207.6	876,643.1	-1.4	B-725	397,099.8	876,111.2	-1.0	126.6
128.7	B-619	397,293.9	876,653.7	-1.7	B-726	396,875.6	876,003.9	-1.4	100.5
215.0	B-620(DH)	397,394.9	876,648.3	-1.5	B-727	397,117.7	875,666.1	-1.3	100.9
126.5	B-621	397,367.6	876,949.3	0.2	B-728	397,070.5	875,620.1	-1.4	126.6
100.2	B-622	397,421.2	876,810.7	0.2	B-729	396,970.7	875,493.4	-1.2	100.9
100.2	B-623	397,422.6	876,523.2	-1.3	B-730	396,868.0	875,621.0	-1.0	103.2
103.2	B-624	397,327.1	876,514.1	-1.4	B-731	396,645.6	875,423.1	-1.5	103.2
126.7	B-625	397,106.5	876,960.5	-1.4	B-732	396,412.1	875,682.4	-1.0	104.5
100.6	B-626	396,874.5	876,857.2	-1.6	B-733	396,117.5	875,897.5	-1.0	103.5
102.0	B-627	396,835.2	876,332.9	-1.3	B-734	395,833.2	875,546.3	-0.6	130.0
127.9	B-628	397,072.9	876,473.2	-1.5	B-735	395,824.7	875,689.4	-0.8	128.0
100.3	B-629	396,971.9	876,346.1	-1.1	B-736	395,808.5	876,107.1	-0.5	125.0
294.0	B-630	396,871.5	876,462.1	-1.5	B-737	395,803.7	876,237.8	-0.6	153.3
100.8	B-631	396,655.1	876,514.1	-1.2	B-738	397,728.1	875,607.3	0.1	101.2
100.3	B-632	396,432.4	876,737.0	-1.6	B-739	396,962.9	876,149.6	-1.6	101.0
100.4	B-633	396,113.3	876,993.9	-1.5	B-740(DHT)	397,137.2*	875,841.7*	-0.8	150.0
127.5	B-634	395,758.2	876,677.2	-0.7	B-802	398,817.1	876,265.7	-1.5	128.5
128.5	B-635	395,770.9	876,798.2	-0.9	B-805	396,883.0	877,239.5	-1.6	125.3
126.0	B-636	395,714.8	877,193.2	-1.1	B-806	395,288.3	877,237.4	-0.4	127.4
150.0	B-637	395,693.1	877,310.3	-0.2	B-807	395,277.5	875,987.8	-0.7	128.5
102.6	B-639	396,963.5	876,998.2	-1.4	B-808	396,204.9	875,331.8	-1.0	126.4
150.0	B-640(DHT)	397,116.6	876,528.3	-0.3	B-809	397,028.0	875,151.3	-1.3	124.5
615.5	B-701(DH)	396,976.1	875,792.3	-1.1	B-810	397,806.7	875,012.4	-1.2	127.0
202.5	B-702	397,017.9	875,745.9	-1.2	B-811	398,325.2	874,953.8	-1.4	127.3
15.0	B-703	397,018.1	875,846.1	-1.3	B-812	398,913.2	875,043.1	-1.4	128.7

Turkey Point Units 6 & 7
COL Application
Part 2 — FSAR

PTN COL 2.5-6

Table 2.5.4-212 (Sheet 2 of 2)
As-built Boring and CPT Probe Information

Depth (ft)	Boring/CPT/TP Number	Northing (U.S. ft) ^(a)	Easting (U.S. ft) ^(a)	Ground Surface El. (ft) ^(b)	Boring/CPT/TP Number	Northing (US ft) ^(a)	Easting (US ft) ^(a)	Ground Surface El. (ft) ^(b)	Depth (ft)
151.5	B-704(DH)	396,930.7	875,741.7	-1.4	B-813	399,047.6	876,097.3	-1.3	126.5
163.5	B-704G(DH)	396,938.6	875,749.0	-1.3	B-814	399,138.9	877,404.8	9.0	153.2
200.0	B-705	396,919.2	875,846.4	-1.3	C-601	397,129.8	876,361.3	-0.1	120– 226.5
151.9	B-706	396,962.5	875,885.3	-1.2	C-602 A	397,116.6	876,528.3	-0.5	120– 221.7
152.0	B-707	396,828.8	875,790.8	-1.8	C-701	397,100.2	875,839.3	-1.4	120– 289.7
266.5	B-708(DH)	396,829.7	875,885.7	-1.4	C-702	397,149.4	876,042.2	0.3	120– 220.8
150.0	B-709	396,760.5	875,840.6	-1.3	—	—	—	—	—
250.9	B-710(DH)	397,086.9	875,792.9	-1.3	—	—	—	—	—

(a) Horizontal northing and easting data are Florida state plane coordinates NAD 83/Adjustment of 1990, Florida East, Zone 0401

(b) Ground surface elevation is with reference to NAVD 88

* Location adjacent to PVC pipe in hole.

CPT = cone penetration test, TP = test pit

Data from [Reference 257](#)

Turkey Point Units 6 & 7
COL Application
Part 2 — FSAR

PTN COL 2.5-6

Table 2.5.4-213
Summary of Test Pit Location

Boring/CPT/TP Number	Northing (US ft) ^(a)	Easting (US ft) ^(a)	Ground Surface Elevation (ft) ^(b)
TP-601	397,105.6	876,035.8	-1.4
TP-701	396,988.2	875,508.5	-1.4

(a) Horizontal northing and easting data are Florida state plane coordinates NAD 83/ Adjustment of 1990, Florida East, Zone 0401

(b) Ground surface elevation is with reference to NAVD 88

CPT = Cone penetration test

TP = Test pit

Data from [Reference 257](#)

PTN COL 2.5-7

Table 2.5.4-214
Summary of Laboratory Compaction, and CBR Results

Test Pit Number	Sample Depth (ft.)	USCS Symbol	Moisture-Density		LBR (%)	CBR			
			Max. Dry Density (pcf)	Optimum Moisture (%)		Molded Density (pcf)	Molded Moisture (%)	Soaked CBR (0.10")	Soaked CBR (0.20")
TP-601	3.2-5	SP-SM	106.5	16.3	112	103.0	15.9	66.5	63.9
						104.5	16.5	69.1	65.8
						107.5	16.9	67.3	78.9
TP-701	3-4.5	SM	106.9	17.4	129	96.1	16.2	22.2	20.9
						96.8	16.5	24.9	21.2
						105.5	16.4	58.9	61.4

Data from [Reference 257](#)

LBR = Lime rock ratio

CBR = California bearing ratio

USCS = Unified Soil Classification System (SM = Silty sand; SP = Poorly graded sand)

Turkey Point Units 6 & 7
COL Application
Part 2 — FSAR

PTN COL 2.5-6

Table 2.5.4-215 (Sheet 1 of 4)
Summary of Measured Shear Wave Velocities and Compressive Wave Velocities

Depth	Moist Unit Weight	Shear Wave Velocity, V_s			Compressive Wave Velocity, V_p		
		Average	Average – stdev	Average + stdev	Average	Average – stdev	Average + stdev
(ft)	(lb/ft ³)	(ft/s)	(ft/s)	(ft/s)	(ft/s)	(ft/s)	(ft/s)
0	80	2,233	—	—	6,322	—	—
5	80	2,233	—	—	6,322	—	—
5	125	2,233	—	—	6,322	—	—
10	125	2,233	—	—	6,322	—	—
10	125	3,961	—	—	8,443	—	—
20	125	3,961	—	—	8,443	—	—
20	125	4,691	—	6,455	9,391	—	11,746
30	125	4,691	2,580	6,455	9,391	6,590	11,746
30	136	5,871	4,785	7,675	11,075	8,983	14,495
40	136	5,871	4,785	7,675	11,075	8,983	14,495
40	136	6,834	5,302	8,194	12,658	9,849	15,339
50	136	6,834	5,302	8,194	12,658	9,849	15,339
50	136	5,665	3,911	7,973	10,676	8,102	14,113
60	136	5,665	3,911	7,973	10,676	8,102	14,113
60	136	4,549	3,186	6,878	9,432	6,881	12,487
70	136	4,549	3,186	6,878	9,432	6,881	12,487
70	136	4,629	2,703	6,413	9,383	6,519	11,984
80	136	4,629	2,703	6,413	9,383	6,519	11,984
80	136	4,570	3,110	6,666	9,130	7,111	12,334
90	136	4,570	3,110	6,666	9,130	7,111	12,334
90	136	4,227	2,548	5,345	8,667	6,470	10,846
100	136	4,227	2,548	5,345	8,667	6,470	10,846
100	136	4,353	2,929	4,900	8,503	7,657	9,437
110	136	4,353	2,929	4,900	8,503	7,657	9,437
110	136	2,072	983	4,843	6,485	5,324	8,950
120	136	2,072	983	4,843	6,485	5,324	8,950
120	120	1,322	1,125	1,624	5,546	5,292	5,808
130	120	1,322	1,125	1,624	5,546	5,292	5,808
130	120	1,748	1,058	2,526	5,953	5,337	6,759
140	120	1,748	1,058	2,526	5,953	5,337	6,759
140	120	1,391	1,025	1,662	5,548	5,235	5,817
150	120	1,391	1,025	1,662	5,548	5,235	5,817

Turkey Point Units 6 & 7
COL Application
Part 2 — FSAR

PTN COL 2.5-6

Table 2.5.4-215 (Sheet 2 of 4)
Summary of Measured Shear Wave Velocities and Compressive Wave Velocities

Depth	Moist Unit Weight	Shear Wave Velocity, V_s			Compressive Wave Velocity, V_p		
		Average	Average – stdev	Average + stdev	Average	Average – stdev	Average + stdev
(ft)	(lb/ft ³)	(ft/s)	(ft/s)	(ft/s)	(ft/s)	(ft/s)	(ft/s)
150	120	1,541	1,129	1,788	5,644	5,276	5,892
160	120	1,541	1,129	1,788	5,644	5,276	5,892
160	120	1,641	1,549	1,791	5,718	5,568	5,873
170	120	1,641	1,549	1,791	5,718	5,568	5,873
170	120	1,585	1,468	1,664	5,682	5,588	5,778
180	120	1,585	1,468	1,664	5,682	5,588	5,778
180	120	1,561	1,430	1,645	5,675	5,556	5,808
190	120	1,561	1,430	1,645	5,675	5,556	5,808
190	120	1,636	1,456	1,814	5,728	5,561	5,890
200	120	1,636	1,456	1,814	5,728	5,561	5,890
200	120	1,769	1,542	1,940	5,761	5,637	5,970
210	120	1,769	1,542	1,940	5,761	5,637	5,970
210	120	2,235	1,802	2,604	6,379	5,827	7,035
220	120	2,235	1,802	2,604	6,379	5,827	7,035
220	120	2,354	1,732	3,059	6,413	5,928	7,039
230	120	2,354	1,732	3,059	6,413	5,928	7,039
230	120	1,925	1,479	2,432	6,020	5,592	6,614
240	120	1,925	1,479	2,432	6,020	5,592	6,614
240	120	2,052	1,555	3,024	6,021	5,458	6,593
250	120	2,052	1,555	3,024	6,021	5,458	6,593
250	120	1,835	1,305	2,263	5,974	5,747	6,207
260	120	1,835	1,305	2,263	5,974	5,747	6,207
260	120	1,666	1,372	2,021	5,865	5,553	6,213
270	120	1,666	1,372	2,021	5,865	5,553	6,213
270	120	1,701	1,621	1,810	5,853	5,600	6,271
280	120	1,701	1,621	1,810	5,853	5,600	6,271
280	120	1,841	1,629	2,183	5,937	5,716	6,229
290	120	1,841	1,629	2,183	5,937	5,716	6,229
290	120	1,747	1,479	2,017	6,013	5,804	6,288
300	120	1,747	1,479	2,017	6,013	5,804	6,288
300	120	1,730	1,489	2,055	5,894	5,656	6,172
310	120	1,730	1,489	2,055	5,894	5,656	6,172
310	120	1,647	1,182	2,137	5,751	5,619	5,848

Turkey Point Units 6 & 7
COL Application
Part 2 — FSAR

PTN COL 2.5-6

Table 2.5.4-215 (Sheet 3 of 4)
Summary of Measured Shear Wave Velocities and Compressive Wave Velocities

Depth	Moist Unit Weight	Shear Wave Velocity, V_s			Compressive Wave Velocity, V_p		
		Average	Average – stdev	Average + stdev	Average	Average – stdev	Average + stdev
(ft)	(lb/ft ³)	(ft/s)	(ft/s)	(ft/s)	(ft/s)	(ft/s)	(ft/s)
320	120	1,647	1,182	2,137	5,751	5,619	5,848
320	120	1,471	1,306	1,719	5,794	5,645	6,005
330	120	1,471	1,306	1,719	5,794	5,645	6,005
330	120	1,423	1,238	1,760	5,707	5,541	5,961
340	120	1,423	1,238	1,760	5,707	5,541	5,961
340	120	1,463	1,207	1,559	5,794	5,598	5,951
350	120	1,463	1,207	1,559	5,794	5,598	5,951
350	120	1,482	1,329	1,617	5,798	5,677	5,995
360	120	1,482	1,329	1,617	5,798	5,677	5,995
360	120	1,480	1,251	1,625	5,872	5,656	6,115
370	120	1,480	1,251	1,625	5,872	5,656	6,115
370	120	1,431	1,263	1,567	5,788	5,588	6,341
380	120	1,431	1,263	1,567	5,788	5,588	6,341
380	120	1,522	1,215	1,641	5,820	5,587	6,060
390	120	1,522	1,215	1,641	5,820	5,587	6,060
390	120	1,431	1,178	1,694	5,769	5,667	5,931
400	120	1,431	1,178	1,694	5,769	5,667	5,931
400	120	1,476	—	—	5,780	—	—
410	120	1,476	—	—	5,780	—	—
410	120	1,442	—	—	5,783	—	—
420	120	1,442	—	—	5,783	—	—
420	120	1,461	—	—	5,878	—	—
430	120	1,461	—	—	5,878	—	—
430	120	1,450	—	—	5,823	—	—
440	120	1,450	—	—	5,823	—	—
450	120	1,450	—	—	5,823	—	—
450	130	4,046	—	—	8,842	—	—
460	130	4,046	—	—	8,842	—	—
470	130	4,046	—	—	8,842	—	—
470	130	4,171	—	—	8,247	—	—
480	130	4,171	—	—	8,247	—	—
480	130	3,818	—	—	7,739	—	—
490	130	3,818	—	—	7,739	—	—

Turkey Point Units 6 & 7
COL Application
Part 2 — FSAR

PTN COL 2.5-6

Table 2.5.4-215 (Sheet 4 of 4)
Summary of Measured Shear Wave Velocities and Compressive Wave Velocities

Depth	Moist Unit Weight	Shear Wave Velocity, V_s			Compressive Wave Velocity, V_p		
		Average	Average – stdev	Average + stdev	Average	Average – stdev	Average + stdev
(ft)	(lb/ft ³)	(ft/s)	(ft/s)	(ft/s)	(ft/s)	(ft/s)	(ft/s)
490	130	3,953	—	—	8,021	—	—
500	130	3,953	—	—	8,021	—	—
500	130	3,917	—	—	8,118	—	—
510	130	3,917	—	—	8,118	—	—
510	130	3,952	—	—	8,261	—	—
520	130	3,952	—	—	8,261	—	—
520	130	3,867	—	—	7,813	—	—
530	130	3,867	—	—	7,813	—	—
530	130	3,860	—	—	8,088	—	—
540	130	3,860	—	—	8,088	—	—
540	130	3,569	—	—	7,873	—	—
550	130	3,569	—	—	7,873	—	—
550	130	3,364	—	—	7,627	—	—
560	130	3,364	—	—	7,627	—	—
560	130	3,083	—	—	7,275	—	—
570	130	3,083	—	—	7,275	—	—
570	130	3,040	—	—	7,398	—	—
580	130	3,040	—	—	7,398	—	—
580	130	3,174	—	—	7,453	—	—
590	130	3,174	—	—	7,453	—	—
590	130	3,741	—	—	8,307	—	—
600	130	3,741	—	—	8,307	—	—
600	130	3,331	—	—	7,847	—	—
610	130	3,331	—	—	7,847	—	—

Data from [Reference 257](#)

Note: stdev = Standard deviation

Turkey Point Units 6 & 7
COL Application
Part 2 — FSAR

PTN COL 2.5-6

Table 2.5.4-216
Summary of Recommended Shear Modulus Degradation and Damping Curves

	Shear Strain, γ (%)	0.0001	0.0003	0.001	0.003	0.01	0.03	0.1	0.3	1
G/G_{max}	Natural Soil (Depth > 159 ft)	1.00	1.00	1.00	1.00	0.95	0.87	0.65	0.42	0.19
	Natural Soil (Depth < 159 ft)	1.00	1.00	1.00	0.99	0.93	0.81	0.56	0.33	0.14
	Miami Limestone	1.00	1.00	1.00	1.00	1.00	0.98	0.87	0.63	0.33
	Structural Fill	1.00	0.96	0.87	0.74	0.55	0.37	0.21	0.11	0.05
D (%)	Natural Soil	0.6	0.6	0.6	0.8	1.3	2.6	5.6	10.4	17.0
	Miami Limestone	0.6	0.6	0.6	0.6	0.6	0.6	2.7	8.2	17.0
	Structural Fill	1.3	1.3	1.6	2.4	4.4	8.2	14.3	20.6	27.9

Data from [Reference 257](#)

PTN COL 2.5-3
PTN COL 2.5-10

Table 2.5.4-217
Summary of Bearing Capacity

Structure	Subsurface	BxL (ftxft) ^(a)		q _{allow} (ksf) ^(b)
		Case I	Case II	Recommended
Reactor & Auxiliary	Lean Concrete Fill on Rock	88x254	159x254	43.0

(a) width x length

(b) Allowable bearing capacity for static and dynamic loading

Data from [Reference 257](#)

Turkey Point Units 6 & 7
COL Application
Part 2 — FSAR

PTN COL 2.5-9

Table 2.5.4-218
Summary of Liquefaction Resistance Calculation Results

Subsurface Data Source	Lowest Calculated Factor of Safety (FOS)	Elevation in feet of Lowest FOS
CPT C-601	1.92	-137.7
CPT C-602	2.06	-137.3
CPT C-701	2.11	-231.5
CPT C-702	1.95	-137.3
SWV B-601	1.50	-152.3
SWV B-620	3.76	-144.2
SWV B-701	4.03	-393.2
SWV B-708	2.14	-121.2

Notes:

SWV = Shear Wave Velocity

CPT = Cone Penetration Test

Calculated Safety Factors Using Shear Wave Velocity Measurements in borings B-604, B-608, B-610, B-704, B-710, and B-720 were greater than 10 or too large to calculate.

Turkey Point Units 6 & 7
COL Application
Part 2 — FSAR

Table 2.5.4-219
Estimated Foundation Settlements

Structure	Contact Pressure (ksf)	Subsurface	B x L (ft x ft)		Low Strain Anticipated Settlement (in.)					
					Center		Mid of Side		Mean	
			Case I	Case II	I	II	I	II	I	II
Reactor & Auxiliary	8.9	Lean Concrete Fill on Rock	88 x 254	159 x 254	1.6	3.4	1.2	1.9	1.4	2.7
Turbine	6.0	Compacted Fill	156 x 309	—	3.6	—	2.2	—	2.9	—
Annex	6.0	Compacted Fill	66 x 405	145 x 405	3.0	3.9	1.8	2.4	2.4	3.15
Radwaste	6.0	Compacted Fill	66 x 175	—	2.8	—	1.6	—	2.2	—

Turkey Point Units 6 & 7
COL Application
Part 2 — FSAR

Figure 2.5.4-201 Site Plan Showing Structures and Finish Grade

PTN COL 2.5-1
PTN COL 2.5-5
PTN COL 2.5-6
PTN COL 2.5-7
PTN COL 2.5-10



Turkey Point Units 6 & 7
COL Application
Part 2 — FSAR

Figure 2.5.4-202 Site Plan Showing Boring Locations

PTN COL 2.5-1
PTN COL 2.5-2
PTN COL 2.5-5
PTN COL 2.5-6
PTN COL 2.5-7

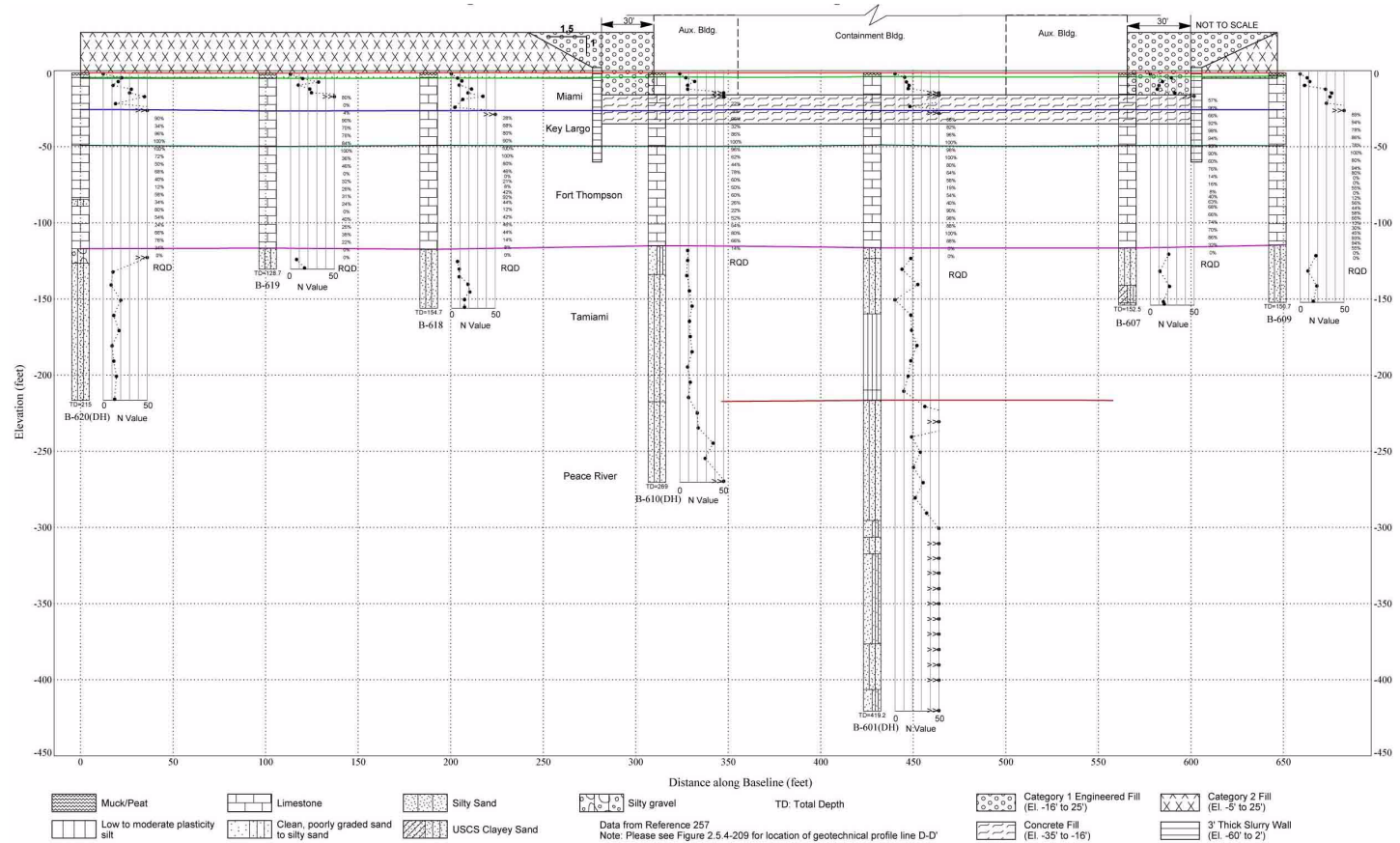


Note: TP = Test pit
CPT = Cone penetration test

Turkey Point Units 6 & 7
COL Application
Part 2 — FSAR

Figure 2.5.4-203 Geotechnical Cross Section D-D' Through Unit 6 Power Block

PTN COL 2.5-1
PTN COL 2.5-5
PTN COL 2.5-6
PTN COL 2.5-7
PTN COL 2.5-10



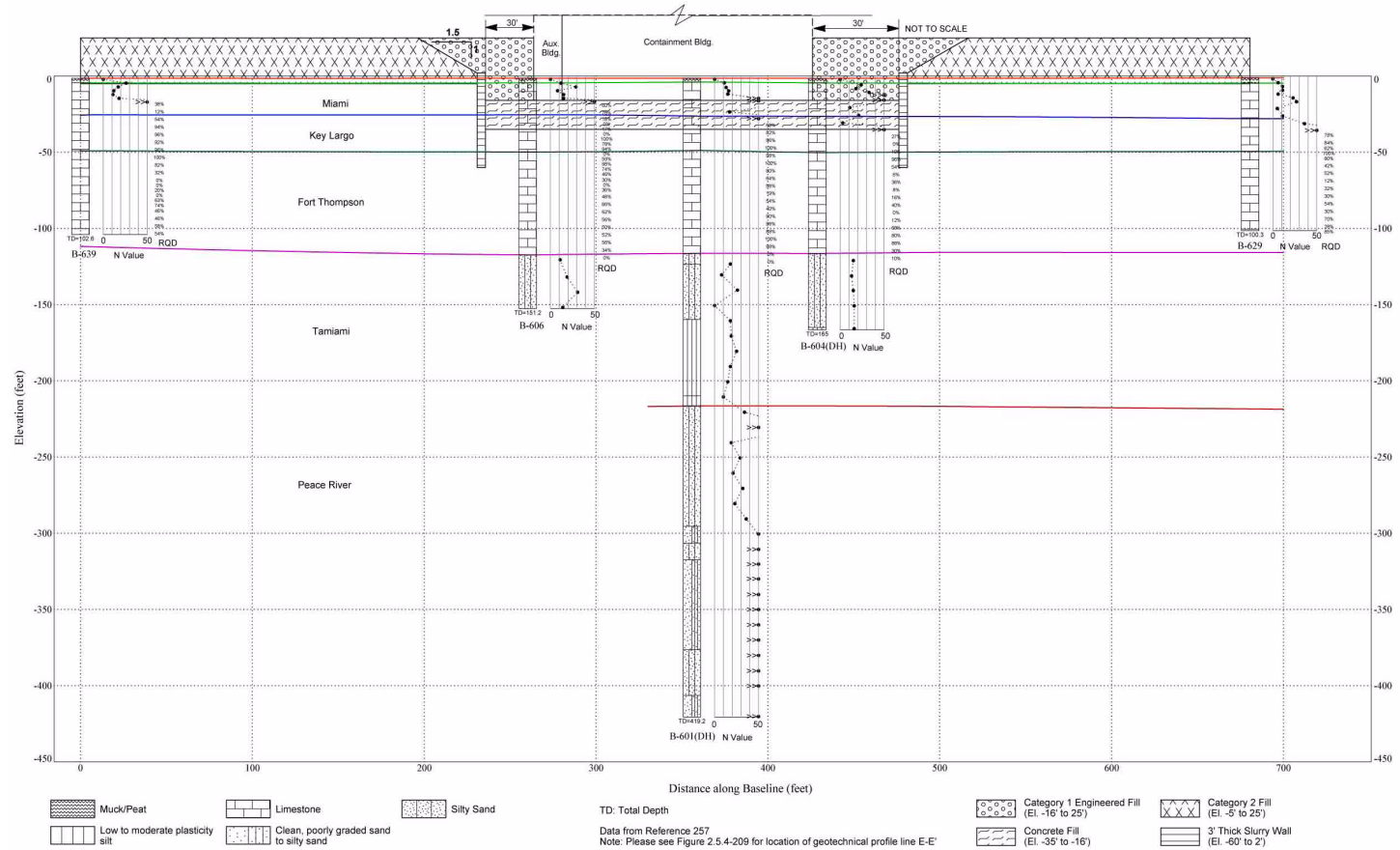
Data from [Reference 257](#)

Note: Please see [Figure 2.5.4-209](#) for location of geotechnical profile line D-D'

Turkey Point Units 6 & 7
COL Application
Part 2 — FSAR

Figure 2.5.4-204 Geotechnical Cross Section E-E' Through Unit 6 Power Block

PTN COL 2.5-1
PTN COL 2.5-5
PTN COL 2.5-6
PTN COL 2.5-7
PTN COL 2.5-10

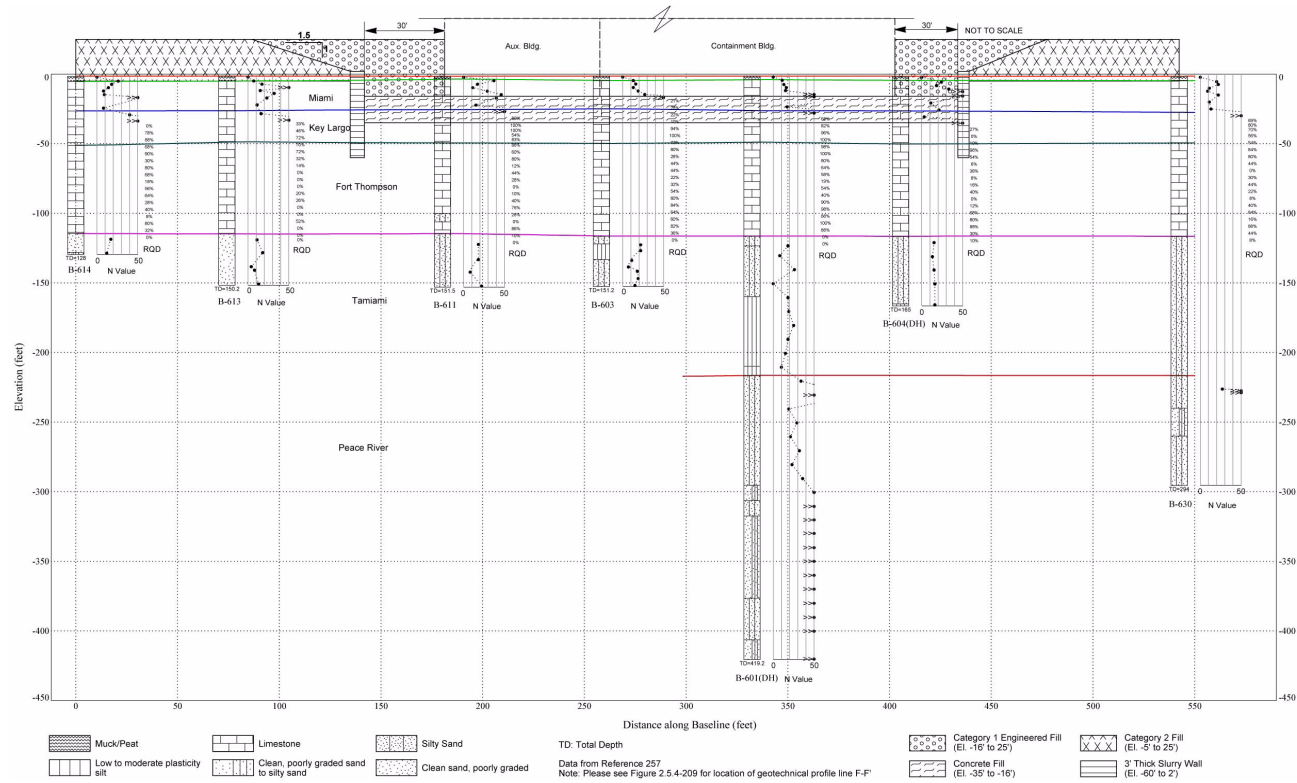


Data from [Reference 257](#)
Note: Please see [Figure 2.5.4-209](#) for location of geotechnical profile line E-E'

Turkey Point Units 6 & 7
COL Application
Part 2 — FSAR

Figure 2.5.4-205 Geotechnical Cross Section F-F' Through Unit 6 Power Block

PTN COL 2.5-1
PTN COL 2.5-5
PTN COL 2.5-6
PTN COL 2.5-7
PTN COL 2.5-10



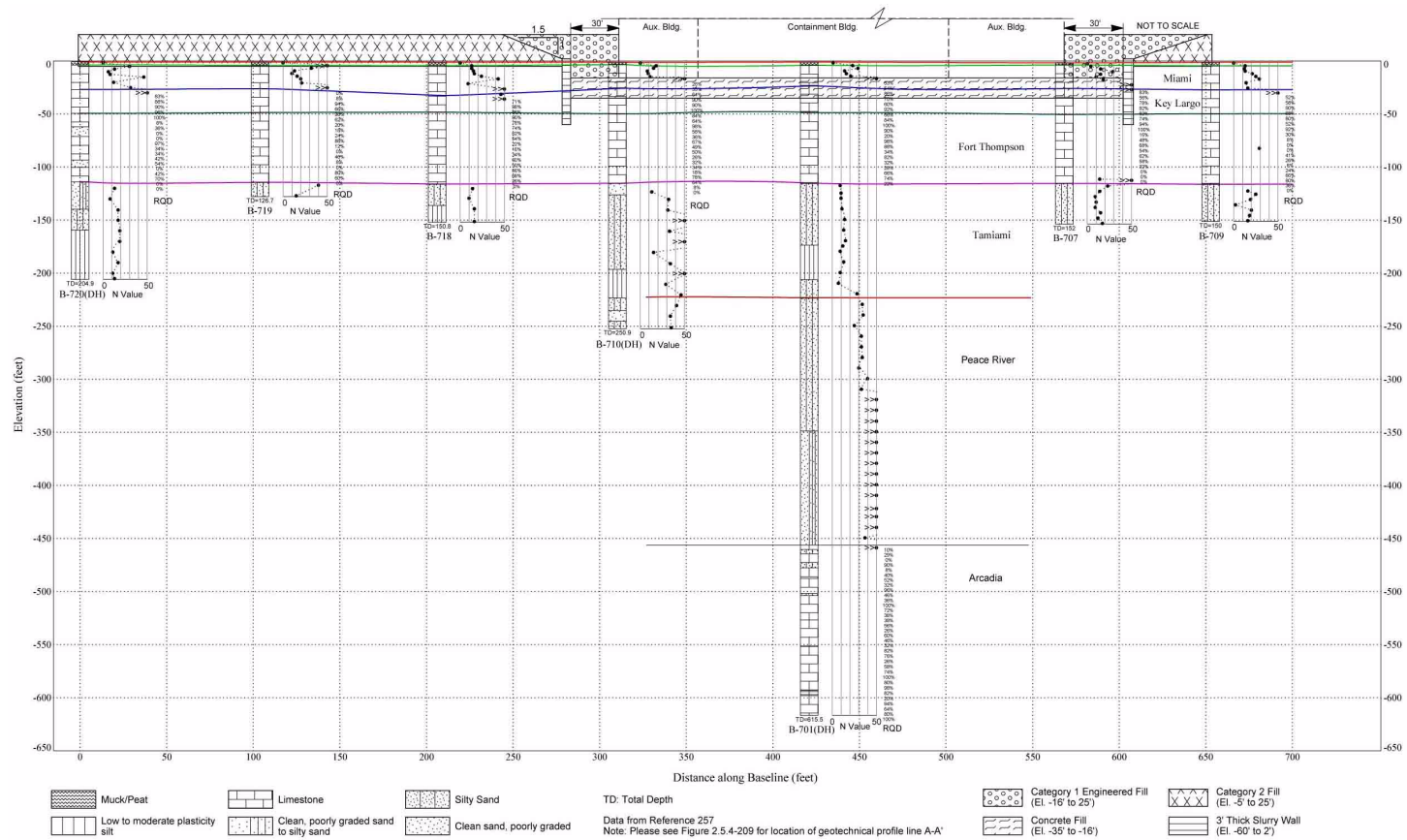
Data from [Reference 257](#)

Note: Please see [Figure 2.5.4-209](#) for location of geotechnical profile line F-F'

Turkey Point Units 6 & 7
COL Application
Part 2 — FSAR

Figure 2.5.4-206 Geotechnical Cross Section A-A' Through Unit 7 Power Block

PTN COL 2.5-1
PTN COL 2.5-5
PTN COL 2.5-6
PTN COL 2.5-7
PTN COL 2.5-10

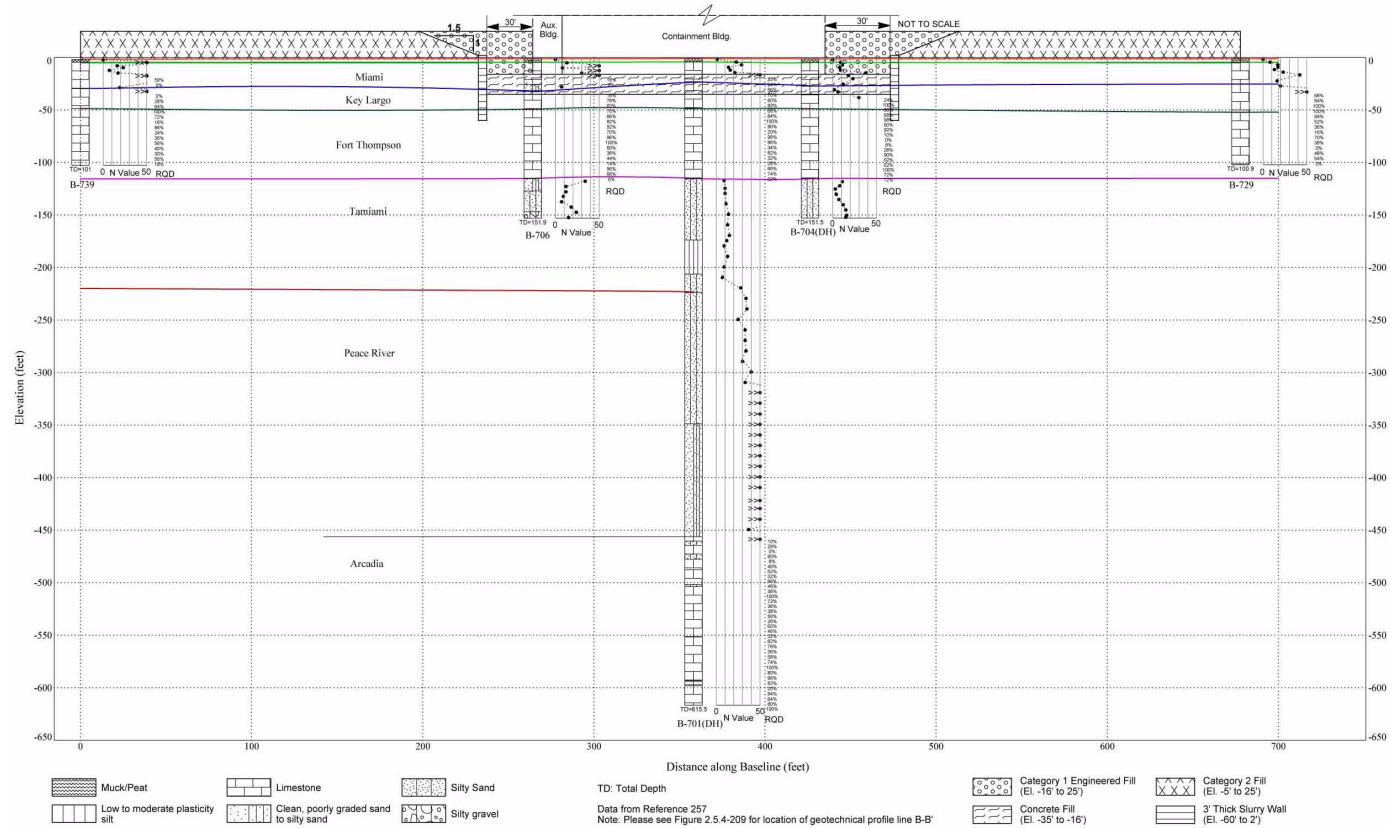


Data from **Reference 257**
Note: Please see **Figure 2.5.4-209** for location of geotechnical profile line A-A'

Turkey Point Units 6 & 7
COL Application
Part 2 — FSAR

Figure 2.5.4-207 Geotechnical Cross Section B-B' Through Unit 7 Power Block

PTN COL 2.5-1
PTN COL 2.5-5
PTN COL 2.5-6
PTN COL 2.5-7
PTN COL 2.5-10



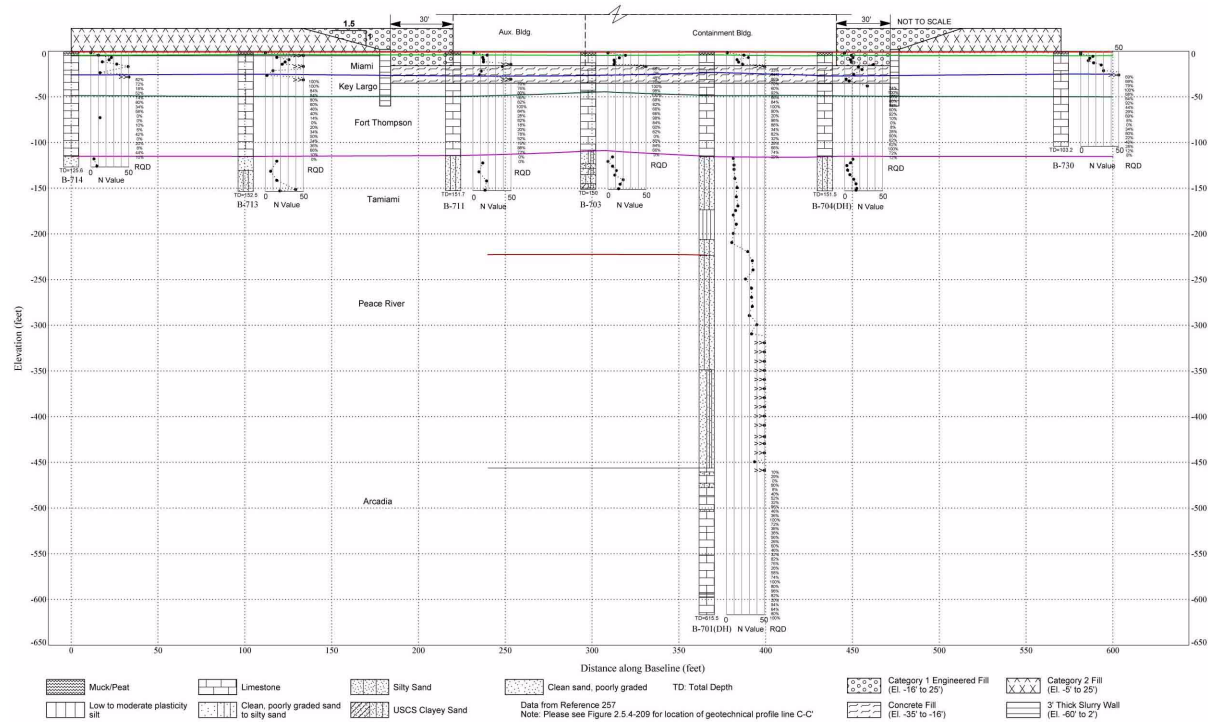
Data from **Reference 257**

Note: Please see **Figure 2.5.4-209** for location of geotechnical profile line B-B'

Turkey Point Units 6 & 7
COL Application
Part 2 — FSAR

Figure 2.5.4-208 Geotechnical Cross Section C-C' Through Unit 7 Power Block

PTN COL 2.5-1
PTN COL 2.5-5
PTN COL 2.5-6
PTN COL 2.5-7
PTN COL 2.5-10

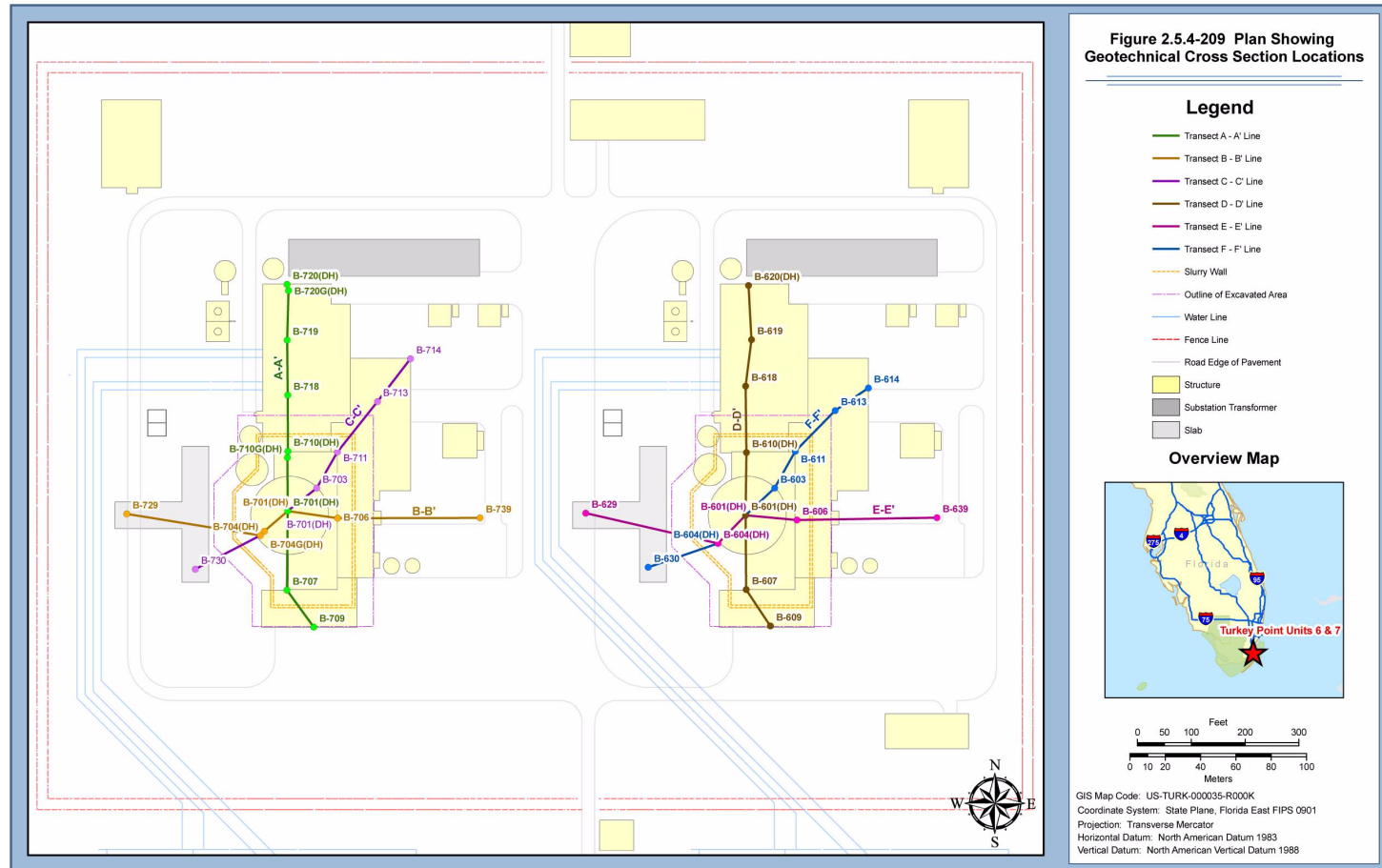


Data from [Reference 257](#)
Note: Please see [Figure 2.5.4-209](#) for location of geotechnical profile line C-C'

Turkey Point Units 6 & 7
COL Application
Part 2 — FSAR

PTN COL 2.5-1
PTN COL 2.5-5
PTN COL 2.5-6
PTN COL 2.5-8

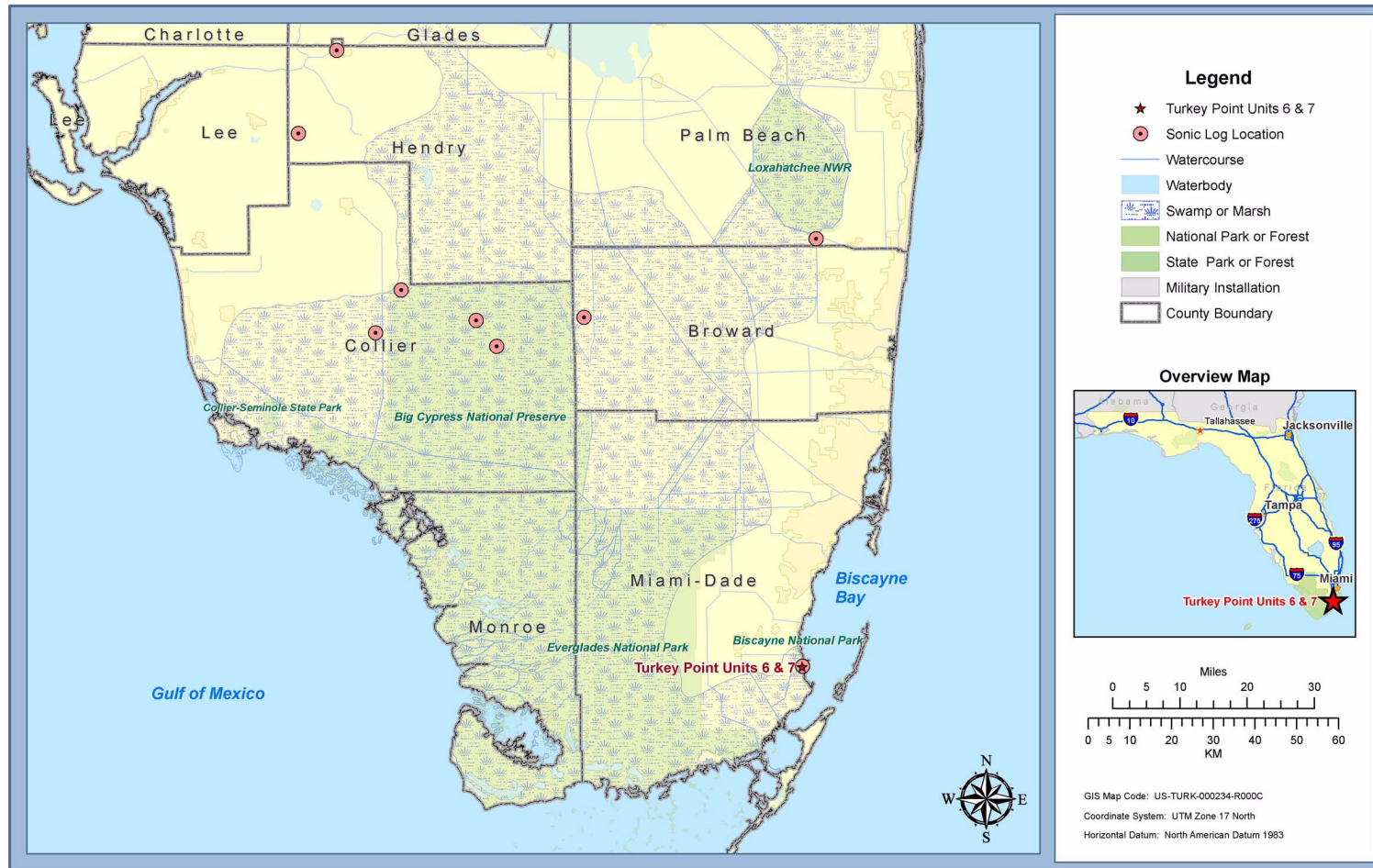
Figure 2.5.4-209 Plan Showing Geotechnical Cross Section Locations



Turkey Point Units 6 & 7
COL Application
Part 2 — FSAR

PTN COL 2.5-2
PTN COL 2.5-6

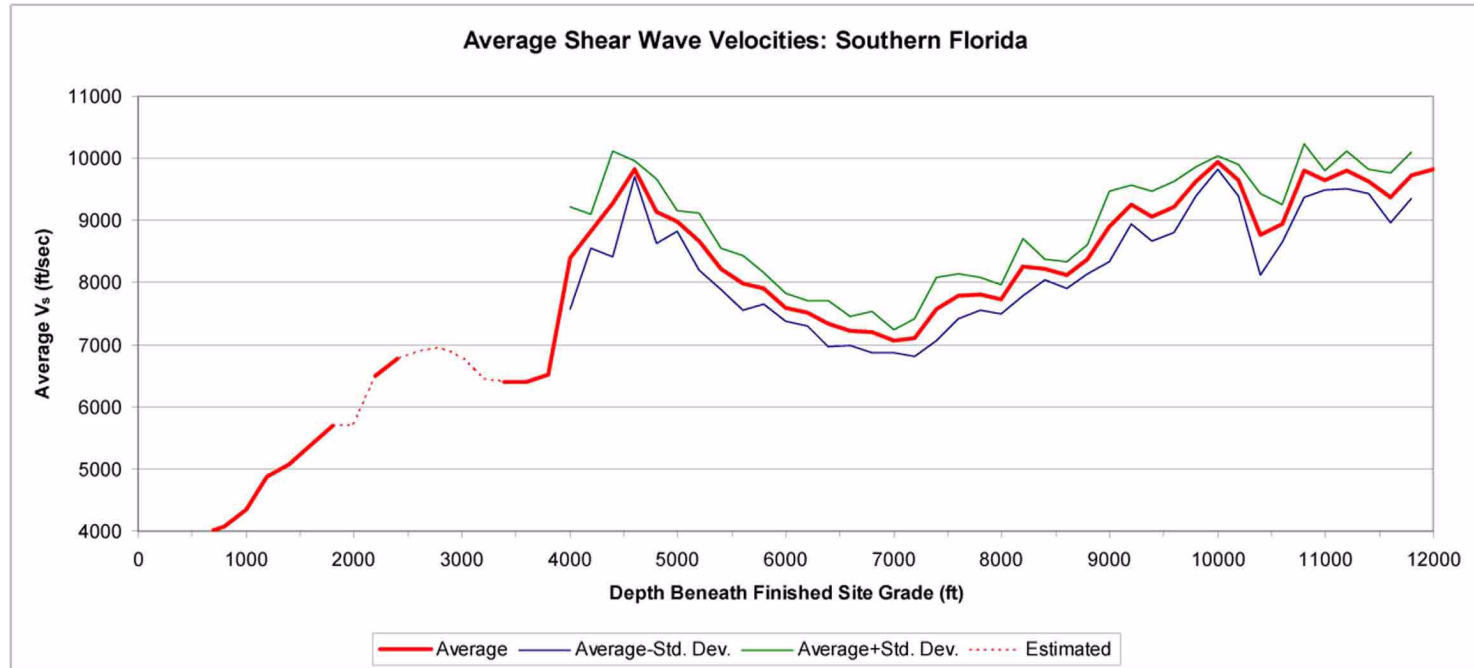
Figure 2.5.4-210 Sonic Log Locations



Turkey Point Units 6 & 7
COL Application
Part 2 — FSAR

PTN COL 2.5-2
PTN COL 2.5-6

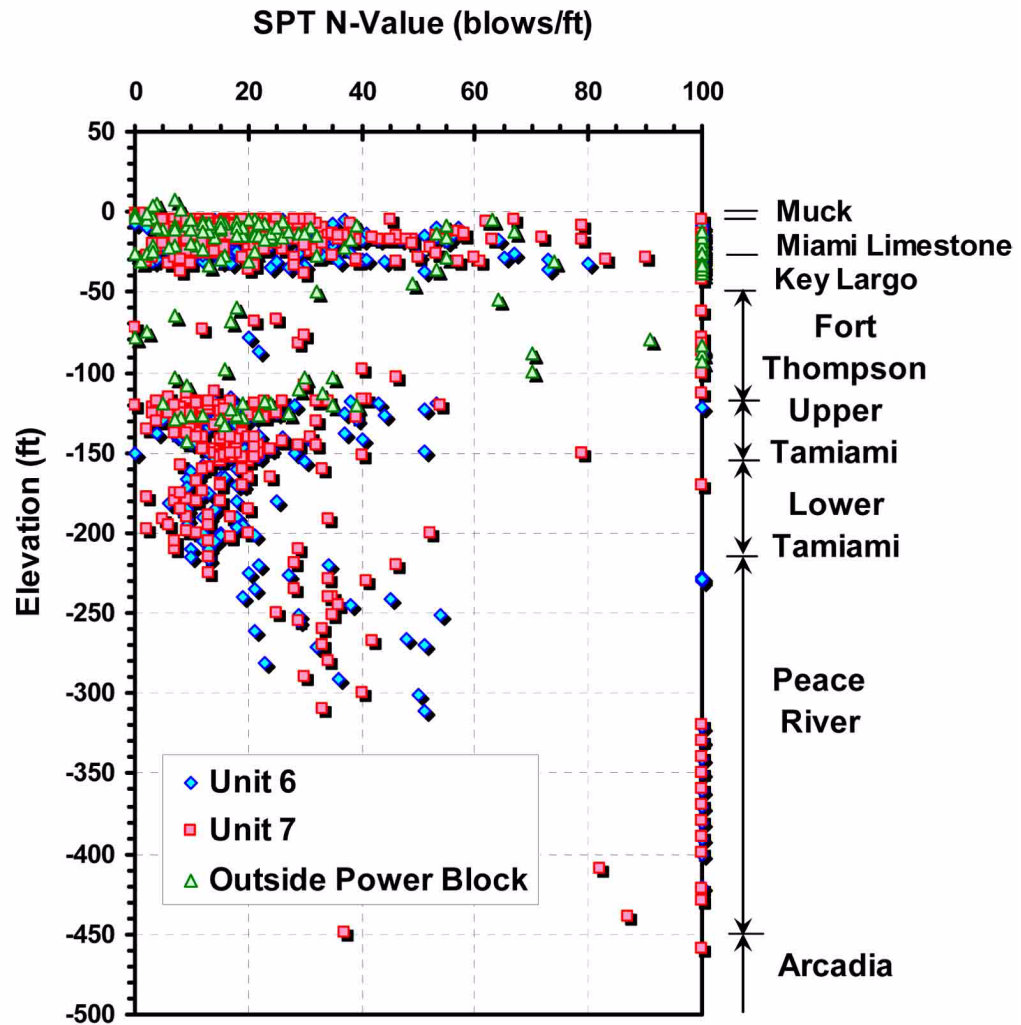
Figure 2.5.4-211 Shear Wave Velocity at Greater Depth



Note: The finished grade is El. 25.5 feet at the nuclear island.

PTN COL 2.5-6

Figure 2.5.4-212 Plot of Uncorrected SPT N-Values with Depth

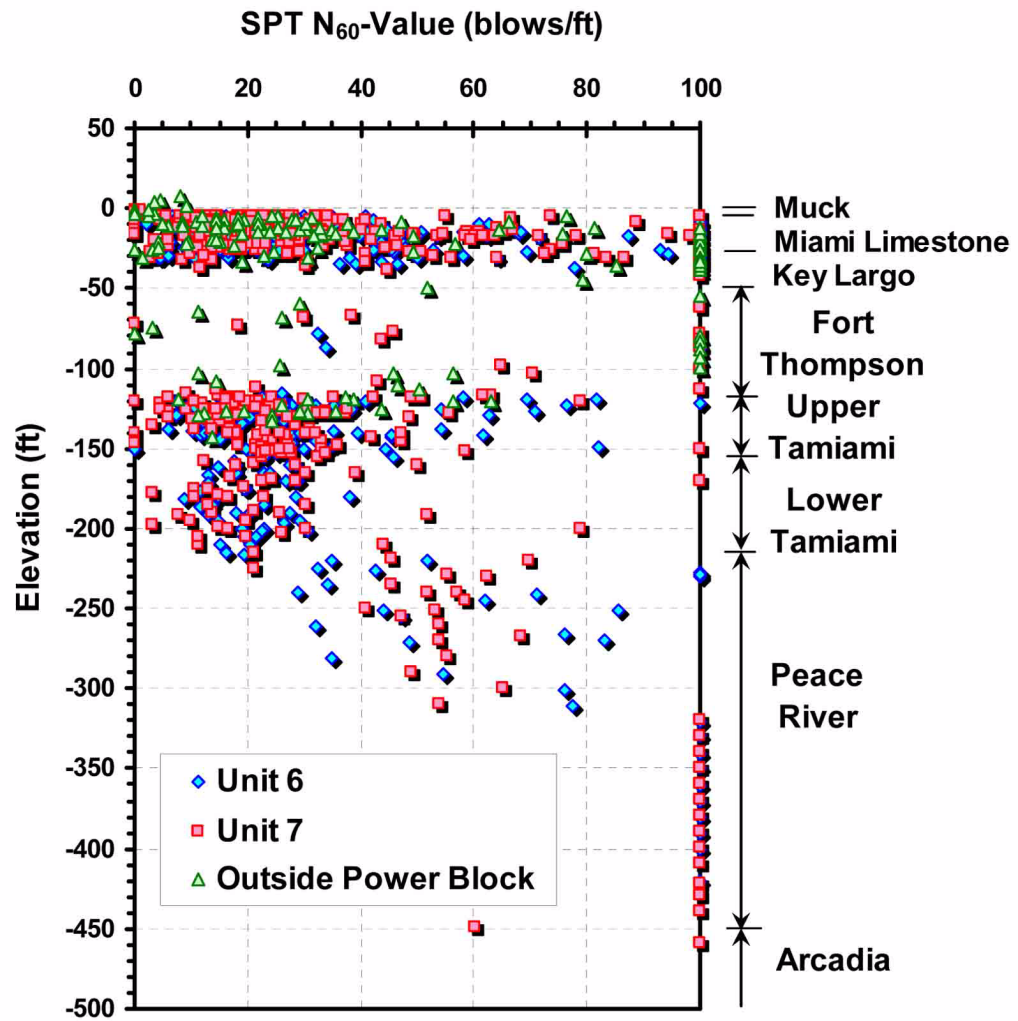


Data from [Reference 257](#)

Notes: Elevation is NAVD 88

PTN COL 2.5-6

Figure 2.5.4-213 Plot of Corrected SPT N_{60} -Values with Depth

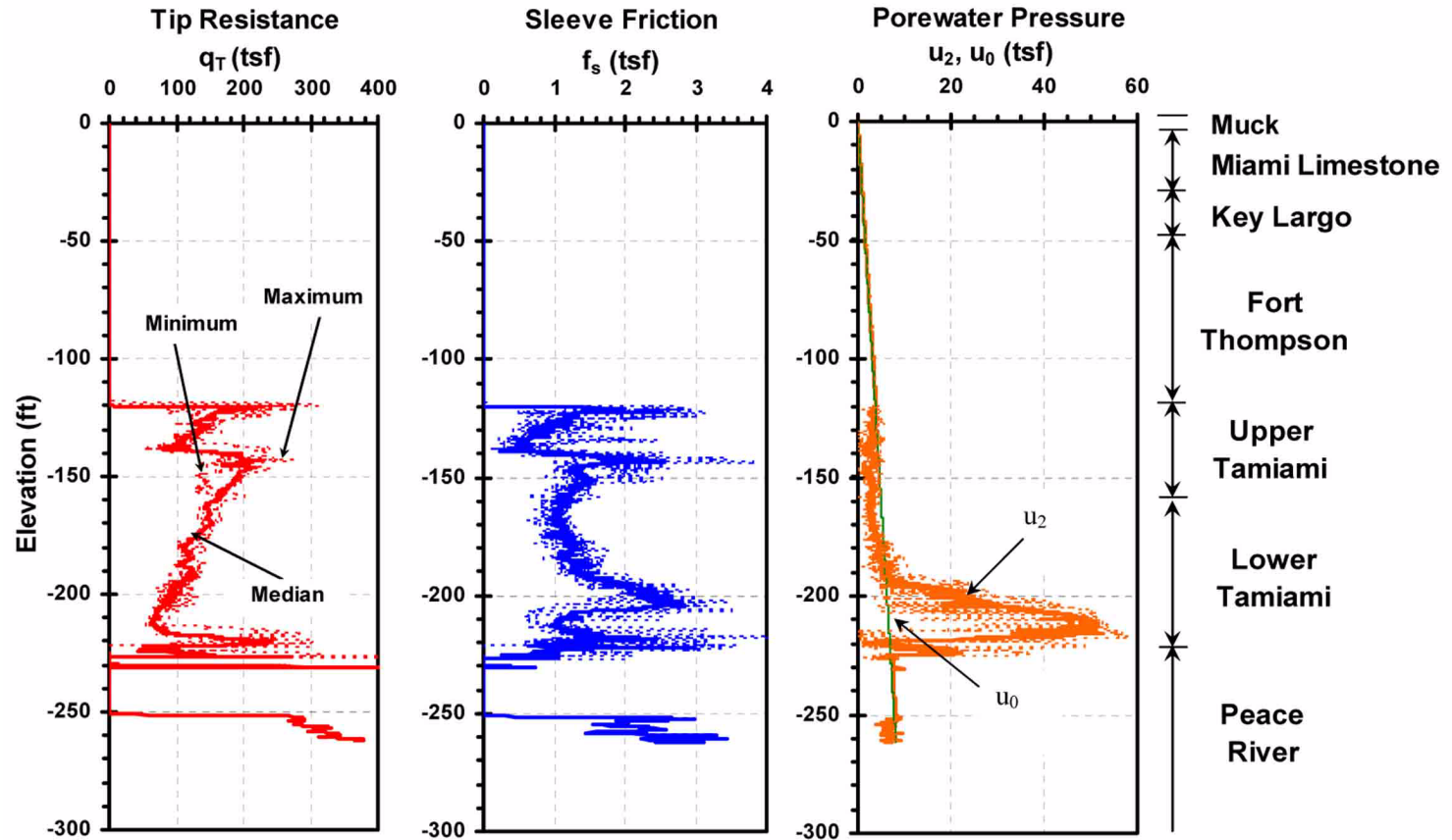


Data from [Reference 257](#)
Note: Elevation is NAVD 88

Turkey Point Units 6 & 7
COL Application
Part 2 — FSAR

PTN COL 2.5-6

Figure 2.5.4-214 Plot of CPT Data with Depth



Data from [Reference 257](#)

Notes:

CPT started at depth of 120 feet in each of the four probes

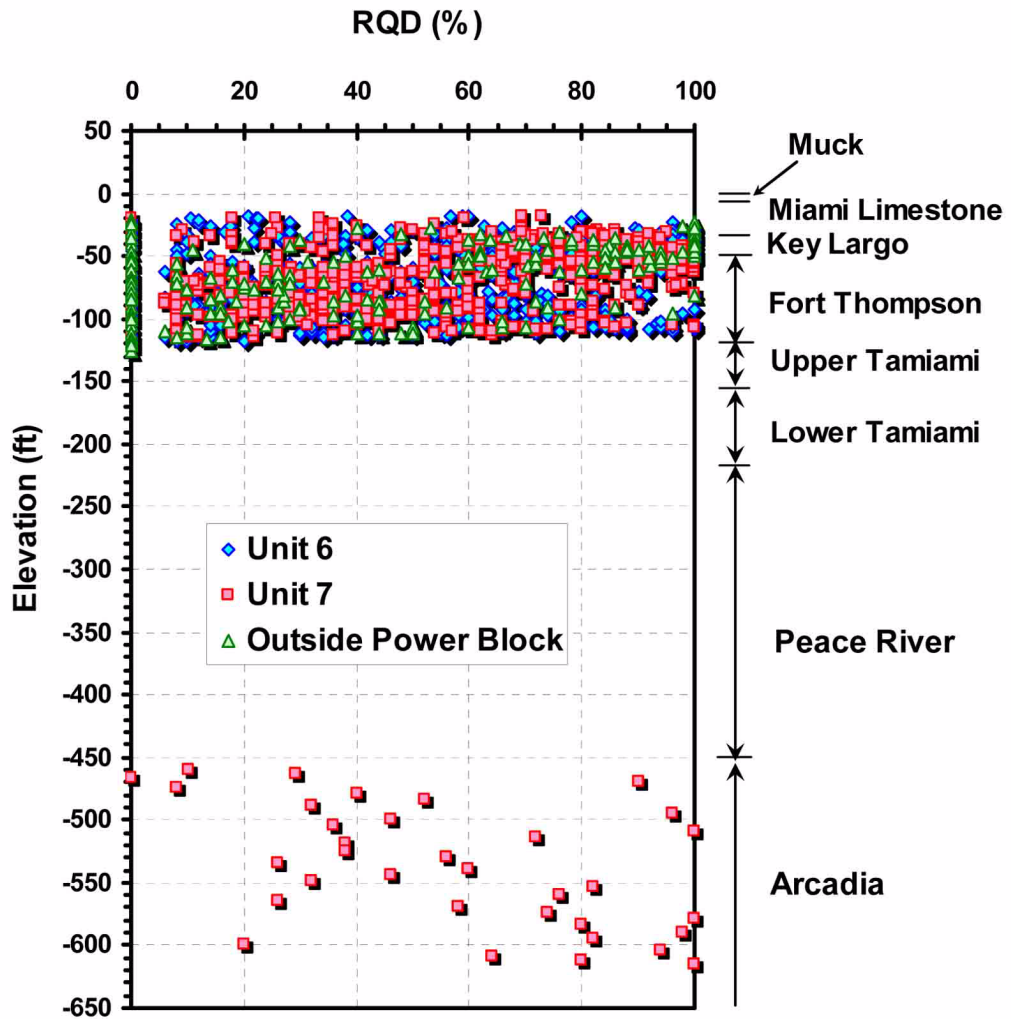
Rock coring was required to advance the CPT between approximate El. -230 and El. -250 feet

u_2 is the porewater pressure measured by CPT

u_0 is the static porewater pressure

PTN COL 2.5-6

Figure 2.5.4-215 Plot of Rock RQD Data with Depth (Sheet 1 of 2)

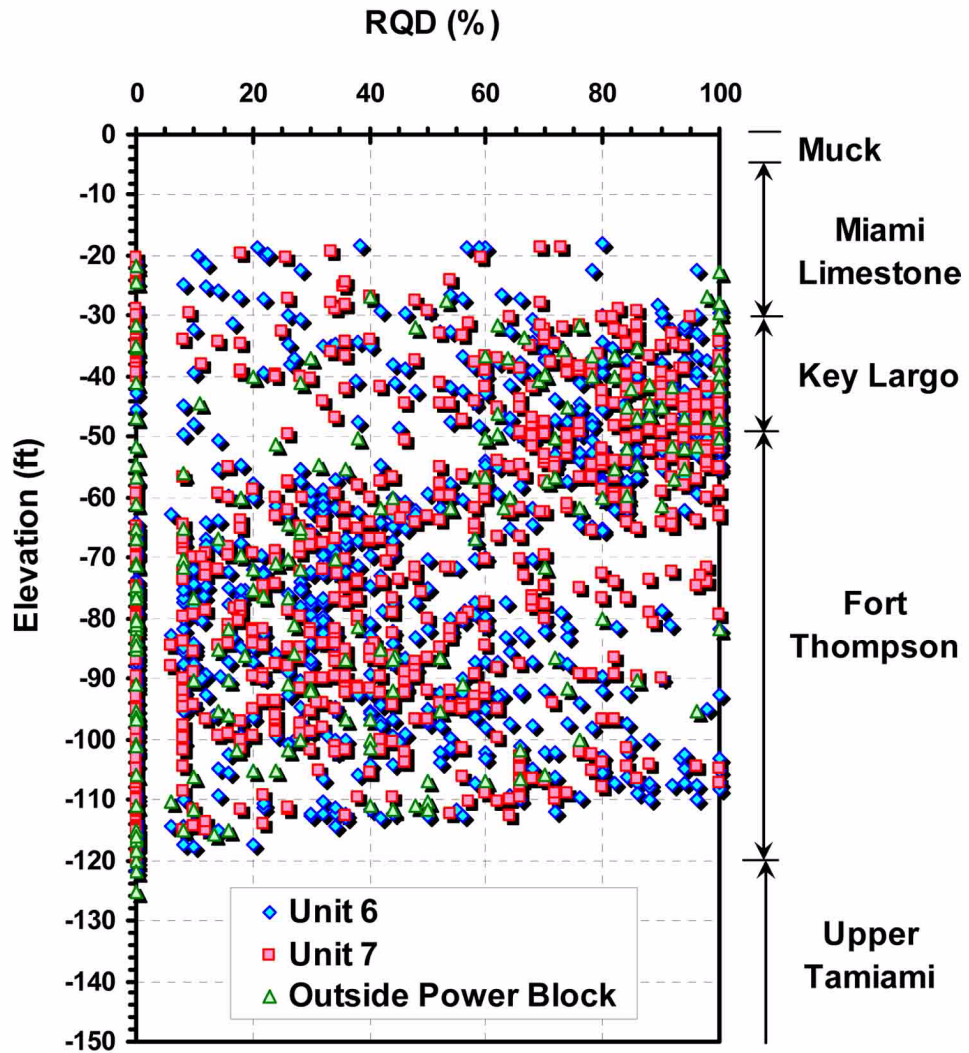


Data from [Reference 257](#)

Turkey Point Units 6 & 7
COL Application
Part 2 — FSAR

PTN COL 2.5-6

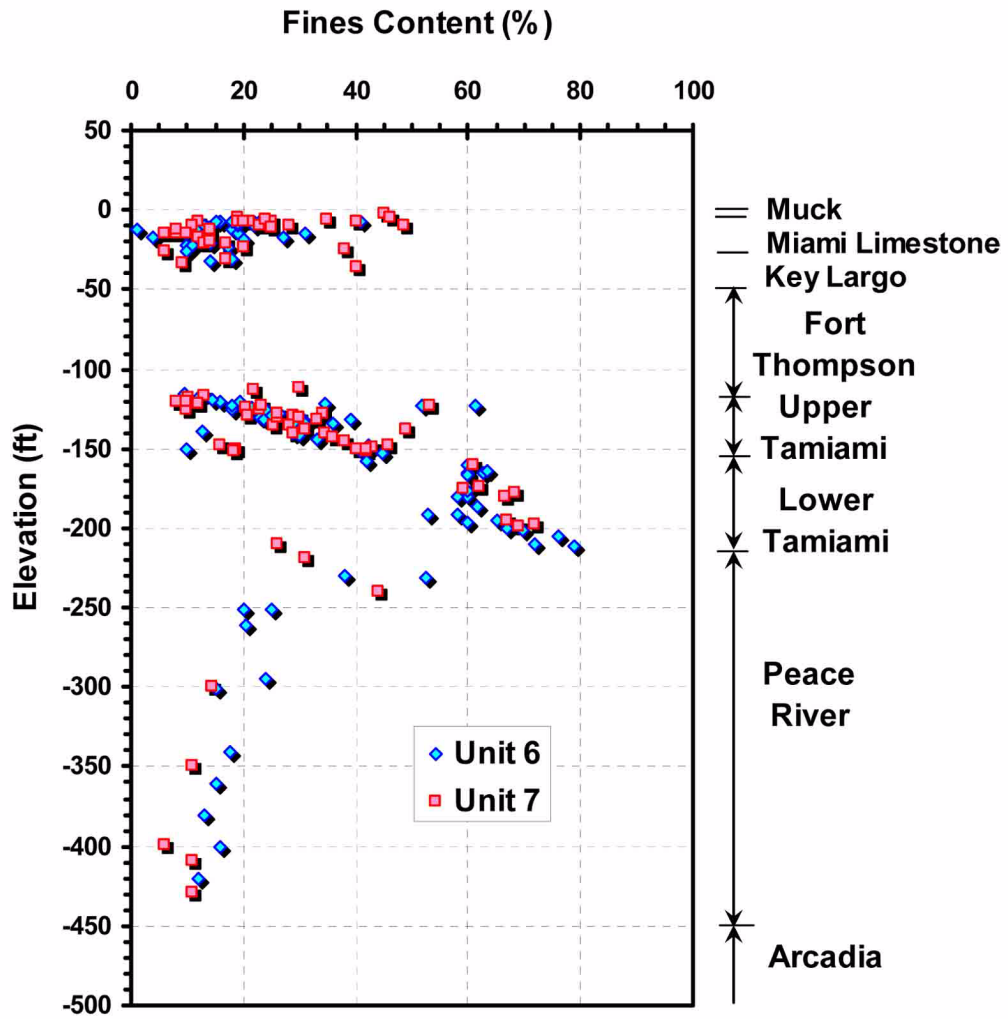
Figure 2.5.4-215 Plot of Rock RQD Data with Depth (Sheet 2 of 2)



Data from [Reference 257](#)

PTN COL 2.5-6

Figure 2.5.4-216 Plot of Fines Content with Depth



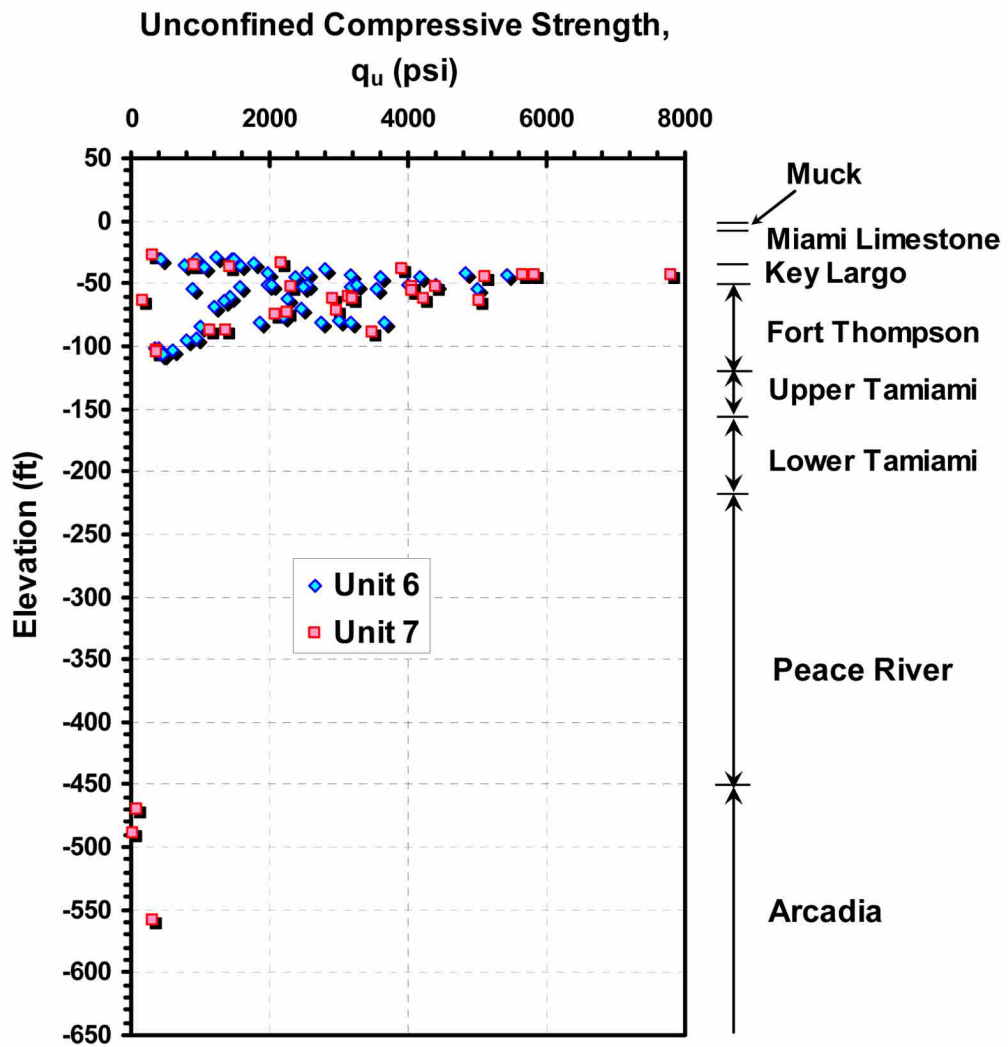
Data from [Reference 257](#)

Notes:

Fines contents were tested from samples collected using SPT and thin-walled tube equipment.
Fines content is the percent of the sample passing the standard number 200 sieve.

PTN COL 2.5-6

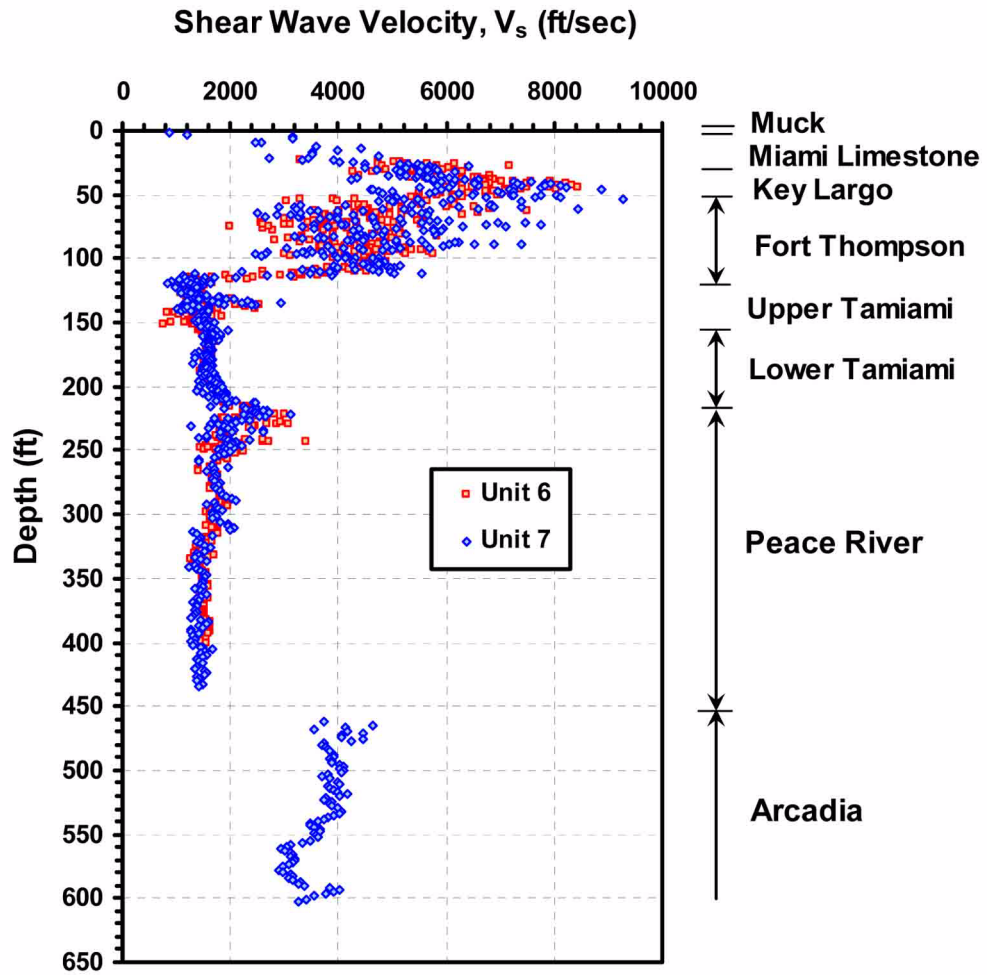
Figure 2.5.4-217 Plot of Rock Unconfined Compressive Strength with Depth



Data from [Reference 257](#)

PTN COL 2.5-6

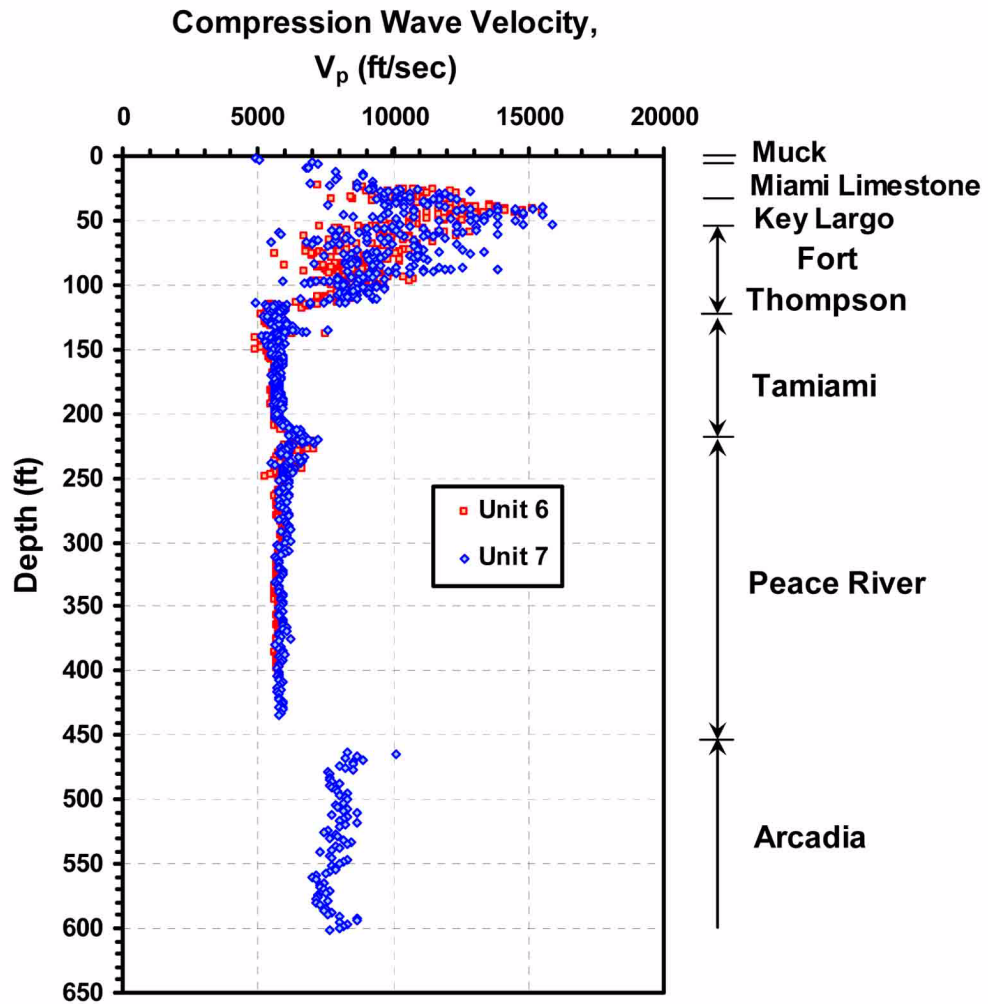
Figure 2.5.4-218 Plot of Shear Wave Velocity Measurements with Depth



Data from [Reference 257](#)

PTN COL 2.5-6

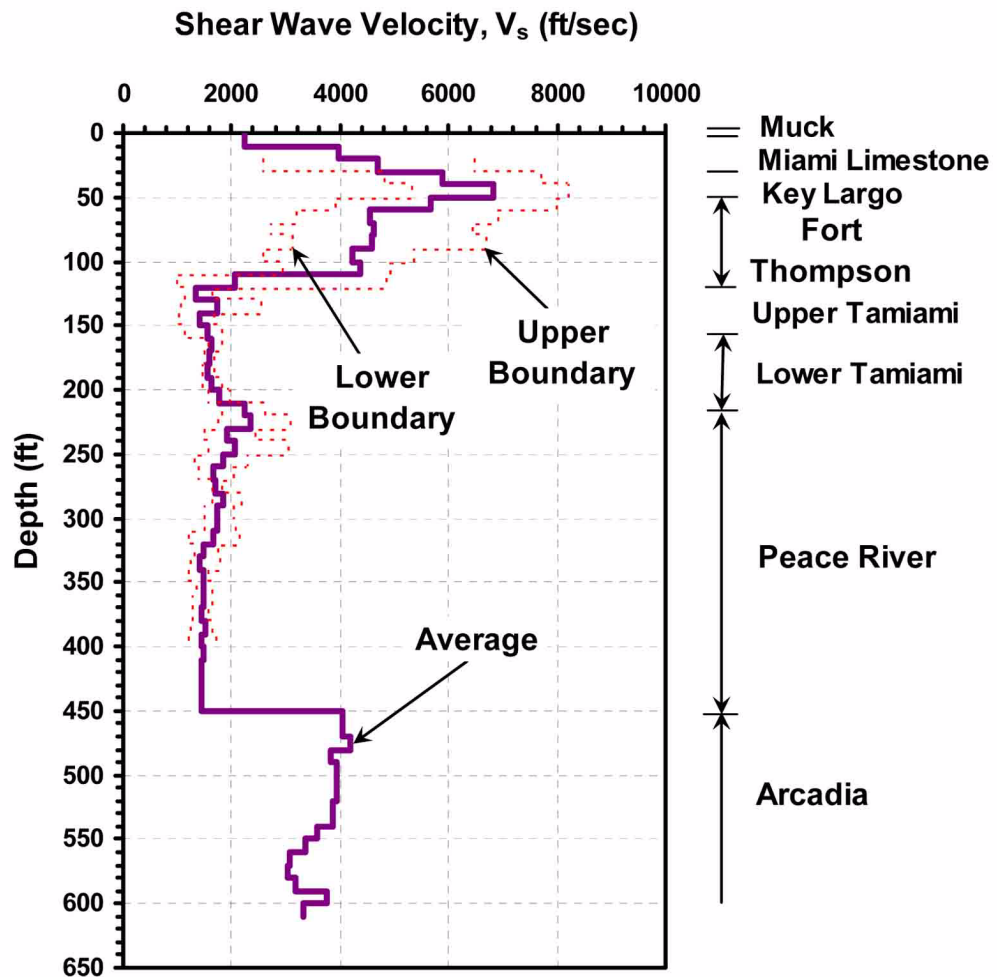
Figure 2.5.4-219 Plot of Compression Wave Velocity with Depth



Data from [Reference 257](#)

PTN COL 2.5-2
PTN COL 2.5-6

Figure 2.5.4-220 Plot of Recommended Shear Wave Velocity with Depth



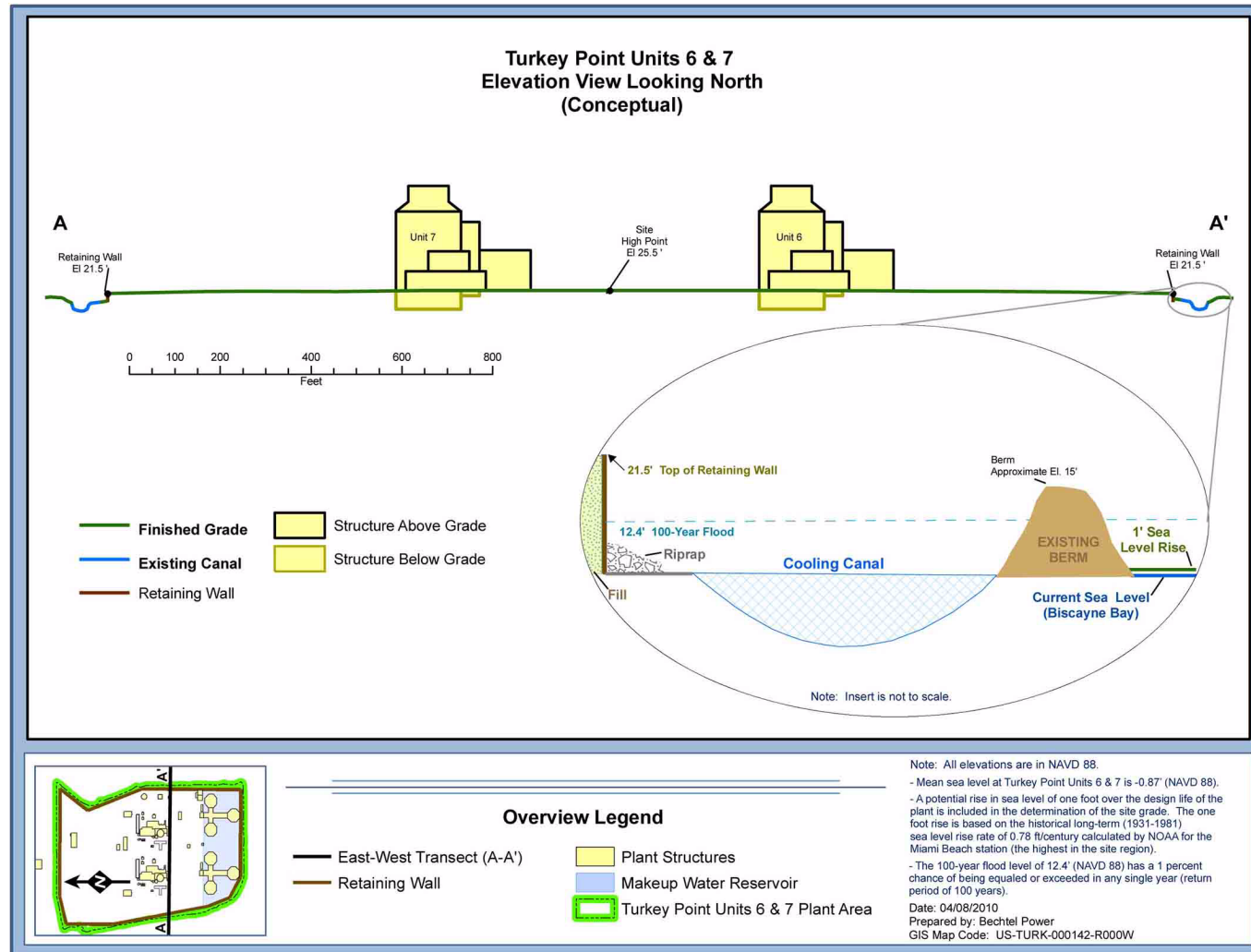
Data from [Reference 257](#)

Note: Average and boundary values above contain both Unit 6 and Unit 7 measurements.

Turkey Point Units 6 & 7
COL Application
Part 2 — FSAR

Figure 2.5.4-221 Profile of Site Grading

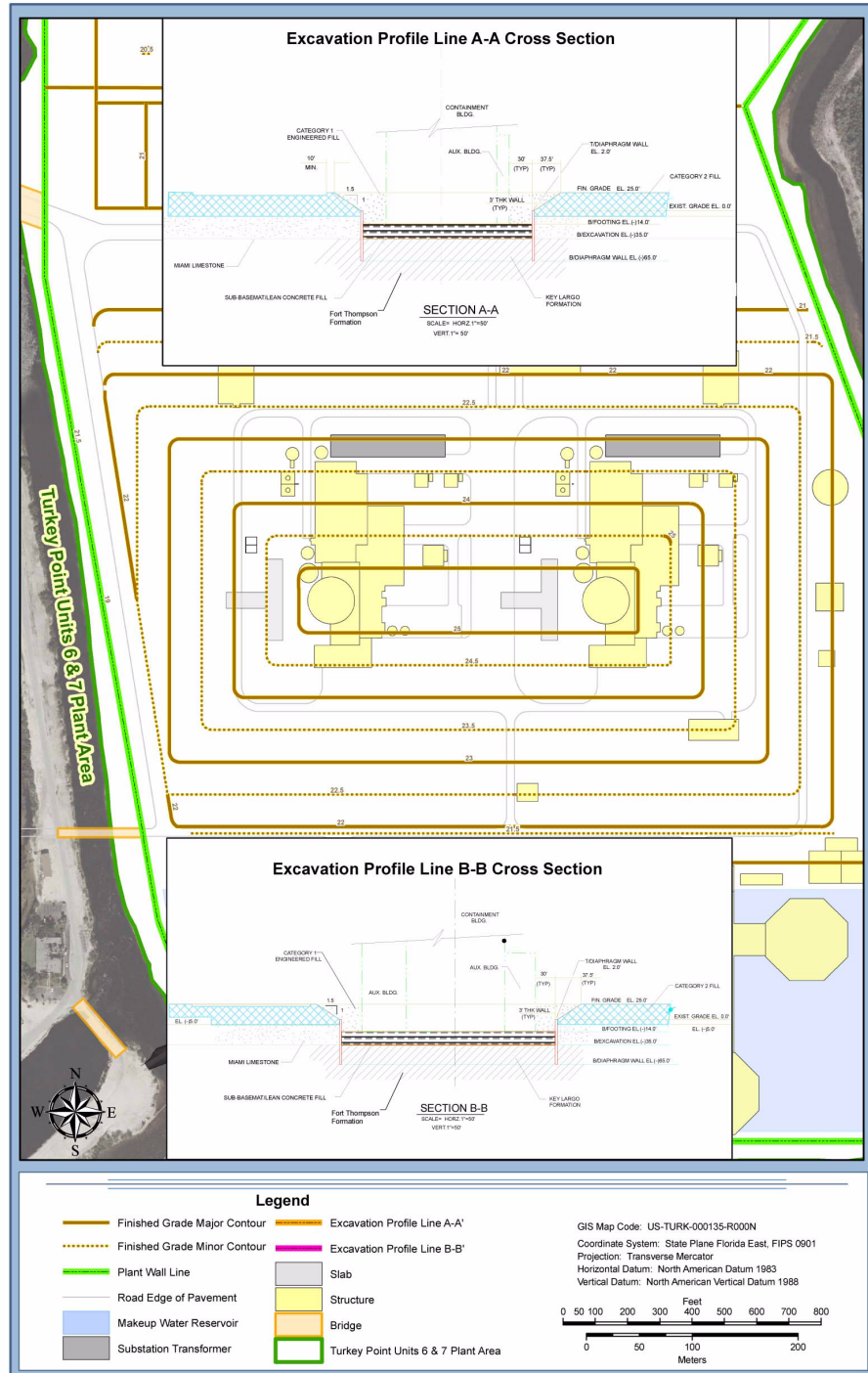
PTN COL 2.5-5
PTN COL 2.5-6
PTN COL 2.5-7



Turkey Point Units 6 & 7
COL Application
Part 2 — FSAR

Figure 2.5.4-222 Excavation at Power Block

PTN COL 2.5-5
PTN COL 2.5-6
PTN COL 2.5-7
PTN COL 2.5-12
PTN COL 2.5-16



Turkey Point Units 6 & 7
COL Application
Part 2 — FSAR

Figure 2.5.4-223 Geophysical Survey Lines

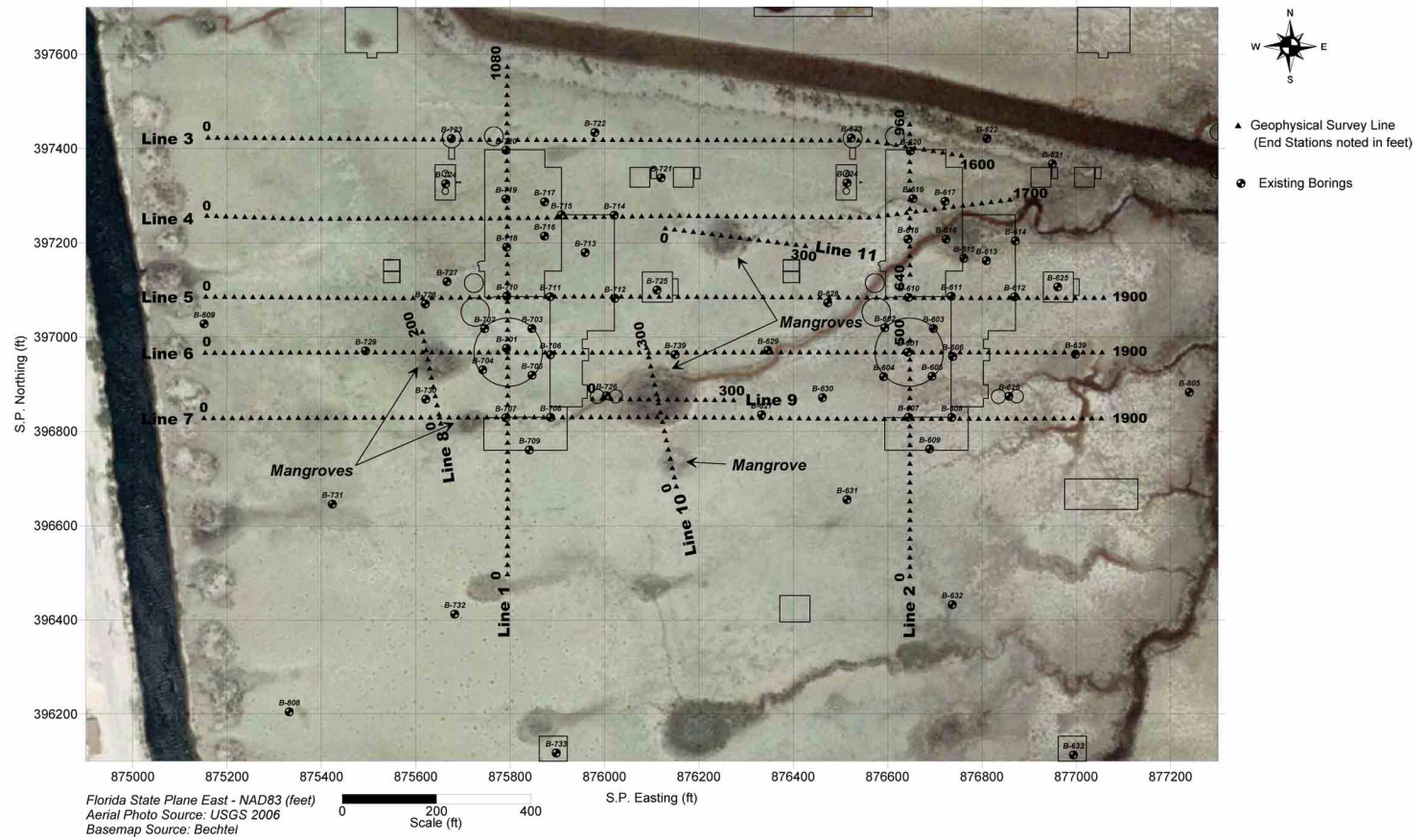
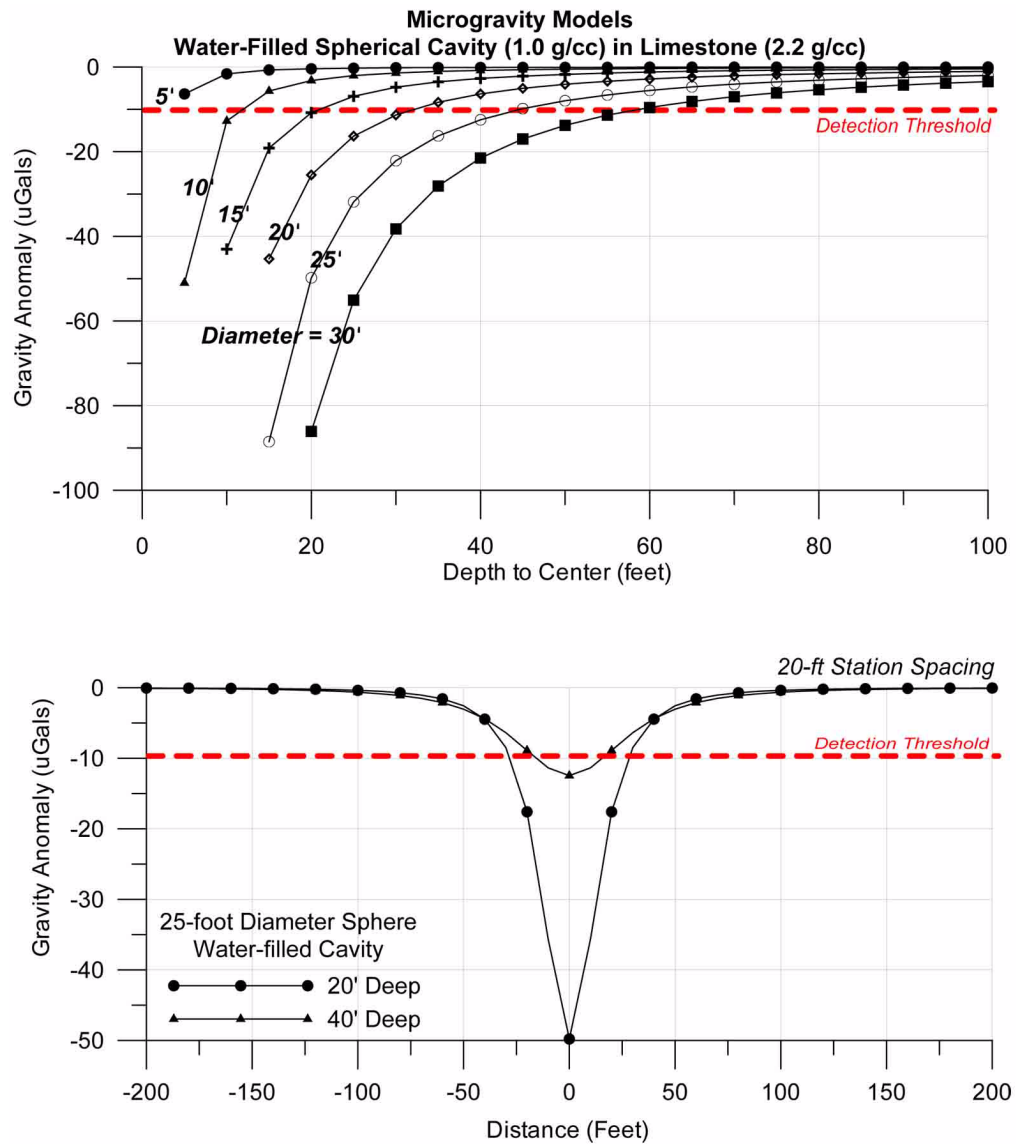
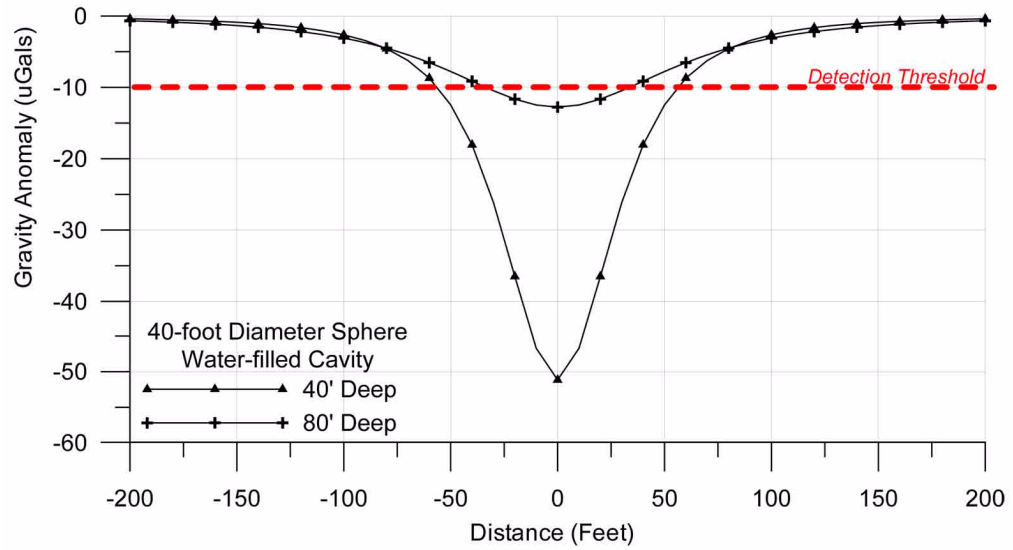


Figure 2.5.4-224 Microgravity Models for Water-Filled Spherical Cavities in Limestone (Sheet 1 of 2)



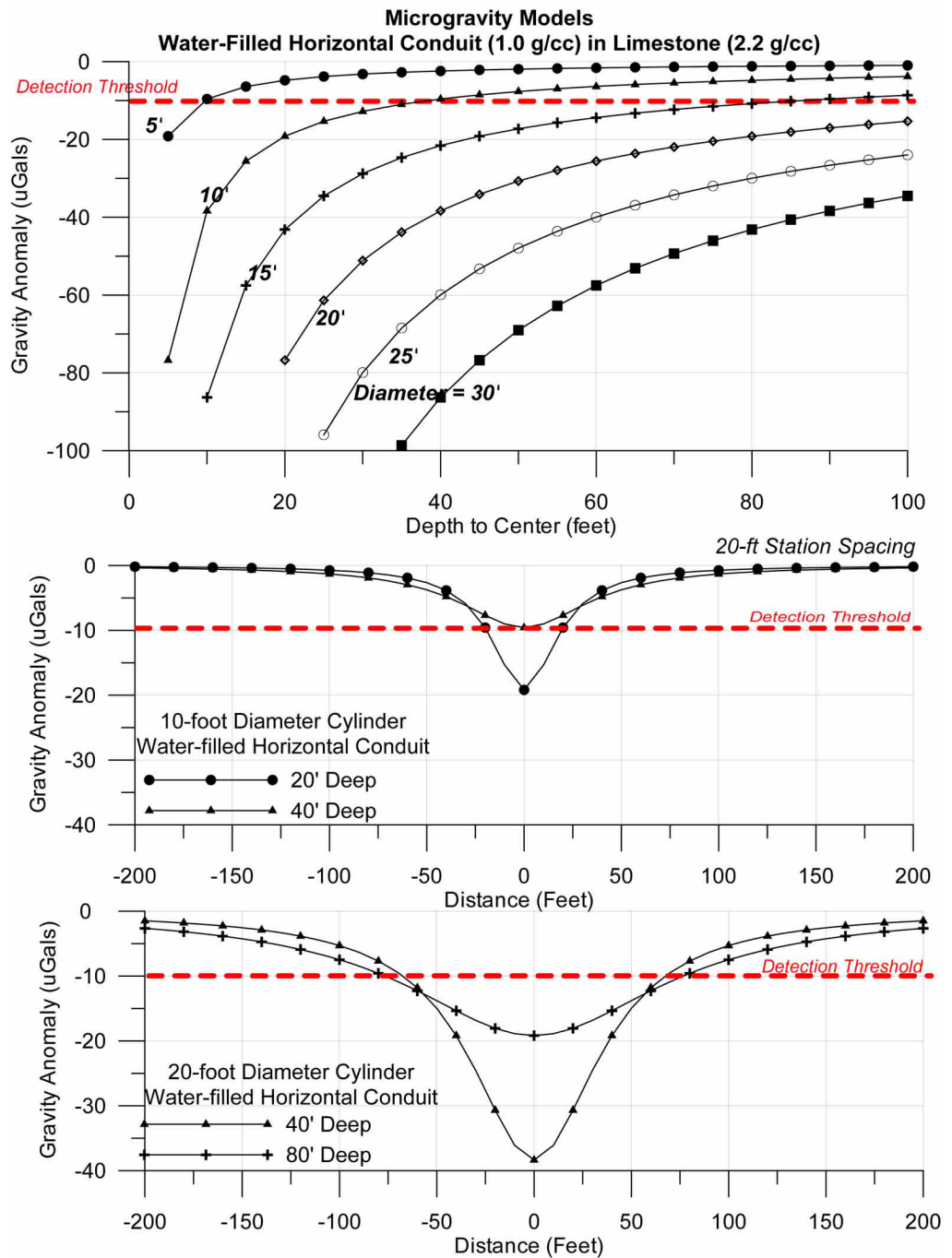
Modified from: [Reference 279](#).

Figure 2.5.4-224 Microgravity Models for Water-Filled Spherical Cavities in Limestone (Sheet 2 of 2)



Modified from: [Reference 279](#).

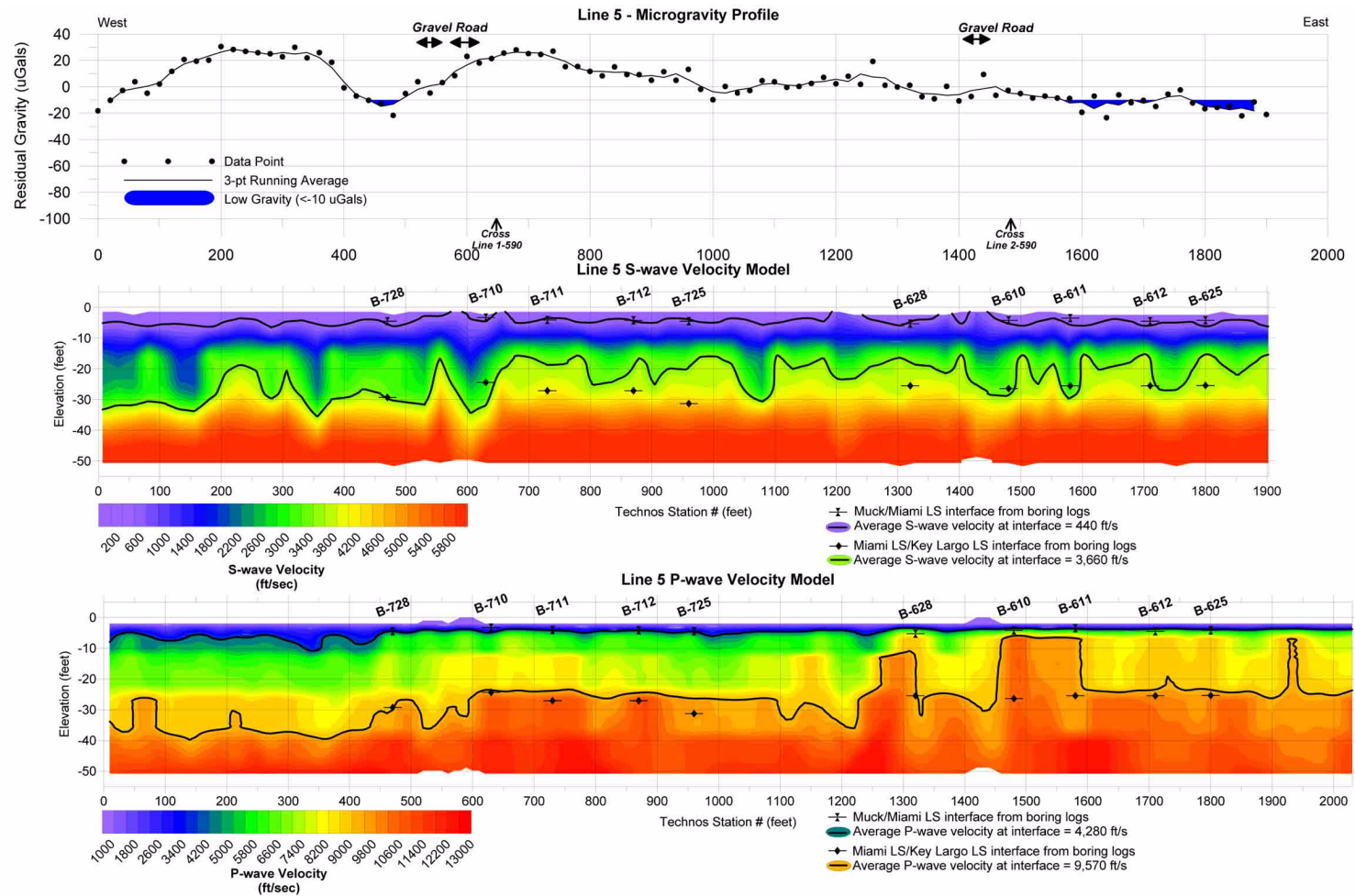
Figure 2.5.4-225 Microgravity Models for Water-Filled Horizontal Conduits in Limestone



Source: [Reference 279](#).

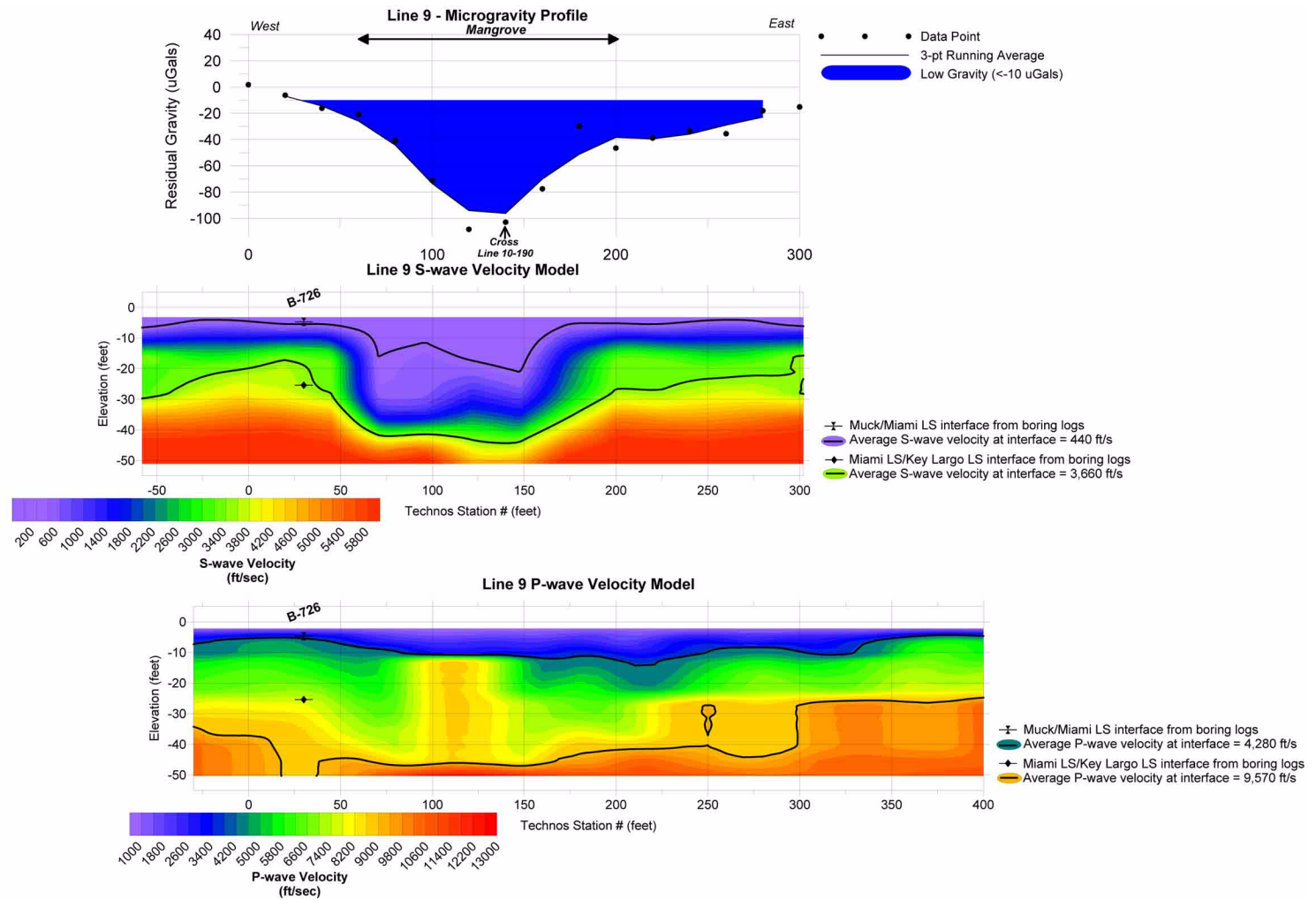
Turkey Point Units 6 & 7
COL Application
Part 2 — FSAR

Figure 2.5.4-226 Line 5 Geophysical Data



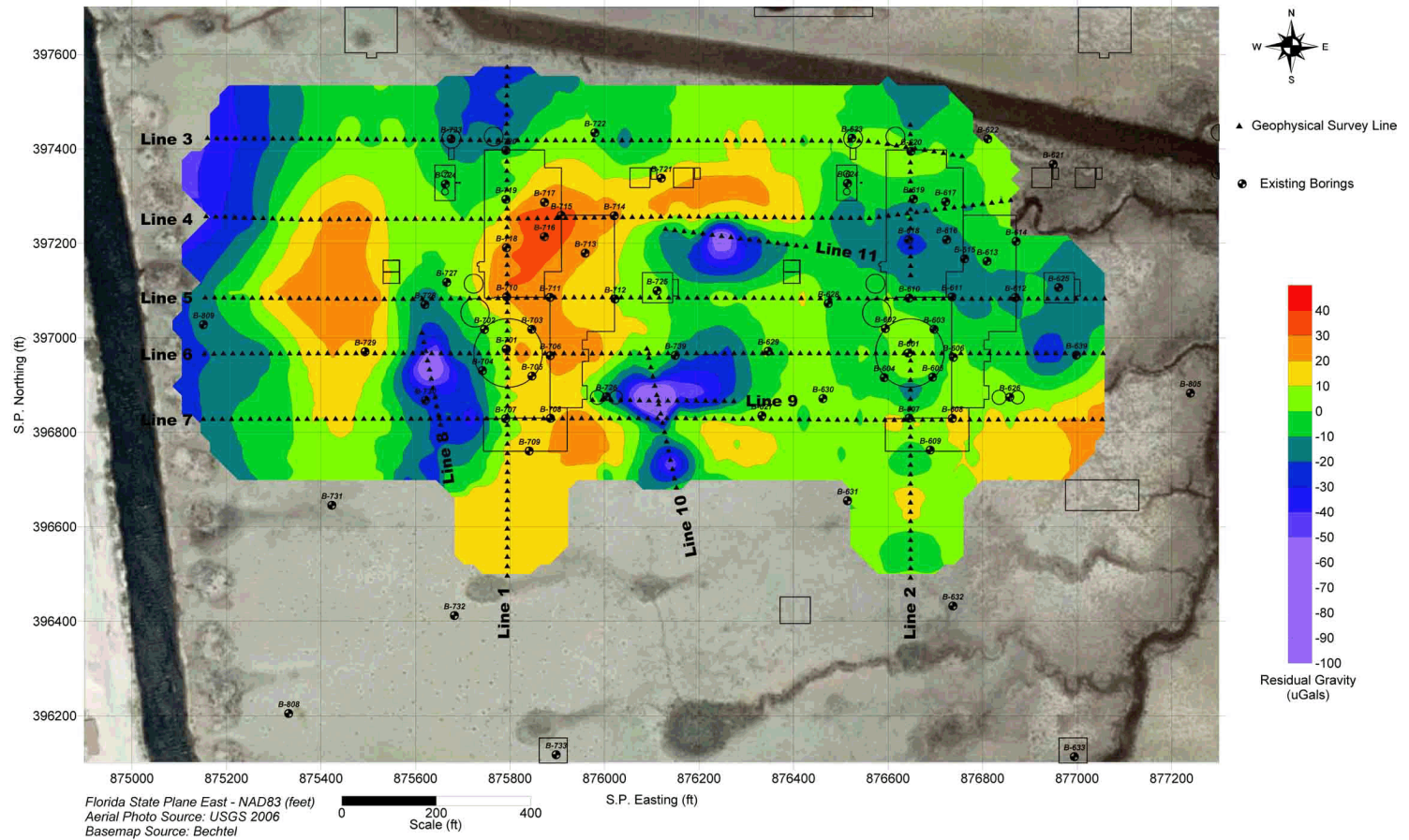
Turkey Point Units 6 & 7
COL Application
Part 2 — FSAR

Figure 2.5.4-227 Line 9 Geophysical Data



Turkey Point Units 6 & 7
COL Application
Part 2 — FSAR

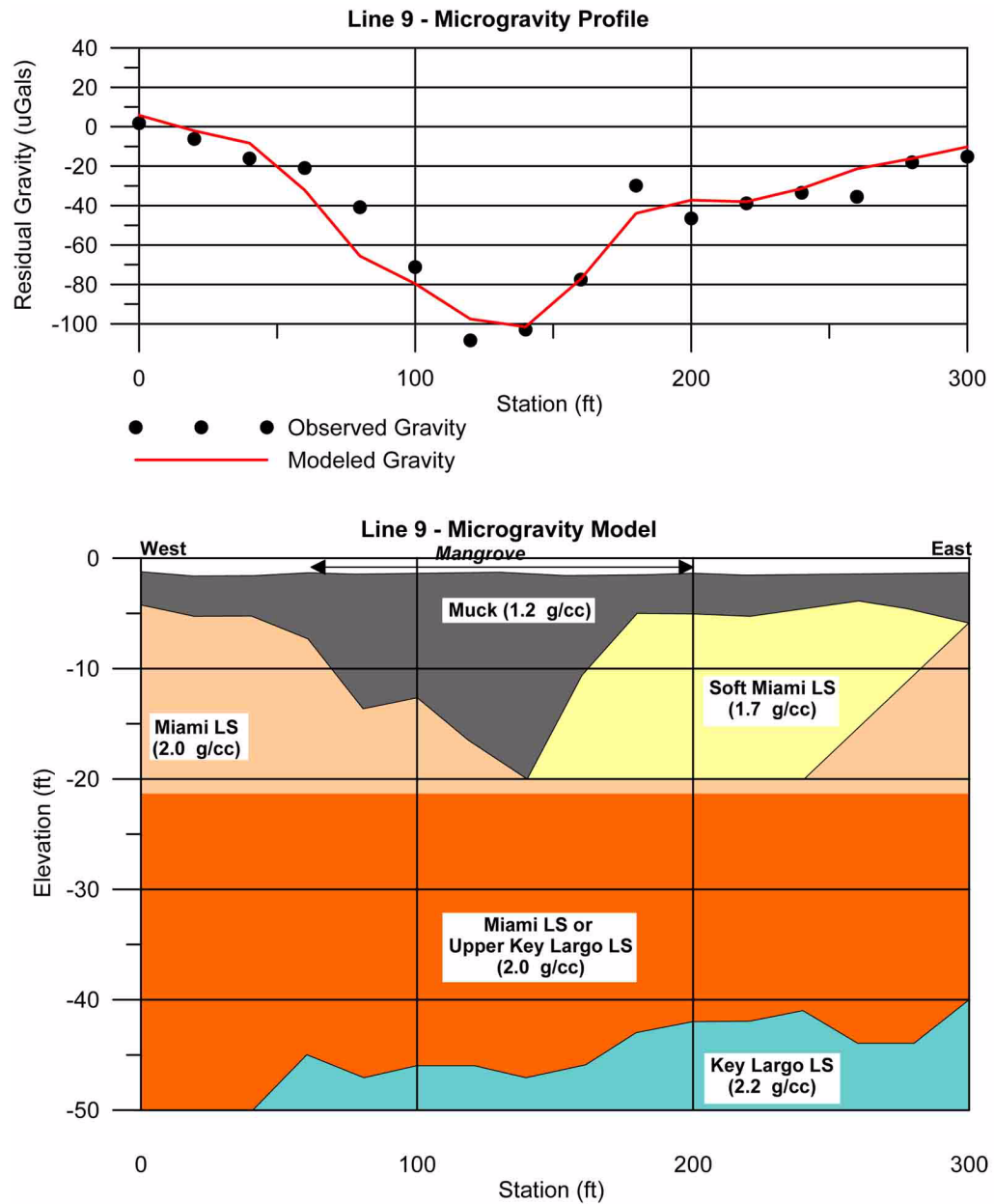
Figure 2.5.4-228 Microgravity Contour Map



Turkey Point Units 6 & 7
COL Application
Part 2 — FSAR

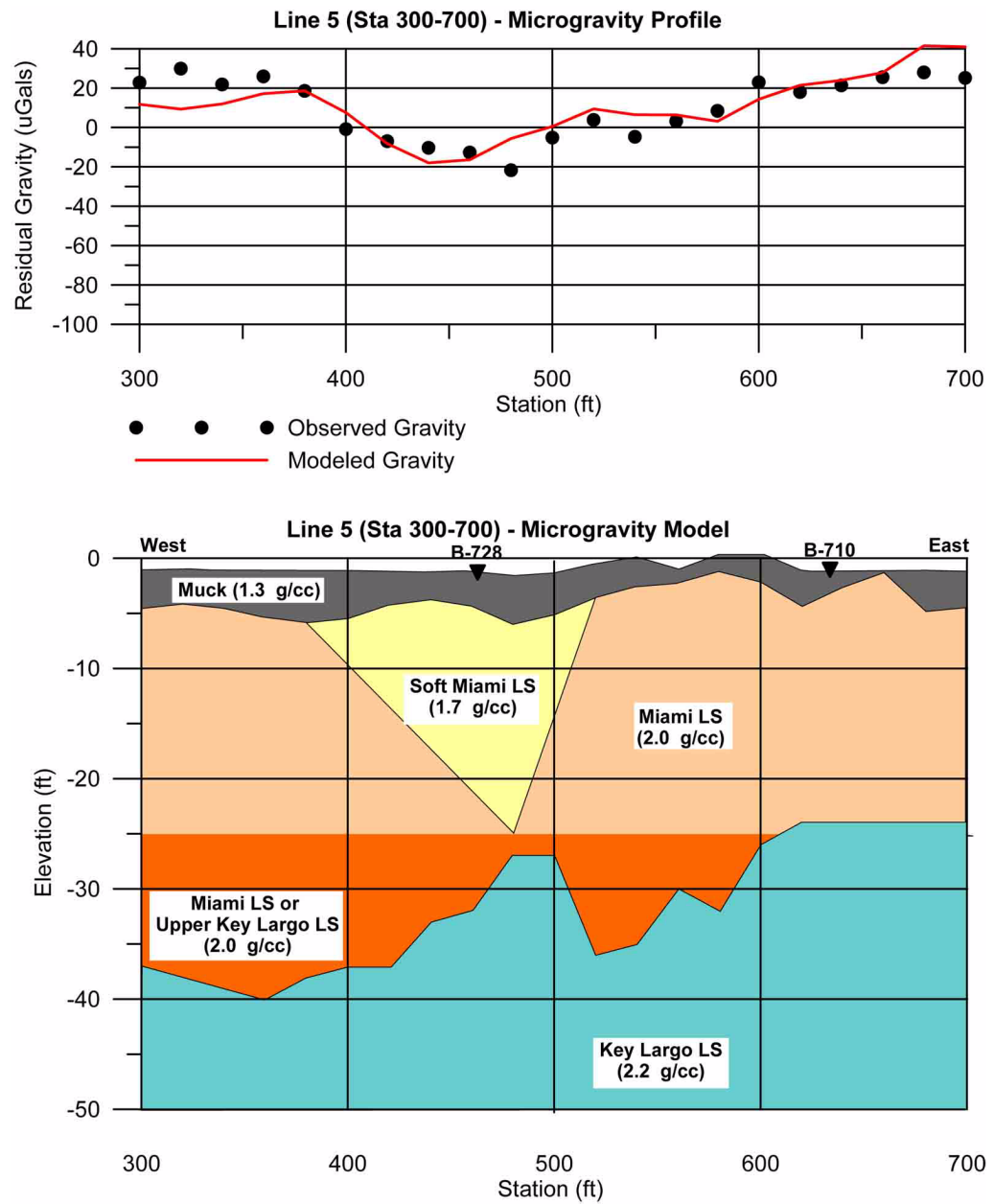
PTN COL 2.5-9

Figure 2.5.4-229 Line 9 Microgravity Model



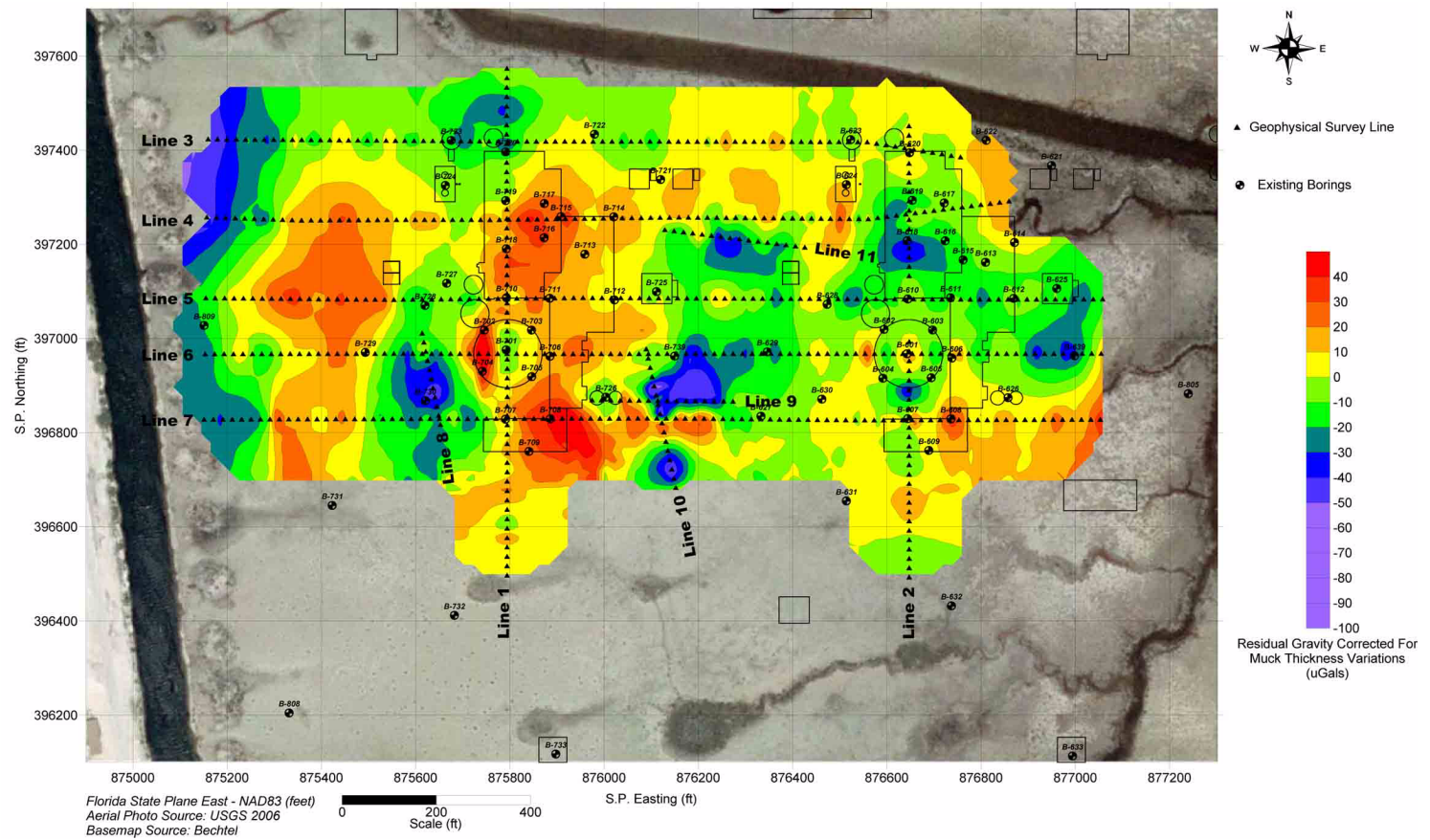
Turkey Point Units 6 & 7
COL Application
Part 2 — FSAR

Figure 2.5.4-230 Line 5 Microgravity Model



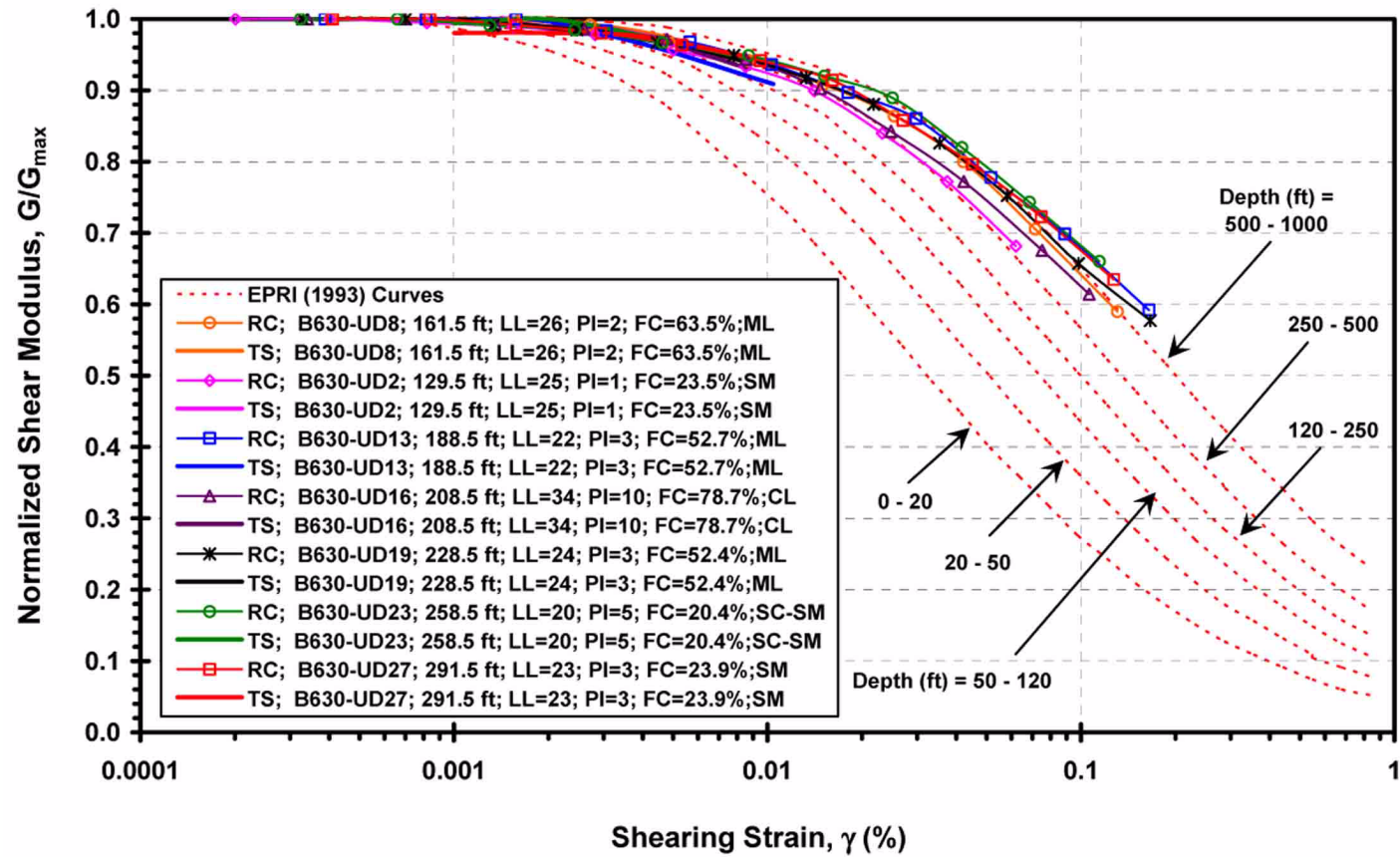
Turkey Point Units 6 & 7
COL Application
Part 2 — FSAR

Figure 2.5.4-231 Microgravity Contour Map with Muck Effects Removed



PTN COL 2.5-2
PTN COL 2.5-6

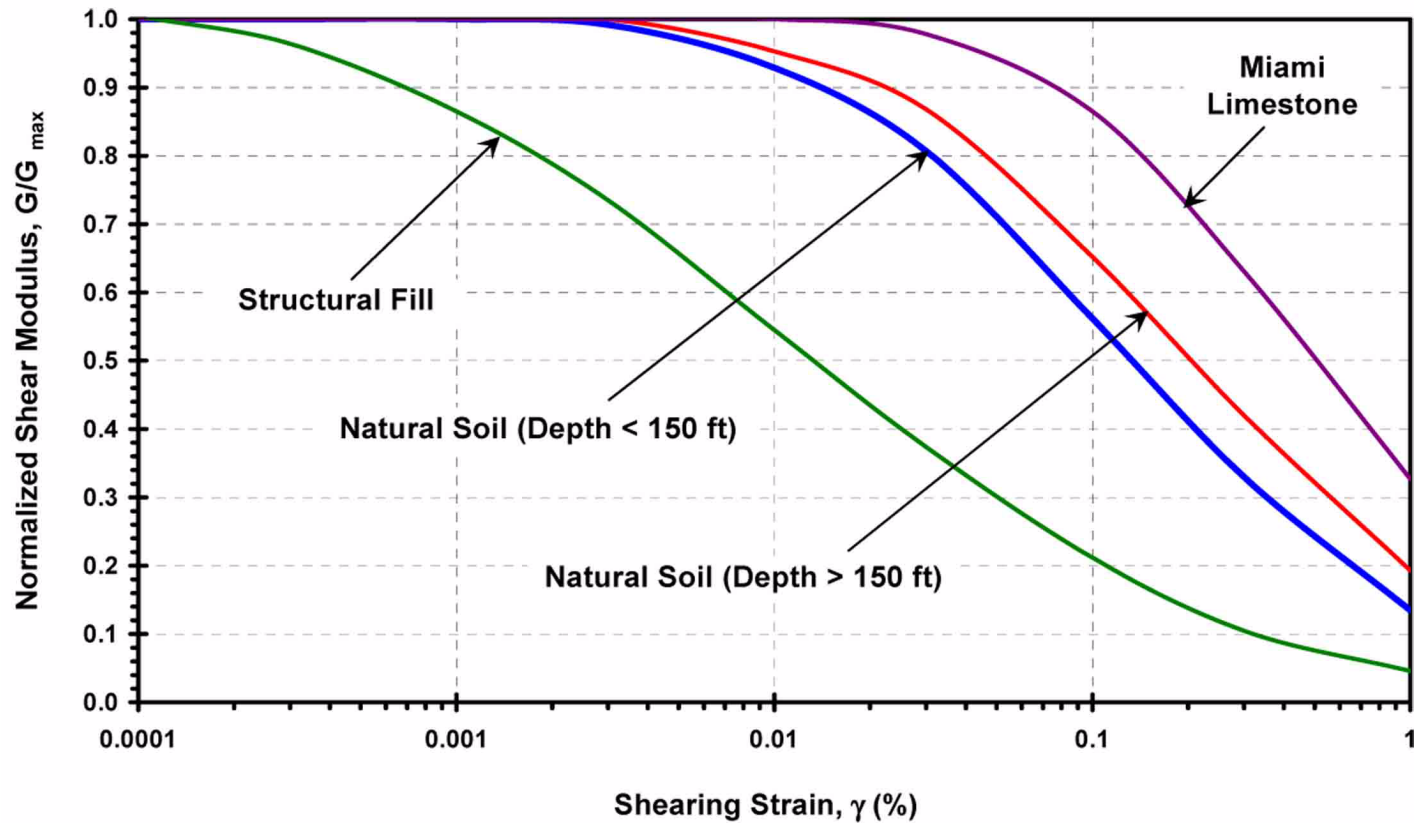
Figure 2.5.4-232 Shear Modulus Degradation Based on RCTS Testing



Data from Reference 257.

Figure 2.5.4-233 Recommended Shear Modulus Degradation Curves

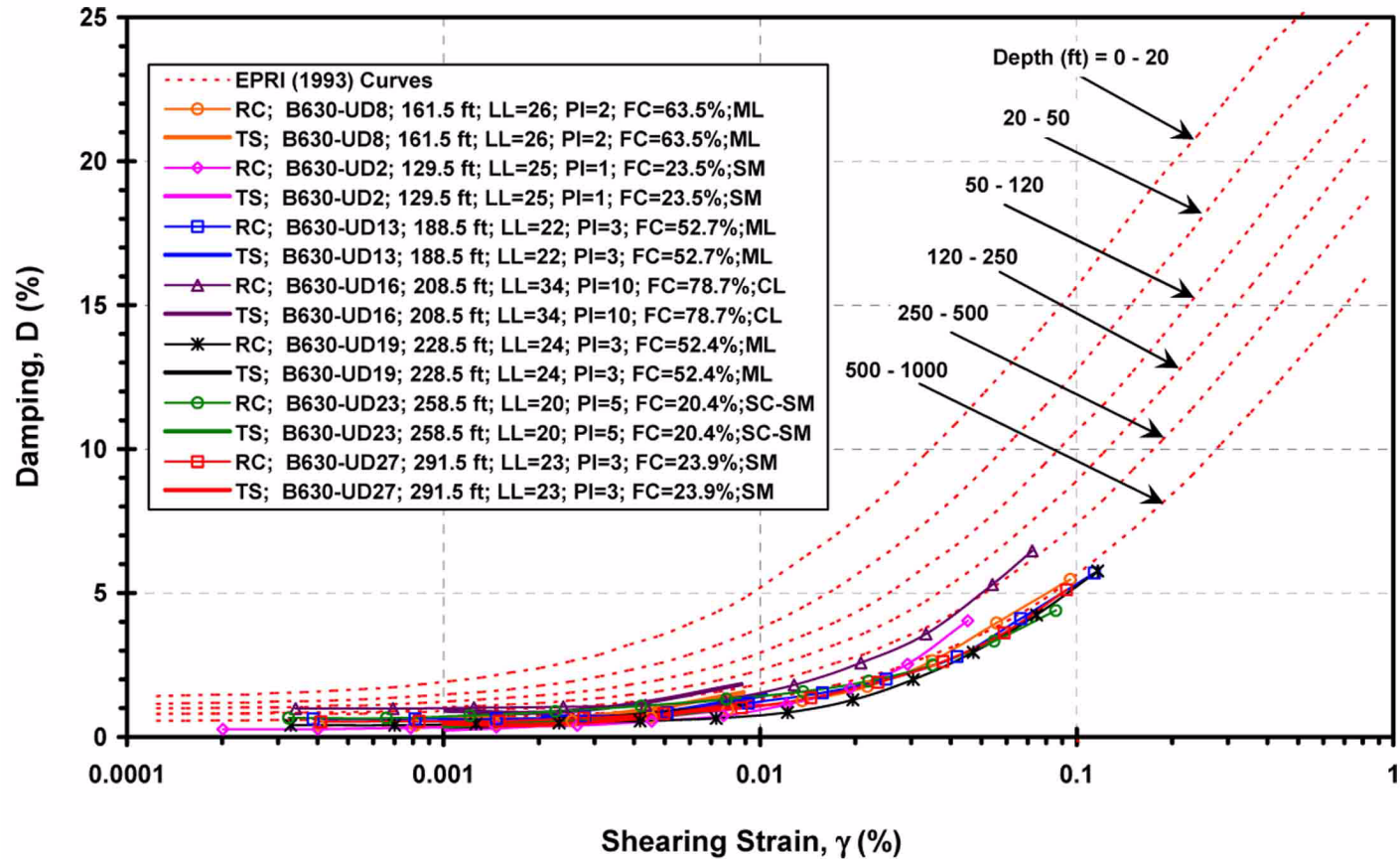
PTN COL 2.5-1
PTN COL 2.5-2
PTN COL 2.5-5
PTN COL 2.5-6
PTN COL 2.5-12
PTN COL 2.5-16



Data from [Reference 257](#) for Miami Limestone and [References 258, 259, and 260](#).

Figure 2.5.4-234 Damping Curve Measurements Based on RCTS Testing

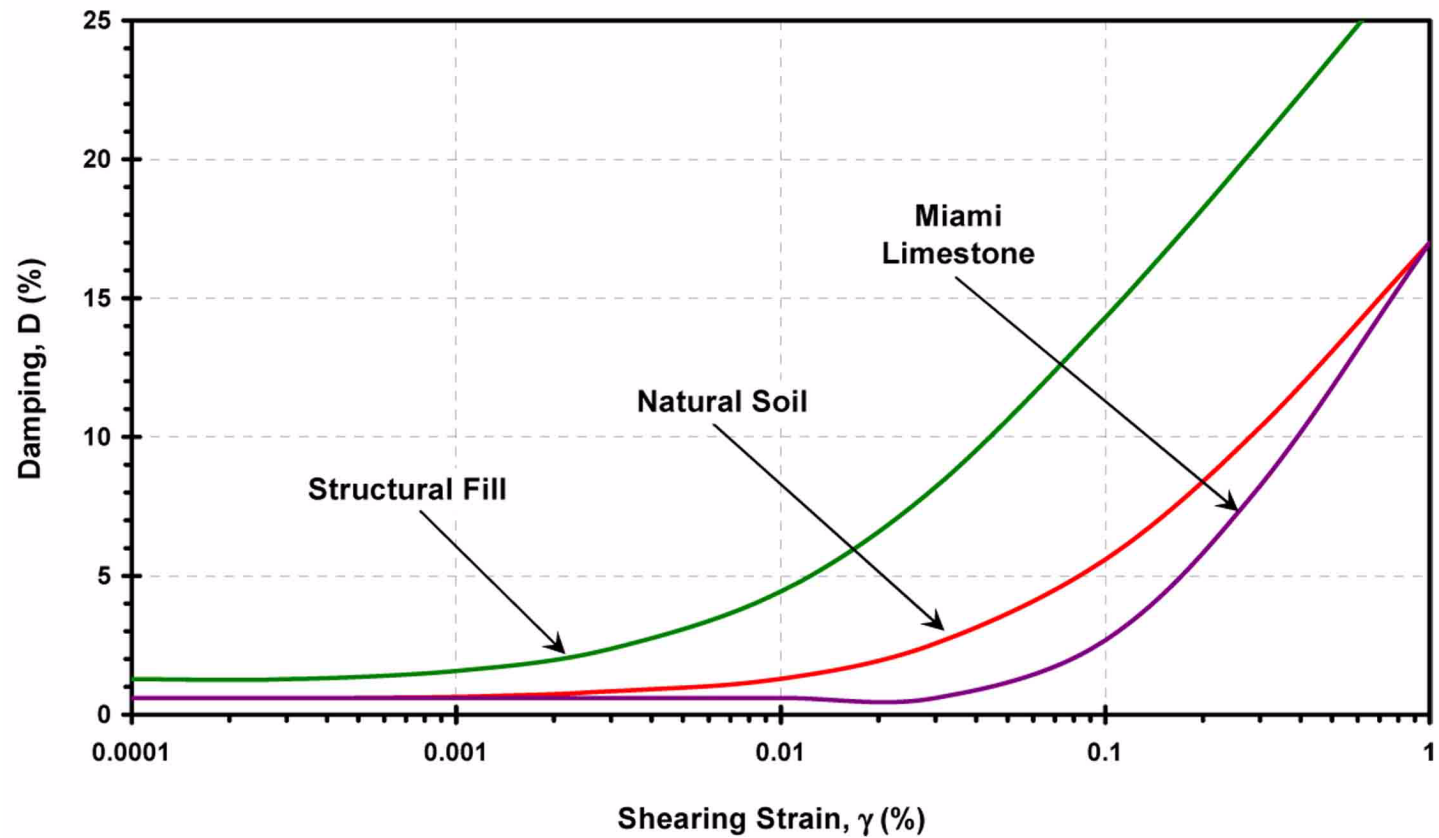
PTN COL 2.5-1
PTN COL 2.5-2
PTN COL 2.5-5
PTN COL 2.5-6



Data from [Reference 257](#).

Figure 2.5.4-235 Recommended Damping Curves

PTN COL 2.5-1
PTN COL 2.5-2
PTN COL 2.5-5
PTN COL 2.5-6

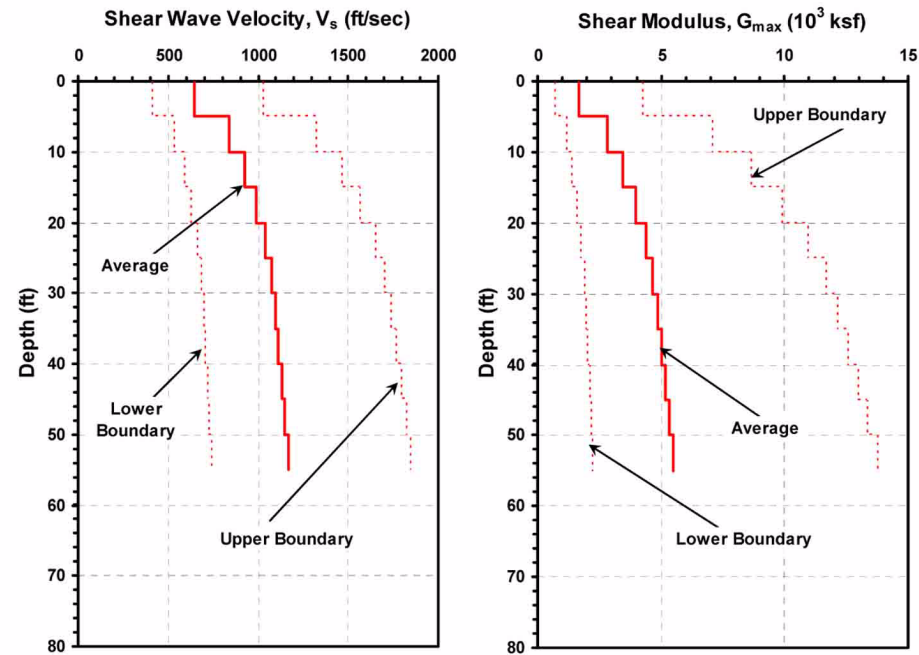


Data from [Reference 257](#) for Miami Limestone and [References 258, 259, and 260](#).

Turkey Point Units 6 & 7
COL Application
Part 2 — FSAR

PTN COL 2.5-2
PTN COL 2.5-6

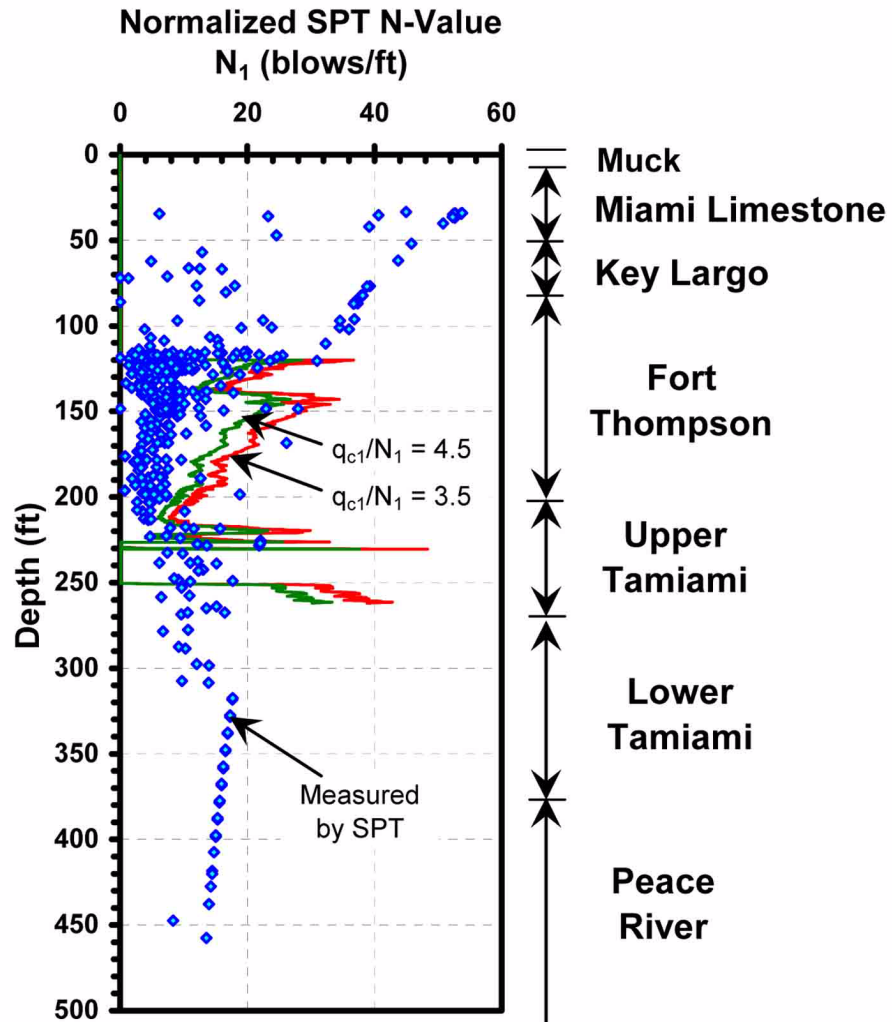
Figure 2.5.4-236 Recommended Shear Wave Velocity and Shear Modulus for Fill



Data from [Reference 257](#).

PTN COL 2.5-9

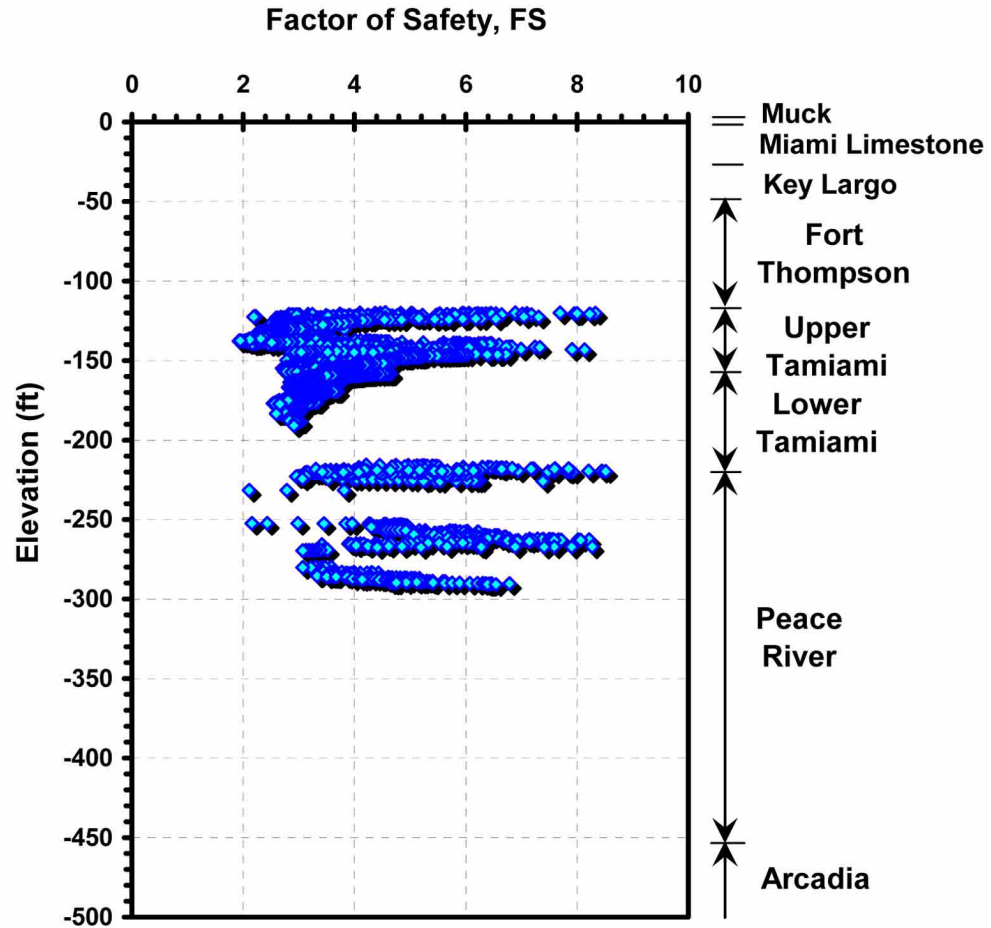
Figure 2.5.4-237 Comparison of Normalized SPT N-Value (N₁) Measured by SPT and Correlated from CPT



Data from [Reference 257](#).

PTN COL 2.5-9

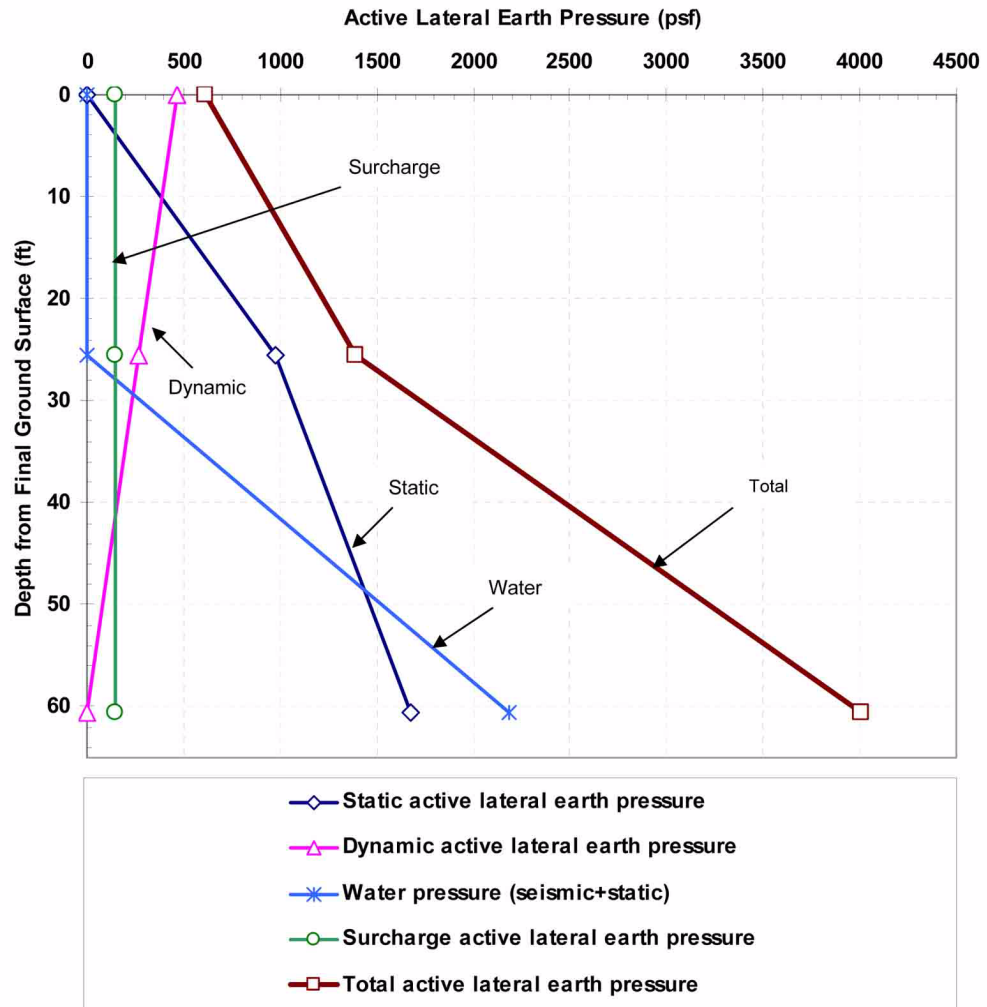
Figure 2.5.4-238 Factor of Safety Against Liquefaction Based on CPT Values



Turkey Point Units 6 & 7
COL Application
Part 2 — FSAR

PTN COL 2.5-3
PTN COL 2.5-7
PTN COL 2.5-11

Figure 2.5.4-239 Lateral Earth Pressure Diagram: Active Case

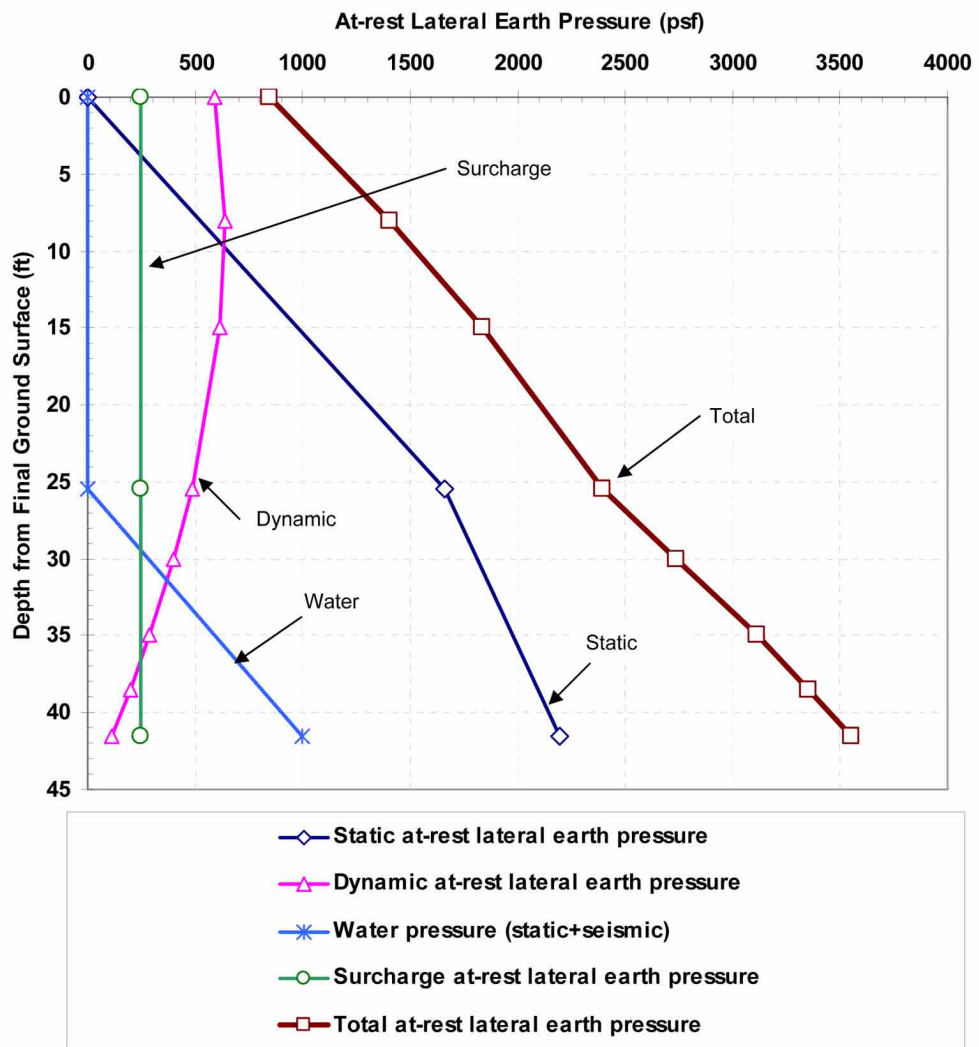


Data from Table 2.5.4-209 for compacted limerock fill.

Turkey Point Units 6 & 7
COL Application
Part 2 — FSAR

PTN COL 2.5-3
PTN COL 2.5-7
PTN COL 2.5-11

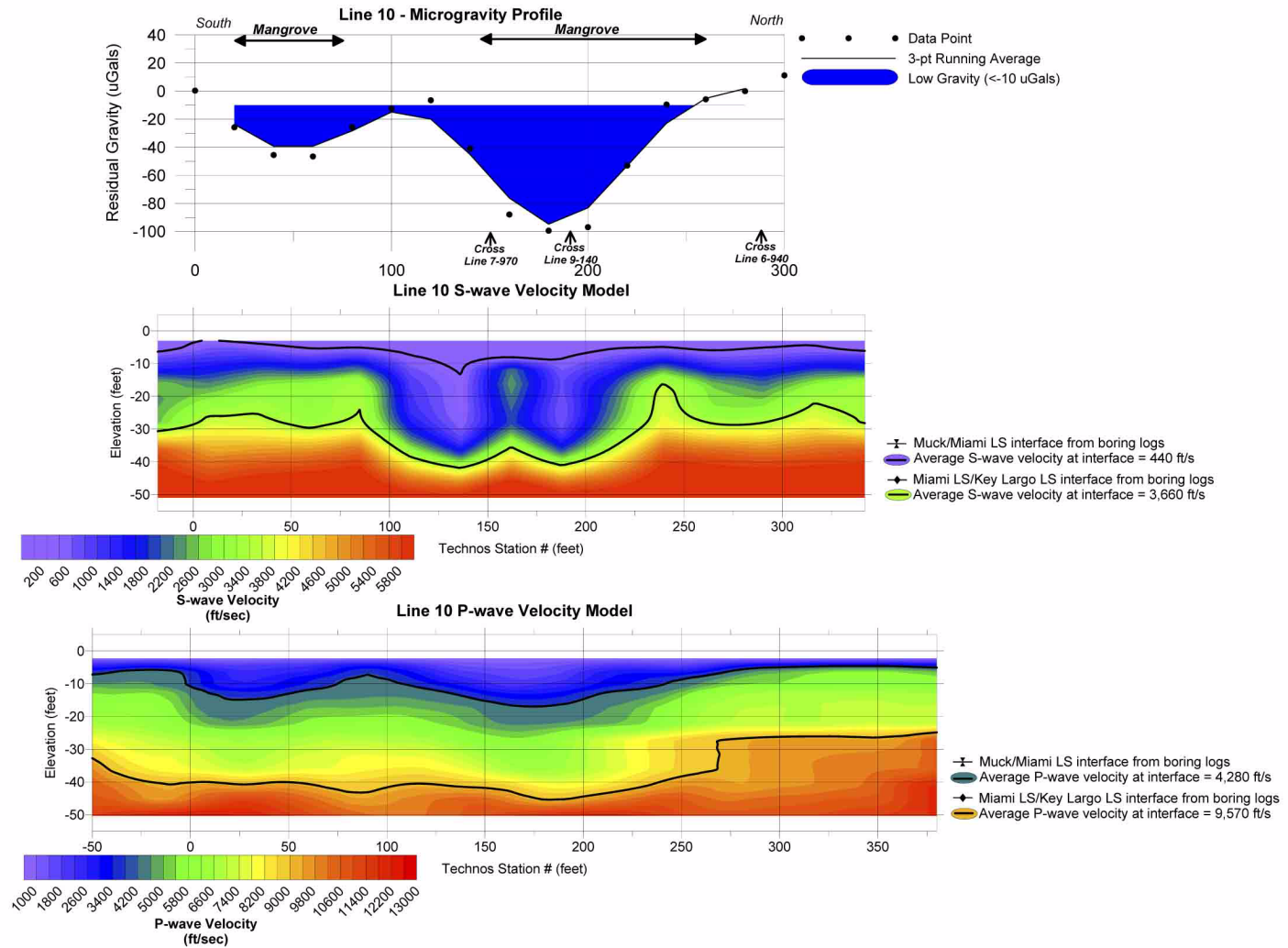
Figure 2.5.4-240 Lateral Earth Pressure Diagram: At-Rest Case



Data from Table 2.5.4-209 for compacted limerock fill.

Turkey Point Units 6 & 7
COL Application
Part 2 — FSAR

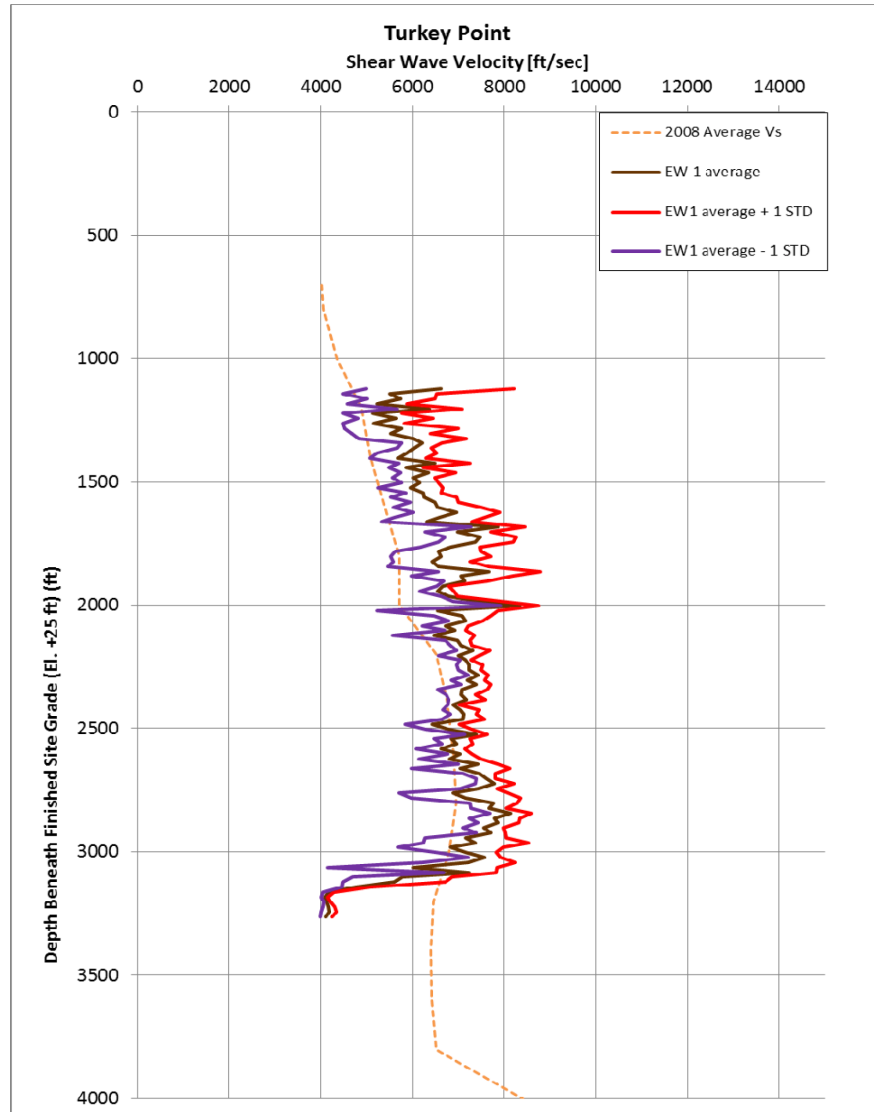
Figure 2.5.4-241 Line 10 Geophysical Data



Source: Reference 286

Turkey Point Units 6 & 7
COL Application
Part 2 — FSAR

Figure 2.5.4-243 EW-1 Profiles of Vs, Average Vs, Standard Deviation, +/- Standard Deviation and 2008 Average Vs versus Depth Beneath Finished Site Grade



Note: The calculated averages for the "2008 Average Vs" values are computed in 100-foot and 200-foot intervals. The EW-1 calculated average Vs values are in 20-foot intervals.

Source; [Reference 287](#)